Utility of cardiovascular magnetic resonance imaging with contrast-enhancement: beyond the scope of viability

Marlon Olimulder

Utility of cardiovascular magnetic resonance imaging with contrast-enhancement: beyond the scope of viability

Marlon Olimulder

UTILITY OF CARDIOVASCULAR MAGNETIC

RESONANCE IMAGING WITH CONTRAST-ENHANCEMENT:

BEYOND THE SCOPE OF VIABILITY

DISSERTATION

to obtain
the degree of doctor at the University of Twente,
on the authority of the rector magnificus,
Prof.dr. H. Brinksma,
on account of the decision of the graduation committee,
to be publicly defended
on day the 25th of June 2014 at 12.45

by

Marlon Anne Gesina Maria Olimulder

Born on 28 August 1982
In Almelo, The Netherlands

This dissertation has been approved by the promotor:
Prof. dr. Clemens von Birgelen

MEMBERS OF THE COMMITTEE

Promotor
Prof. dr. C. von Birgelen   University of Twente, Enschede

Assistant promotor
Dr. M.A. Galjee   Waterlandziekenhuis Purmerend
                         (chairman board of management, cardiologist)
Dr. L.J. Wagenaar   Medisch Spectrum Twente (cardiologist)

Other members
Prof. dr. M.J. IJzerman   University of Twente, Enschede
Prof. dr. ir. C.H. Slump   University of Twente, Enschede
Prof. dr. J.G. Grandjean   University of Twente, Enschede
Prof. dr. A.H.E.M. Maas   University of Nijmegen
Prof. dr. R.J. de Winter   University of Amsterdam
Prof. dr. med. D. Baumgart   University of Duisburg-Essen, Germany

Faculty Management and Governance, department Health Sciences

Table of contents

Chapter 1

General introduction and outline of the thesis

1.1   General Introduction

Cardiovascular magnetic resonance imaging
In 1977, the first magnetic resonance scan of a human body was accomplished, but the required scan time of almost 5 hours prevented use of this technology as a clinical tool.[1] Further refinement of the technique in the 1980's resulted in electrocardiography (ECG)-gated Cardiovascular Magnetic Resonance imaging (CMR) of the heart.[2] As a result of various developments in terms of hardware, pulse sequences, and the ability of post-processsing techniques, CMR nowadays allows us to depict cardiovascular anatomy with a high spatial and temporal resolution. These image sequences permit not only the morphological examination of the heart, including left ventricular dimensions, but they also make functional assessment possible, including accurate and reproducible assessment of left ventricular (LV) function. This has enabled CMR to emerge as a powerful tool for physicians to diagnose various cardiac pathologies, guide therapies, and predict outcome and prognosis.[3]

Gadolinium-enhanced cardiovascular magnetic resonance imaging
One of the most recent developments of CMR is to characterize myocardial tissue after the administration of gadolinum, so-called Late Gadolinium-Enhanced CMR (LGE-CMR),[4] which previously has been referred to as Contrast-Enhanced CMR (CE-CMR) or Delayed-Enhanced CMR (DE-CMR). This technical approach can be valuable for the evaluation of both patients with ischemic heart disease, who developed a myocardial infarction (MI), as well as for patients with non-ischemic heart diseases, as for instance myocarditis. CMR has proven to be equal and sometimes even superior to other imaging modalities such as echocardiography, X-ray angiocardiography, and nuclear imaging.[5;6] Currently, CMR is considered the "gold" standard for non-invasive assessment of LV function and MI tissue characterization.[6;7] CMR is undergoing a rapid, continuous evolution. Other clinical diagnostic applications of CMR, among which the current practice of risk stratification in post-MI patients who are candidates for implantable cardioverter-defibrillator (ICD), will be highlighted in this thesis. CMR is a technically demanding imaging technique; therefore, some methodological and technical aspects of cine and LGE-CMR are illustrated below.

Brief remarks on technical aspects of cine and LGE-CMR assessment
In order to determine ventricular function, a stack of moving images (so called 'cines') of contiguous left ventricular short-axis slices (slice thickness of 5 to 10 mm) from the base of the heart to the apex is made (Figure 1a). Depending on the patient's heart rate, each separate slice is distributed in approximately 30 phases (simplified in Figure 1b). To calculate LV volumes and determine LV ejection fraction (LVEF), the LV endocardial borders are manually or semi-automatically traced on various slices and then Simpson's rule is applied (i.e., summation of LV lumen cross-sectional

area multiplied by thickness of each individual slice). Tracing of the end-diastolic LV epicardial borders in addition to the endocardial borders allows determining LV mass.
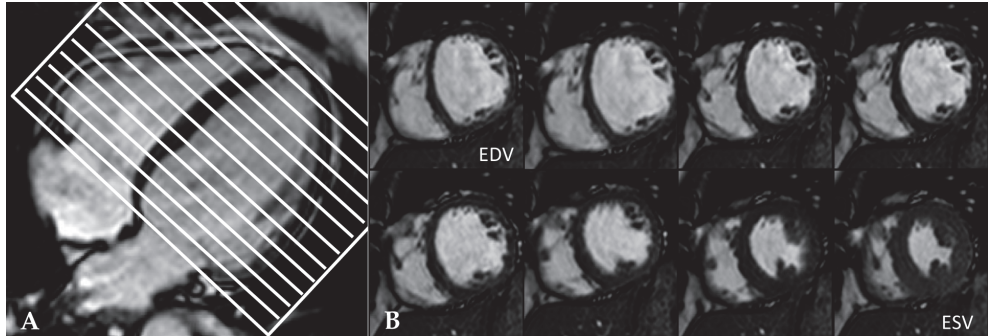
Figure 1. Schematic figure for **A**: multiple short axis slices from basal to apical are made from a four chamber view, **B**: from 1 separate short axis slice, phases from end-diastolic to end-systolic are illustrated.

For making LGE-CMR images, an intravenous contrast agent, such as gadolinium, is injected. Ten to 15 minutes after the injection, the images are collected, hence the name "<u>late</u>" gadolinium-enhanced imaging. Timing of the image acquisition is of paramount importance as too early image acquisition reduces the difference in contrast between normal and damaged myocardium (i.e., myocardial scar, fibrosis) because of insufficient washout of contrast from the normal myocardium, while too late image acquisition can result in an excessive washout of contrast from damaged myocardial tissue.[8]

To quantify the size of infarcted myocardial tissue (i.e., the infarct size), different approaches have been applied.[9] In this thesis, the so-called "full width at half maximum (FWHM) approach" has been applied, which is a semi-automated thresholding technique. The FWHM approach considers myocardial tissue as *infarct core*, if its signal intensity is at least half as high as the highest signal intensity in the region of interest. Scar tissue, which comprises both infarct core and the so-called *heterogeneous zone* (i.e., zone with signal intensity ≥ 35% and < 50% of the maximum), is further quantified according to its location by use of a 17 segmental model.[10] In this model, the *transmural extent* of myocardial scar can be implemented, with transmural scar being present if a LV segment has a scar score of 3 or 4.[11] (A scar score of 0 was defined as normal, 1 as 1-25% scar, 2 as 26-50% scar, 3 as 51-75% scar, and 4 as 76-100% scar of the segmental area). In addition, a segmental *regional scar score* can be calculated to relate scar size to the territories of the three major coronary arteries.[10]

Myocardial infarction and clinical use of LGE-CMR

Coronary artery disease is highly prevalent in countries with western lifestyle, leading in a substantial proportion of patients to acute coronary syndromes and myocardial infarctions.[12] A myocardial infarction, generally occurs as a consequence of a rupture or erosion of an atherosclerotic coronary plaque due to intracoronary thrombus formation at that site, which blocks coronary flow and myocardial oxygen supply.[13] Myocardial necrosis starts to occur after a coronary occlusion for at least 20 to 30 minutes (without sufficient collateral blood supply), and after 2-3 hours the necrosis is generally transmural.[14-16] A heterogeneous mixture of scar tissue and vital cardiomyocytes is generally found in the border zone of an infarcted LV area.[17;18]

In the early phase of MI, cellular degradation in the infarcted myocardium results in an increase in cellular permeability and enlargement of the extravascular space (edema), and thus, in an increased distribution volume for the contrast agent. In a later phase of MI, due to different wash-in and washout kinetics, myocardial scars retain the contrast agent longer than the normal myocardium. The net result of both mechanisms is that infarcted myocardium appears bright on LGE-T1-weighted images.[19] The bright myocardial region generally shows a typical pattern that is related to the perfusion area of the culprit vessel.

Depending on the duration of coronary occlusion, myocardial changes (and thus LGE) may be limited to the subendocardium or may further extend to full transmural necrosis and ultimately scar (Figure 2a,b). In general, a standardized 17 segment-model is used to report the results of myocardial viability assessment by LGE-CMR (Figure 3).[10] In patients with prior MI, a high interobserver agreement for the assessment of presence and extent of LGE is found. In addition, presence, location, and extent of LGE correspond well with histology.[9;20;21] Quantitative assessment of infarct tissue characteristics (including size, heterogeneity, and transmural extent) have been shown to be clinically useful. For instance, the assessment of myocardial viability following MI can help to tailor therapy, as only viable myocardium can benefit from coronary revascularization.[22]

Quantification of infarct tissue characteristics may also help to prognosticate left ventricular remodeling.[23] The transmural extent of infarcted tissue as determined by LGE-CMR has been shown to be a powerful predictor of the contractile response to both medical therapy and coronary revascularization.[24] Another area of increased interest is the assessment of characteristics of the infarcted myocardial tissue as potential predictor of life-threatening ventricular arrhythmias. It has been demonstrated that the heterogeneity of the infarcted tissue by LGE-CMR can be a potentially important predictor of ventricular arrhythmia.[25;26]
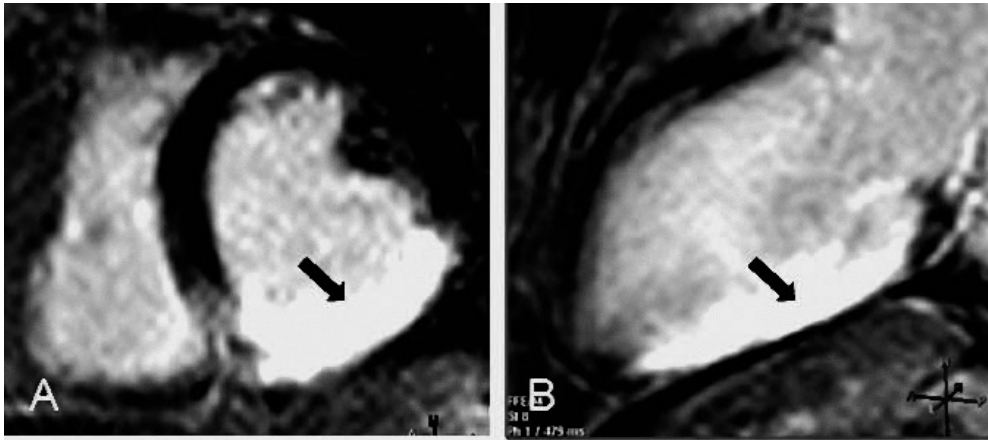
Figure 2. LGE-CMR patterns post myocardial infarction. **A,B**: LGE short axis and long axis view showing transmural inferior infarction (black arrow).
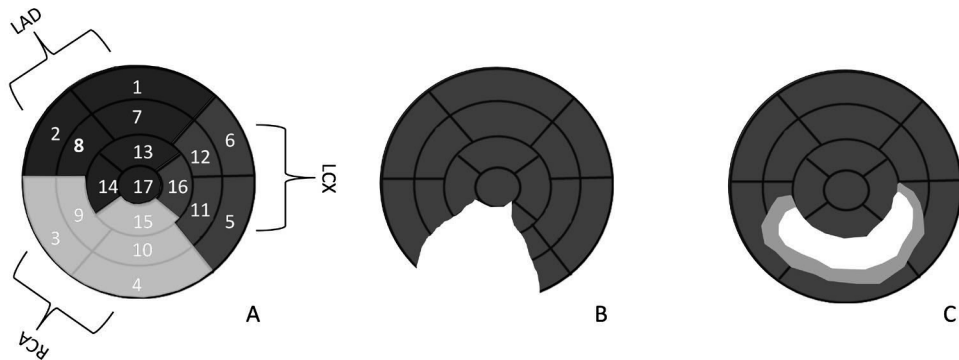
Figure 3. Bull's eye scheme according to the 17 segmental model, demonstrating LGE characteristics post myocardial infarction. **A**: assignment of the 17 segments to one of the 3 major coronary arteries, with segment 1, 2, 7, 8, 13, 14, and 17 corresponding to the left anterior descending coronary artery; segments 3, 4, 9, 10 and 15 corresponding to the right coronary artery when it is dominant; and segments 5, 6, 11, 12, and 16 are assigned to the left circumflex artery. **B**: Transmural inferior MI. **C**: Inferoseptal MI with a core zone (white area) and a peri-infarction zone (grey area).

Myocardial inflammation and its assessment with LGE-CMR

Myocarditis is the name for inflammatory diseases of the myocardium that can be caused by different viruses or can be initiated by post-infectious immune or primarily organ-specific autoimmune responses.[27] Diagnosing acute myocarditis is challenging because of its often-diverse clinical presentation (that may mimic an MI) and the limited sensitivity of histophathological assessment of endomyocardial biopsies.

In the setting of myocarditis, the increased permeability of myocytes in the region of inflammation and the edema increase the distribution volume for a CMR contrast agent. Increased recognition

of myocardial inflammatory changes has led to a rise in interest in LGE-CMR as a diagnostic tool.[28;29] The presence of LGE has been reported in 44-95% of patients with acute myocarditis,[30;31] and LGE-CMR has been shown to indicate areas of myocardial damage with a sensitivity of 100% and a specificity of 90% (as compared to histopathology).[30] In addition, the LGE technique is capable of ruling out an ischemic cause in the differential diagnosis of myocarditis because in the setting of myocardial infarction the subendocardial myocardial layer is always involved. In acute myocarditis, LGE is most frequently located in the lateral wall and originates from the epicardial layer.[32] In contrast to patients with coronary artery disease who suffered from an MI, the subendocardium is generally not involved in a myocarditis, with the exception of eosinophilic myocarditis. (Figure 4).[33;34]

Patients mostly recover from an acute myocarditis without any late sequelae, but they may infrequently develop a chronic myocarditis and/or a dilated cardiomyopathy. This sometimes leads to life-threatening complications such as severe heart failure and malignant cardiac arrhythmias.[35] In the chronic stage of myocarditis, LGE-CMR has identified areas of myocardial damage in 70% of patients with biopsy-proven chronic myocarditis, with a predilection pattern of changes in the LV midwall and/or subepicardial wall.[36] LGE may provide additional information that could help to differentiate between viral origins of the inflammation, as in the majority of parvovirus B19 patients LGE is found in the lateral free wall, whereas in many patients with human herpes virus 6 LGE involves the midwall of the interventricular septum.[31;32]
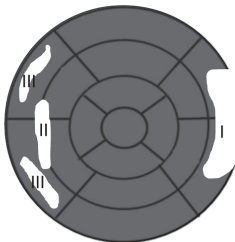
Figure 4. Bull's eye scheme according to the 17 segmental model, demonstrating typical LGE patterns in myocarditis and cardiac involvement of other diseases.
Myocarditis with LGE frequently located in the lateral wall originating from the epicardium (I). LGE patterns in myocarditis differ according to viral origin, with parvovirus B19 having LGE in the lateral free wall (I), HHV6 having LGE frequently in the midwall of the interventricular septum (II), and chronic fatigue syndrome myocarditis having LGE anteroseptal and inferoseptal (III).

1.2   Outline of the thesis

The general aim of this thesis is to evaluate and discuss the value of LGE-CMR, which allows to assess LV functional parameters and myocardial tissue characteristics. The present first chapter gives a brief overview of the technique of CMR, including the LGE technique and its use in the

clinical setting of MI and myocarditis–the two main clinical applications of LGE-CMR in this thesis.

Clinical studies and histopathological examinations have suggested that early revascularization for an MI limits the size, transmural extent, and homogenetiy of myocardial necrosis, however, the long-term effect of early revascularization on infarct tissue characteristics is largely unknown. In **chapter 2**, we investigated with LGE-CMR the long-term effects of early revascularization for acute MI on infarct tissue characteristics (i.e. size, location, transmural extent and heterogeneity of scar).

As LV remodeling following MI is the result of complex interactions between various factors– including the presence or absence of early revascularization, we studied in **chapter 3** the impact of early revascularization for MI on the relationship between (LGE)-CMR assessed infarct tissue characteristics and LV remodeling.

There is also great interest in the potential impact of various risk factors on LV remodeling. Previous research has suggested that LV remodeling is not caused by a single factor or circumstance, but that a number of cardiovascular risk factors may be involved. The Framingham Risk Score is an established cardiovascular event risk score that is mostly used in the field of primary cardiovascular prevention, but recently it has been shown in human subjects that it also predicts the likelihood of certain adaptive changes in LV structure and function during lifetime. Therefore, in **chapter 4**, we used LGE-CMR in a consecutive series of patients with a first STEMI, successful primary percutaneous coronary intervention (PCI), and single-vessel coronary artery disease to assess the potential relationship between the Framingham Risk Score and both parameters of LV remodeling and infarct tissue characteristics at 6-month follow-up.

Ventricular arrhythmias are a major cause of sudden cardiac death in patients with prior MI. Knowledge about potential differences in infarct tissue characteristics between patients with prior life-threatening ventricular arrhythmia versus patients who prophylactically receive an ICD, might ultimately help improve risk stratification in post-MI patients considered for ICD implantation. In **chapter 5**, these potential differences were investigated by use of LGE-CMR in a consecutive series of ICD recipients for primary and secondary prevention following MI.

As Microvolt T-Wave Alternans (MTWA) is an electrocardiographic marker for predicting sudden cardiac death (SCD), in **chapter 6**, we assessed potential relationships between MTWA and scar/fibrosis by LGE-CMR in both patients with ischemic cardiomyopathy and patients with dilated cardiomyopathy.

LGE-CMR is not only valuable in the setting of ischemic heart disease. In **chapter 7**, we discuss the current role of LGE-CMR in the evaluation of myocarditis-induced, inflammatory cardiomyopathies.

In patients with chronic fatigue syndrome, previous histopathological studies have demonstrated the presence of cardiomyopathic changes in samples from the myocardium, suggesting that viral persistence may lead to myocardial damage in certain patients with chronic fatigue syndrome.

We therefore studied patients with chronic fatigue syndrome with a combined CMR approach and evaluated the potential cardiac involvement, which is reported in **chapter 8**.

Finally, **chapter 9** provides an overview of LGE-CMR use beyond the applications that are highlighted in chapters 1–8 of this thesis. More specifically, the role of LGE-CMR in non-ischemic cardiomyopathies and other (relatively rare) cardiac diseases are discussed. In addition, we address the future perspective of CMR.

References

(1)   Damadian R, Goldsmith M, Minkoff L. NMR in cancer: XVI. FONAR image of the live human body. Physiol Chem Phys 1977;9:97-100, 108.

(2)   Didier D, Ratib O. Dynamic cardiovascular MRI:Principles and practical examples. Thieme 2003

(3)   Bruder O, Wagner A, Lombardi M et al. European Cardiovascular Magnetic Resonance (EuroCMR) registry--multi national results from 57 centers in 15 countries. J Cardiovasc Magn Reson 2013;15:9.

(4)   Schulz-Menger J, Bluemke DA, Bremerich J et al. Standardized image interpretation and post processing in cardiovascular magnetic resonance: Society for Cardiovascular Magnetic Resonance (SCMR) board of trustees task force on standardized post processing. J Cardiovasc Magn Reson 2013;15:35.

(5)   Pennell DJ, Sechtem UP, Higgins CB et al. Clinical indications for cardiovascular magnetic resonance (CMR): Consensus Panel report. Eur Heart J 2004;25:1940-1965.

(6)   Pilz G, Heer T, Harrer E, Ali E, Hoefling B. Clinical applications of cardiac magnetic resonance imaging. Minerva Cardioangiol 2009;57:299-313.

(7)   Child NM, Das R. Is cardiac magnetic resonance imaging assessment of myocardial viability useful for predicting which patients with impaired ventricles might benefit from revascularization? Interact Cardiovasc Thorac Surg 2012;14:395-398.

(8)   Vogel-Claussen J, Rochitte CE, Wu KC et al. Delayed enhancement MR imaging: utility in myocardial assessment. Radiographics 2006;26:795-810.

(9)   Hsu LY, Natanzon A, Kellman P, Hirsch GA, Aletras AH, Arai AE. Quantitative myocardial infarction on delayed enhancement MRI. Part I: Animal validation of an automated feature analysis and combined thresholding infarct sizing algorithm. J Magn Reson Imaging 2006;23:298-308.

(10) Cerqueira MD, Weissman NJ, Dilsizian V et al. Standardized myocardial segmentation and nomenclature for tomographic imaging of the heart. A statement for healthcare professionals from the Cardiac Imaging Committee of the Council on Clinical Cardiology of the American Heart Association. Circulation 2002;105:539-542.

(11) Roes SD, Kelle S, Kaandorp TA et al. Comparison of myocardial infarct size assessed with contrast-enhanced magnetic resonance imaging and left ventricular function and volumes to predict mortality in patients with healed myocardial infarction. Am J Cardiol 2007;100:930-936.

(12) Murray CJ, Lopez AD. Alternative projections of mortality and disability by cause 1990-2020: Global Burden of Disease Study. Lancet 1997;349:1498-1504.

(13) Erdmann J, Stark K, Esslinger UB et al. Dysfunctional nitric oxide signalling increases risk of myocardial infarction. Nature 2013;504:432-436.

(14) Edelman RR. Contrast-enhanced MR imaging of the heart: overview of the literature. Radiology 2004;232:653-668.

(15) Jennings RB, Ganote CE. Structural changes in myocardium during acute ischemia. Circ Res 1974;35 Suppl 3:156-172.

(16) Thygesen K, Alpert JS, Jaffe AS et al. Third universal definition of myocardial infarction. J Am Coll Cardiol 2012;60:1581-1598.

(17) Bolick DR, Hackel DB, Reimer KA, Ideker RE. Quantitative analysis of myocardial infarct structure in patients with ventricular tachycardia. Circulation 1986;74:1266-1279.

(18) Cardinal R, Vermeulen M, Shenasa M et al. Anisotropic conduction and functional dissociation of ischemic tissue during reentrant ventricular tachycardia in canine myocardial infarction. Circulation 1988;77:1162-1176.

(19) Wu KC, Lima JA. Noninvasive imaging of myocardial viability: current techniques and future developments. Circ Res 2003;93:1146-1158.

(20) Amado LC, Gerber BL, Gupta SN et al. Accurate and objective infarct sizing by contrast-enhanced magnetic resonance imaging in a canine myocardial infarction model. J Am Coll Cardiol 2004;44:2383-2389.

(21) Bello D, Fieno DS, Kim RJ et al. Infarct morphology identifies patients with substrate for sustained ventricular tachycardia. J Am Coll Cardiol 2005;45:1104-1108.

(22) Kim RJ, Wu E, Rafael A et al. The use of contrast-enhanced magnetic resonance imaging to identify reversible myocardial dysfunction. N Engl J Med 2000;343:1445-1453.

(23)   Orn S, Manhenke C, Anand IS et al. Effect of left ventricular scar size, location, and transmurality on left ventricular remodeling with healed myocardial infarction. Am J Cardiol 2007;99:1109-1114.

(24)   Weinsaft JW, Klem I, Judd RM. MRI for the assessment of myocardial viability. Cardiol Clin 2007;25:35-56, v.

(25)   Pascale P, Schlaepfer J, Oddo M, Schaller MD, Vogt P, Fromer M. Ventricular arrhythmia in coronary artery disease: limits of a risk stratification strategy based on the ejection fraction alone and impact of infarct localization. Europace 2009;11:1639-1646.

(26)   Roes SD, Borleffs CJ, van der Geest RJ et al. Infarct tissue heterogeneity assessed with contrast-enhanced MRI predicts spontaneous ventricular arrhythmia in patients with ischemic cardiomyopathy and implantable cardioverter-defibrillator. Circ Cardiovasc Imaging 2009;2:183-190.

(27)   Caforio AL, Mahon NJ, Tona F, McKenna WJ. Circulating cardiac autoantibodies in dilated cardiomyopathy and myocarditis: pathogenetic and clinical significance. Eur J Heart Fail 2002;4:411-417.

(28)   bdel-Aty H, Boye P, Zagrosek A et al. Diagnostic performance of cardiovascular magnetic resonance in patients with suspected acute myocarditis: comparison of different approaches. J Am Coll Cardiol 2005;45:1815-1822.

(29)   Gutberlet M, Spors B, Thoma T et al. Suspected chronic myocarditis at cardiac MR: diagnostic accuracy and association with immunohistologically detected inflammation and viral persistence. Radiology 2008;246:401-409.

(30)   Mahrholdt H, Goedecke C, Wagner A et al. Cardiovascular magnetic resonance assessment of human myocarditis: a comparison to histology and molecular pathology. Circulation 2004;109:1250-1258.

(31)   Mahrholdt H, Wagner A, Deluigi CC et al. Presentation, patterns of myocardial damage, and clinical course of viral myocarditis. Circulation 2006;114:1581-1590.

(32)   Yelgec NS, Dymarkowski S, Ganame J, Bogaert J. Value of MRI in patients with a clinical suspicion of acute myocarditis. Eur Radiol 2007;17:2211-2217.

(33)   Bohl S, Wassmuth R, bdel-Aty H et al. Delayed enhancement cardiac magnetic resonance imaging reveals typical patterns of myocardial injury in patients with various forms of non-ischemic heart disease. Int J Cardiovasc Imaging 2008;24:597-607.

(34)   Debl K, Djavidani B, Buchner S et al. Time course of eosinophilic myocarditis visualized by CMR. J Cardiovasc Magn Reson 2008;10:21.

(35)   Zagrosek A, Wassmuth R, bdel-Aty H, Rudolph A, Dietz R, Schulz-Menger J. Relation between myocardial edema and myocardial mass during the acute and convalescent phase of myocarditis--a CMR study. J Cardiovasc Magn Reson 2008;10:19.

(36)   De CF, Pieroni M, Esposito A et al. Delayed gadolinium-enhanced cardiac magnetic resonance in patients with chronic myocarditis presenting with heart failure or recurrent arrhythmias. J Am Coll Cardiol 2006;47:1649-1654.

Chapter 2

Infarct tissue characteristics of patients with versus without early revascularization for acute myocardial infarction: a contrast-enhancement cardiovascular magnetic resonance imaging study

Olimulder MA, Kraaier K, Galjee MA, Scholten MF, van Es J, Wagenaar LJ, van der Palen J, von Birgelen C.

Abstract

Background: Histopathological studies suggested that early revascularization for acute myocardial infarction (MI) limits size, transmural extent, and homogeneity of myocardial necrosis. However, the long-term effect of early revascularization on infarct tissue characteristics is greatly unknown. Cardiovascular magnetic resonance (CMR) imaging with contrast enhancement (CE) allows non-invasive examination of infarct tissue characteristics and left ventricular (LV) dimensions and function in one examination.

Methods: A total of 69 patients, referred for cardiac evaluation for various clinical reasons, were examined with CE-CMR >1 month (median 6, range 1-213) post-acute MI. We compared patients with (n=33) versus without (n=36) successful early revascularization for acute MI. Cine-CMR measurements included left ventricular (LV) end-diastolic and end-systolic volumes, LV ejection fraction (LVEF,%), and wall motion score index (WMSI). CE images were analyzed for core, peri, and total infarct size (%), and for the number of transmural segments.

Results: In our population, patients with successful early revascularization had better LVEF (46±16 vs.34±14%;P<0.01), superior WMSI (0.53, range 0.00-2.29 vs.1.42, range 0.00-2.59;P<0.01), and smaller end-systolic volumes (121±70 vs.166±82;P=0.02). However, there was no difference in core (9±6 vs. 11±6%), peri (9±4 vs.10±4%), and total infarct size (18±9 vs.21±9%;P>0.05 for all comparisons); only transmural extent (P=0.07) and infarct age (P=0.06) tended to be larger in patients without early revascularization.

Conclusion: CMR wall motion abnormalities are significantly better after revascularization, these differences are particularly marked later after infarction. The difference in scar size is more subtle and does not reach significance in this study.

Introduction

In the setting of an acute myocardial infarction (MI), early revascularization within 6-12 hours by means of primary percutaneous coronary interventions (PCI) reduces the infarct size and improves clinical outcome.[1-4] Post-mortem studies on infarcted hearts previously showed that necrosis was uniform after permanent occlusion of the culprit coronary artery, whereas some myocardium survived in the necrotic region following early revascularizon.[5] While early revascularization may alter infarct morphology by salvage of myocardial cells,[6-8] a significant proportion of patients still develops transmural myocardial necrosis.[9]

Cardiovascular magnetic resonance (CMR) imaging in combination with the contrast enhancement (CE) technique permits detailed noninvasive cardiac assessment of survivors of MI. This technique has the unique capability of studying myocardial tissue characteristics (size, heterogeneity, and transmurality of necrosis) as well as geometry and function of the left ventricle.[10] However, to the best of our knowledge, CE-CMR has not yet been used to assess potential differences in tissue characteristics between patients with versus without early revascularization for acute MI.

Therefore, in a consecutive series of patients with prior MI in whom CE-CMR was performed for clinical reasons, we compared data from patients with versus without early revascularization for acute MI. Based on the findings of previous histopathological studies, we hypothesized that in patients with early revascularization, infarct areas may be smaller, less homogeneous, and less transmural on CE-CMR than in patients without early revascularization.

Methods

Patient population

We conducted this study between October 2007 and January 2010 at Thoraxcentrum Twente in a consecutive series of patients with prior MI, who were referred for cardiac evaluation for various clinical reasons (e.g., viability and/or LV function, residual ischaemia, selection for implantable cardioverter defibrillator therapy). Patients were included in the study if (1) the MI occurred at least one month prior to CMR (according to the definition of a healed MI),[11] (2) complete CE-CMR data were obtained, and (3) a positive infarct pattern of CE was found. To reduce the change of having an impaired function of the LV that was not mainly due to the MI, patients with CMP (i.e idiopathic dilated, hyperthrophic) ore relevant concomitant disease (e.g myocarditis, tachycardiomyopathy) were excluded from this study.

The clinical charts, electrocardiograms (ECG), and angiographies of included MI patients were carefully examined to classify patients into two groups: patients with versus without successful early revascularization. The early revascularization group consisted of patients who underwent successful (vessel patency and/or resolution of ST-segment elevation and relief of symptoms) early

revascularization by means of PCI (in the revascularizatin era) within 12 hours after the start of symptoms.[12] Patients without early revascularization fulfilled at least one of these criteria: (1) (late) presentation of MI > 12 hours after the onset of symptoms, (2) conservative treatment, or (3) failed revascularization procedure (narrowed culprit artery).

CMR data acquisition

CMR examination was performed on a 1.5-T whole body scanner (Achieva Scan, Philips Medical System, Best, the Netherlands) using commercially available cardiac CMR software. For signal-reception a five-element cardiac synergy coil was used. Electrocardiogram triggering was performed with a vector-ECG set-up. Subjects were examined in the supine position. Morphologic images in the multislice cardiac short axis, four chamber long axis, three chamber, and two chamber long axis, and left ventricular outflow tract views were acquired by using fast field echo cine images (slice thickness 8.0mm, repetition time 3.4ms; echo time 1.7ms; flip angle 60°; matrix 256×256). Papillary muscles were regarded as part of the ventricular cavity. Myocardial scar was assessed on CE multislice short- axis, long-axis, and four chamber views, obtained 10 minutes after intravenous bolus injection of 0.2mmol gadolinium/kg body weight (Shering AG, Berlin, Germany). A three-dimensional Turbo Field Echo-inversion recovery T1-weighted sequence was used with the following parameters: repetition time 4.0ms; echo time 1.3ms; flip angle 15°; inversion time individually optimized to null myocardial signal (usually between 180-250ms); matrix 157; and slice thickness 10 mm.

CMR data analysis and definitions

CMR data were analyzed on a workstation using dedicated software for cardiac analysis (Philips MR workspace, Release 2.5.3.0 2007-12-03; Philips, The Netherlands).

LV geometry and function: Left ventricular end-diastolic and end-systolic volumes (EDV and ESV; ml), left ventricular ejection fraction (LVEF; %), and end-diastolic wall mass (EDWM; g) were calculated from contiguous short-axis loops by segmentation of endocardial and epicardial borders on each frame. Papillary muscles were regarded as part of the ventricular cavity. End-diastolic wall thickness (EDWT; mm) at the infarcted wall area was measured quantitatively at the center of the infarct region.[13]

The left ventricular wall regions were further divided into 17 segments according to a standardized myocardial segmentation model.[14] Wall motion of all 17 separate segments was assigned the following scores: normal wall motion was 0, hypokinesia 1, severe hypokinesia 2, akinesia 3, and dyskinesia 4. The wall motion score index (WMSI) was calculated by dividing the sum of scores in each segment by the total number of segments (17 segments). WMSI of 0 was considered as normal, 0-1 as moderate, 1-2 as poor, and >2 as bad.

Infarct tissue characteristics: The infarcted myocardium was defined as the zone of hyper-enhancement on the CE images, in contrast with the dark-gray signal of the normal myocardium. Infarct size was quantified by a semi-automatic thresholding technique with the full width at half-maximum approach as previously validated to maximize accuracy and reproducibility.[15-17] After outlining the myocardial segment containing the region with high signal intensity, the maximum signal intensity region was determined. Scar was divided into an infarct core zone and a heterogeneous zone (i.e., peri infarct zone). Infarct core was then defined as myocardium with a signal intensity ≥ 50% of the maximal signal intensity. The heterogeneous zone was defined as myocardium with a signal intensity between ≥35% and <50% of maximal signal intensity. Total scar was defined as the sum of infarct core plus heterogeneous zone.[18] By use of planimetry, the extent of CE was first determined on contiguous short-axis images, then summed up to a volume, and finally expressed as a percentage of the total myocardial volume.

Scar tissue characteristics were further quantified according to location by use of a 17 segmental model.[14] Each segment was scored as follows: a scar score of 0 was considered as normal, 1 as 1-25% scar, 2 as 26-50% scar, 3 as 51-75% scar, and 4 as 76-100% scar of the segmental area.

The segmental scar score was calculated by dividing the sum of the individual segmental scores by the total number of observed segments. The *transmural extent* of myocardial scar was defined as the number of segments with a scar score 3 or 4. In addition, a segmental *regional scar score* was calculated in order to relate scare size to the territories of the 3 major coronary arteries according as previously described in detail.[14]

Statistical analysis

Continuous variables had a normal distribution and were expressed as mean ± standard deviation (SD). Categorical data were expressed as frequencies and percentages. To compare patients with versus without early revascularization, Student's t-test and Mann-Whitney U test were used to compare continuous variables, and chi-square and Fisher exact test were used to compare categorical variables. P-values <0.05 were considered statistically significant. A post hoc analysis was accomplished in order to assess the difference in infarct size characteristics that could be detected with the available sample size; presented as detectable alternatives. Linear regression was performed to correct for confounding factors.

Results

Study patients

A total of 69 patients (59±11 years old; 56 men) with a median of 6 (range: 1-213) months after acute MI were examined in this study. Almost half of the patients (n=33, 48%) had undergone successful early revascularization by means of PCI. The group of patients without early revascularization (n=36, 52%) consisted of patients with subclinical MI (n=12), late clinical presentation of MI (n=16), or failed revascularization therapy (n=8). All patients with early succesful revascularization demonstrated ST-elevation on the ECG. In patients without early revascularization, 11 patients demonstrated ST-elevation, and 25 patients had q waves on the ECG. Demographics and baseline characteristics did not differ between groups, except for the prevalention of diabetes mellitus (9% vs. 26%; P=0.04) and diuretic usage (33% vs. 58%; P=0.02), which were both more presented in patients without early revascularization. Infarct age did not significantly differ between both subgroups. See also table 1.

Table 1. Patient characteristics

	Overall study population (n=69)	Early revascularization (n=33)	No early revascularization (n=36)	P
Male sex, n	56 (81)	26 (79)	30 (83)	0.43
Age, y	59±11	58±11	58±11	0.53
Hypertension, n	32 (46)	18 (55)	14 (39)	0.13
Diabetes, n	12 (17)	2 (6)	10 (28)	0.02
Alcohol, n	35 (51)	19 (58)	16 (43)	0.40
Current smoking, n	27 (39)	14 (42)	13 (36)	0.69
Medication				
- B-blocker, n	55 (80)	26 (79)	29 (81)	0.52
- Ace inhibitor, n	39 (56)	16 (49)	23 (64)	0.12
- Diuretic, n	33 (48)	11 (33)	21 (58)	0.02
- Statin, n	66 (96)	32 (97)	34 (94)	0.53
Infarct location				0.56
- anterior, n	27 (39)	14 (42)	13 (36)	
- nonanterior, n	30 (43)	16 (48)	14 (39)	
- both, n	12 (18)	3 (10)	9 (25)	
Infarct age*, months	6 (1-213)	5 (1-80)	11 (1-213)	0.06

Continuous data are expressed as mean ± standard deviation or median with range if appropriate; and categorical data as frequencies and percentage. *The group of patients without succesful early revascularization comprised 9 patients with silent MI. As a matter of course, median infarct age was calculated from data of all but these 9 patients.

CMR results

CE-CMR was performed for viability and/or LV function (n=29), selection of implantable cardioverter defibrillator therapy (n=26), residual ischemia (n=5), or other reasons (n=9). No significant difference (P=0.56) between both subgroups according to clinical indication for CMR was found.

LV geometry and function: In the early revascularization group, LVEF was significantly higher (46±16 vs. 34±14%; P=<0.01), WMSI was superior (0.53 (range: 0.00-2.29) vs. 1.42 (range: 0.00-2.59); P=<0.01), ESV was significantly smaller (121±70 vs. 166±82; P=0.02), and EDWT at the infarct centre was larger (5.99±2.98 vs. 4.40±2.27). In addition, in patients with early revascularization, a trend towards a lower LV EDV (210±61 vs. 24073; P=0.07) was found. All cine CMR data are presented in Table 2. Because of the almost significant (p=0.06) difference in infarct age between both groups, we performed a linear regression analysis to see if the difference in LV function (i.e LVEF and WMSI) remained significant after correction for infarct age. This resulted in a non-significant difference in LVEF of 6.5% (p=0.13) and a significant difference in WMSI of 0.38 (p=0.04) between revascularized and non-revascularized patients in favor of the group with early successful revascularization.

Infarct tissue characteristics: There was no significant difference in size of infarct core (9±6 vs. 11±6%; P=0.17; detectable alternative 4), peri-infarct zone (9±4 vs. 10±4%; P=0.34; detectable alternative 3), and total infarct area (18±9 vs. 21±9%; P=0.18; detectable alternative 6); additionally, regional scar scores did not differ between groups. Only the transmural extent of infarction tended to be greater in patients without early revascularization (2.18±1.94 vs. 3.08±2.08; P=0.07). All CE-CMR data are presented in table 3. (Figure 1.)

Table 2. Cine CMR results for patients with versus without early revascularization following MI.

	Overall study population (n=69)	Early revascularization (n=33)	No early revascularization (n=36)	P
LV geometry and function				
EDV, ml	225±68	210±61	240±73	0.07
ESV, ml	145±79	121±70	166±82	0.02
EDWM, g	138±35	133±33	143±36	0.23
LVEF, %	40±16	46±16	34±14	<0.01
WMSI	1.09 (0.00-2.59)	0.53 (0.00-2.29)	1.42 (0.00-2.59)	<0.01
EDWT infarct centre, mm	5.15±2.72	5.99±2.98	4.40±2.27	0.02

Data are presented as mean ± SD or median with range if appropriate. Categorical data are presented as frequencies and percentages. EDV = end diastolic volume, ESV = end systolic volume, EDWM = end diastolic wall mass, LVEF = left ventricular ejection fraction, WMSI = wall motion score index, EDWT = end diastolic wall thickness, PCI = percutaneous coronary intervention.
Data in a subgroup analysis of early revascularization patients performed by PCI (n=33), rather than the combination of PCI and thrombolysis are presented in italic.

Table 3. CE-CMR results for patients with versus without early revascularization following MI.

	Overall study population (n=69)	Early revascularization (n=33)	No early revascularization (n=36)	P
Infarct characteristics				
Infarct size – core, %	10±6	9±6	11±6	0.17
Infarct size – peri, %	10±4	9±4	10±4	0.34
Infarct size – total, %	19±9	18±9	21±8	0.18
Infarct location				
- LAD score	1.14 (0.14-3.00)	1.14 (0.14-2.57)	1.21 (0.14-3.00)	0.51
- RCA score	1.40 (0.20-2.60)	1.20 (0.20-2.60)	1.40 (0.20-2.60)	0.43
- LCX score	0.80 (0.20-2.40)	*0.80 (0.20-2.40)*	0.80 (0.20-2.20)	0.67
Transmural extent	2.61±1.99	2.18±1.94	3.08±2.08	0.07

Data are presented as mean ± SD or median and range. Categorical data are presented as frequencies and percentages. LAD = left anterior descending, RCA = right coronary artery, LCX= left circumflex, PCI = percutaneous coronary intervention.
Data in a subgroup of early revascularization patients with PCI (n=33) rather than the combination of PCI and thrombolysis are presented in italic.
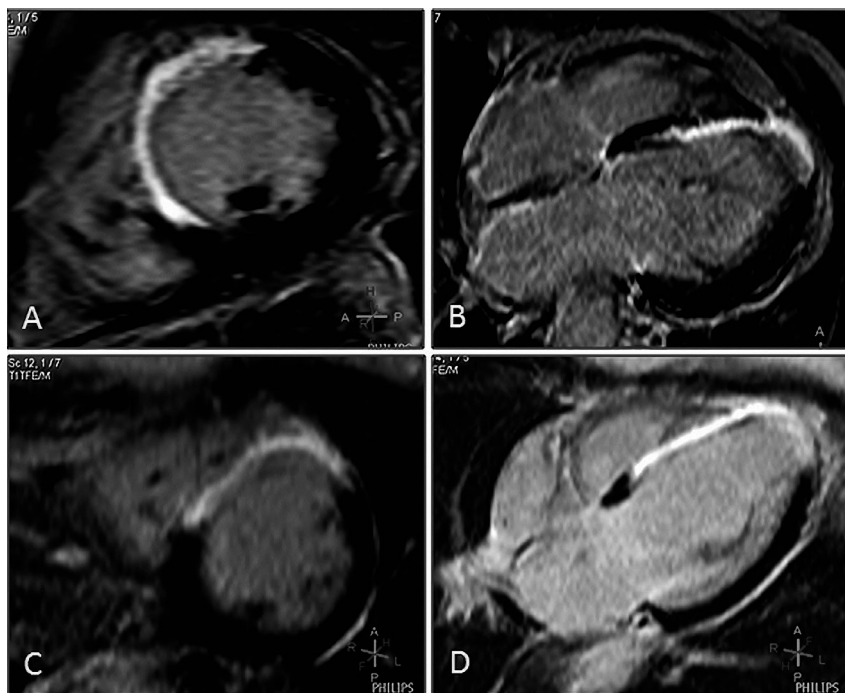
Figure 1. CE-CMR results in a patient with and a patient without early revascularization.
A,B: CE-CMR imaging short axis and four chamber view in an early revascularized patient; presence of transmural CE is observed anteroseptal and apical. **C,D**: CE-CMR imaging short axis view and four chamber view in a patient without early revascularization; presence of transmural CE is observed anteroseptal and apical.

Discussion

To the best of our knowledge, this is the first study to evaluate infarct tissue characteristics in patients with versus without successful early revascularization for acute MI using CE-CMR. The main findings of the present study in patients with vs. without successful early revascularization for acute MI were (I) that in this population infarct tissue characteristics did not differ significantly between groups (only transmural infarction tended to be smaller after early revascularization), while (II) in the latter group LV function (LVEF,WMSI) was significantly worse, and the myocardium at infarct site and LV dimensions were less preserved (i.e., more LV remodelling).

Both study groups showed no significant difference in baseline characteristics except for a higher prevalention of diabetics and a higher diuretic usage in the group of patients without early revascularization. This may actually be expected as diabetics are known to have more silent MI (50% in our population) without the chance to perform an early revascularization therapy,[19] and diuretics are a substitue for severe heart failure, and thus reflect a poor clinical condition caused by LV dysfunction which was significantly more represented in patients without early revascularization.

Revascularization and infarct tissue characteristics

Previous *histopathological postmortem* studies assessed hearts 0-9 days after acute MI to find that permanent occlusion of the culprit coronary artery resulted in a uniform transmural necrosis in the infarcted area, while after early revascularization heterogeneously infarcted tissue was observed.[5;7] Previous *clinical* studies using various non-invasive imaging modalities to evaluate the impact of early revascularization on infarct tissue characteristics reported conflicting results. Compared to our present data, these studies were performed much earlier after an acute MI. The group Schomig et al. found by use of scintigraphy 10-14 days after the index MI no significant relation between time to revascularization and infarct size.[20] However, Schomig et al. also found that following randomly assigned invasive or conservative treatment of patients with acute MI more than 12 hours after symptom onset, invasive treatment still reduced infarct size as determined by scintigraphy.[21] More recently, Francone et al. assessed 3 ± 2 days after the index MI the relation between CE-CMR determined infarct size vs. time-to-revascularization. They found that revascularization ≤90 minutes after the onset of symptoms was associated with a smaller infarct size and a larger area of salvaged myocardium, whereas revascularization >360 minutes after symptom onset was associated with a larger infarct size and a very limited myocardial salvage.[1] Also recently investigated, in a chronic ischemic heart disease population, Heidary et al. recently found no difference in infarct tissue characteristics between patients with medical management only versus patients with previous revascularizations.[22]

Nevertheless, while in our specific study population no significant difference in core, peri and total infarct size was found, total infarct size was 14% smaller in revascularized patients compared to nonrevascularized patients (18% vs 21%) which may actually be of clinical importance. In addition, there was a strong but non-significant trend towards less transmural extent of infarct tissue in favor of early revascularized patients. This is in agreement with the fact that a successful early revascularization reduces in particular the transmural expansion of necrosis from the endocardial to the epicardial myocardium.

Conversely, while ace-inhibitor therapy was initially allocated for higher-risk subgroups patients (i.e. large anterior MI),[23] our findings indirect support recent guidelines that recommend a broad application of ACE-inhibitors post-MI, not only restricted to high-risk patients.[12]

The results in our study population cannot be extrapolated to an "all comers" population. First of all, patients were only selected if there was a clinical indication to perform CE-CMR imaging and if the MI had occurred at least one month prior to CMR. In addition, our study population represents a series of long-term survivors of MI. The median infarct age in our study population was 6 months (range 1-213), whereas previous (histopathological and clinical) studies investigated differences in infarct tissue characteristics no more than half a month after the index MI. In addition, previous histopathological studies examined patients with fatal outcome after very recent MI only. Differences in study design and the inherent selection bias may affect the likelihood of detecting differences in infact size. This may explain differences between the results of the present study and previous histopathological studies (in patients with lethal course of the disease) and clinical studies in other types of patient populations.

During the process of infarct healing, which is generally considered to occur within 1 month after the MI, infarct tissue characteristics may change as a result of replacement of necrotic tissue by scar tissue.[11] Further gradual changes of infarct tissue may occur after this process of infarct healing (i.e. >1 month after MI) in response to residual myocardial ischemia, increased wall stress, arterial hypertension, or medical therapy.[24;25]

Recent data from electro-anatomic mapping in long-term survivors of MI (13±9 years) suggested that infarct tissue characteristics are different in patients with vs. without revascularization during index MI,(24) but these data were obtained in a patient population with documented episodes of sustained monomorphic ventricular tachycardia which represents another significant selection bias.

Revascularization and LV remodelling

Infarct size has been regarded as the primary determinant of LV remodelling and is associated with an adverse left ventricular function.[26-28] A *scintigraphic* study previously investigated the impact of early revascularization on LV remodelling in patients one month after index MI; this study showed following early revascularization a smaller infarct size, smaller LVEDV and LVESV, and a higher LVEF.[29]

In our present study, LV function (i.e. LVEF and WMSI) was also significantly better after successful early revascularization and LV dimensions and wall thickness in the infarct area tended to be more preserved, whereas patients without early revascularization showed a greater extent of remodelling late after the index MI. However, between both groups we found no difference in infarct tissue characteristics as determined with CE-CMR.

Our findings (based on available CE-CMR data of a specific patient population referred for cardiac evaluation for various clinical reasons) may suggest that the process of remodelling >1 month post-MI - especially in patients without early revascularization - is greatly determined by mechanisms that go beyond the extent of infarct size. Potential mechanisms involved may be pressure- and volume overload hypertrophy, compensatory neurohormonal mechanisms, and genetic mechanisms such as adapted gene expression in the setting of heart failure.[30;31] The results of our regression analysis suggest that infarct age should be taken into account when investigating LV (dys)function in patients with previous myocardial infarction.

Our data underline the importance of investigating the various mechanisms that are potentially involved in the process of LV remodelling, both in basic research and in clinical studies.

Limitations

As in most previous CE-CMR studies, sample size was relatively small. Our study population represents long-term survivors of MI. Because of our study design we cannot exclude a certain bias towards patients with a more favorable or fatal clinical course, following MI. But notably, other studies on infarct tissue characteristics which were histopathological studies had other significant selection biases, as they only examined patients following fatal MI. A prospective study design therefore would be ideal to investigate differences in infarct tissue characteristics in patients with versus without successful early revascularization for acute MI using CE-CMR.

Conclusion

CMR wall motion abnormalities are significantly better after revascularization, these differences are particularly marked later after infarction. The difference in scar size is more subtle and does not reach significance in this study.

References

(1)   Francone M, Bucciarelli-Ducci C, Carbone I, Canali E, Scardala R, Calabrese FA, Sardella G, Mancone M, Catalano C, Fedele F, Passariello R, Bogaert J, Agati L (2009) Impact of primary coronary angioplasty delay on myocardial salvage, infarct size, and microvascular damage in patients with ST-segment elevation myocardial infarction: insight from cardiovascular magnetic resonance. J Am Coll Cardiol;54(23):2145-53.

(2)   Fibrinolytic Therapy Trialists' (FTT) Collaborative Group (1994) Indications for fibrinolytic therapy in suspected acute myocardial infarction: collaborative overview of early mortality and major morbidity results from all randomised trials of more than 1000 patients. Lancet;343(8893):311-22.

(3)   Collaborative Group (1993) Randomised trial of late thrombolysis in patients with suspected acute myocardial infarction. EMERAS (Estudio Multicentrico Estreptoquinasa Republicas de America del Sur) . Lancet;342(8874):767-72.

(4)   Feng Y, Shen C, Ma G, Wang J, Chen Z, Dai Q, Zhi H, Yang C, Fu Q, Shang G, Guan Y (2010) Prolonged pain to hospital time is associated with increased plasma advanced oxidation protein products and poor prognosis in patients with percutaneous coronary intervention for ST-elevation myocardial infarction. Heart Vessels;25(5):374-8.

(5)   Matsuda M, Fujiwara H, Onodera T, Tanaka M, Wu DJ, Fujiwara T, Hamashima Y, Kawai C (1987) Quantitative analysis of infarct size, contraction band necrosis, and coagulation necrosis in human autopsied hearts with acute myocardial infarction after treatment with selective intracoronary thrombolysis. Circulation;76(5):981-9.

(6)   Eitel I, Desch S, Sareban M, Fuernau G, Gutberlet M, Schuler G, Thiele H (2009) Prognostic significance and magnetic resonance imaging findings in aborted myocardial infarction after primary angioplasty. Am Heart J;158(5):806-13.

(7)   Karagueuzian HS, Fenoglio JJ, Jr., Weiss MB, Wit AL (1979) Protracted ventricular tachcardia induced by premature stimulation of the canine heart after coronary artery occlusion and reperfusion. Circ Res;44(6):833-46.

(8)   Michelson EL, Spear JF, Moore EN (1980) Electrophysiologic and anatomic correlates of sustained ventricular tachyarrhythmias in a model of chronic myocardial infarction. Am J Cardiol;45(3):583-90.

(9)   O'Regan DP, Ahmed R, Neuwirth C, Tan Y, Durighel G, Hajnal JV, Nadra I, Corbett SJ, Cook SA. (2009) Cardiac MRI of myocardial salvage at the peri-infarct border zones after primary coronary intervention. Am J Physiol Heart Circ Physiol;297(1):H340-H346.

(10)   Friedrich MG (2008) Tissue characterization of acute myocardial infarction and myocarditis by cardiac magnetic resonance. JACC Cardiovasc Imaging;1(5):652-62.

(11)   Thygesen K, Alpert JS, White HD (2007) Universal definition of myocardial infarction. Eur Heart J;28(20):2525-38.

(12)   Van de WF, Bax J, Betriu A, Blomstrom-Lundqvist C, Crea F, Falk V, Filippatos G, Fox K, Huber K, Kastrati A, Rosengren A, Steg PG, Tubaro M, Verheugt F, Weidinger F, Weis M, Vahanian A, Camm J, De CR, Dean V, Dickstein K, Filippatos G, Funck-Brentano C, Hellemans I, Kristensen SD, McGregor K, Sechtem U, Silber S, Tendera M, Widimsky P, Zamorano JL, Aguirre FV, Al Attar N, Alegria E, Andereotti F, Benzer W, Breithardt O, Danchin N, Di Mario C, Dudek D, Gulba D, Halvorsen S, Kaufmann P, Kornowski R, Lip GY, RUtten F (2008) Management of acute myocardial infarction in patients presenting with persistent ST-segment elevation: the Task Force on the Management of ST-Segment Elevation Acute Myocardial Infarction of the European Society of Cardiology. Eur Heart J;29(23):2909-45.

(13)   Roes SD, Kelle S, Kaandorp TA, Kokocinski T, Poldermans D, Lamb HJ, Boersma E, van der Wall EE, Fleck E, de RA, Nagel E, Bax JJ (2007) Comparison of myocardial infarct size assessed with contrast-enhanced magnetic resonance imaging and left ventricular function and volumes to predict mortality in patients with healed myocardial infarction. Am J Cardiol15;100(6):930-6.

(14)   Cerqueira MD, Weissman NJ, Dilsizian V, Jacobs AK, Kaul S, Laskey WK, Pennell DJ, Rumberger JA, Ryan T, Verani MS (2002) Standardized myocardial segmentation and nomenclature for tomographic imaging of the heart: a statement for healthcare professionals from the Cardiac Imaging Committee of the Council on Clinical Cardiology of the American Heart Association. Circulation;105(4):539-42.

(15) Amado LC, Gerber BL, Gupta SN, Rettmann DW, Szarf G, Schock R, Nasir K, Kraitchman DL, Lima JA (2004) Accurate and objective infarct sizing by contrast-enhanced magnetic resonance imaging in a canine myocardial infarction model. J Am Coll Cardiol21;44(12):2383-9.

(16) Bondarenko O, Beek AM, Hofman MB, Kuhl HP, Twisk JW, van Dockum WG, Visser CA, van Rossum AC (2005) Standardizing the definition of hyperenhancement in the quantitative assessment of infarct size and myocardial viability using delayed contrast-enhanced CMR. J Cardiovasc Magn Reson;7(2):481-5.

(17) Beek AM, Bondarenko O, Afsharzada F, van Rossum AC (2009) Quantification of late gadolinium enhanced CMR in viability assessment in chronic ischemic heart disease: a comparison to functional outcome. J Cardiovasc Magn Reson;11(1):6.

(18) Roes SD, Borleffs C, van der Geest RJ, Westenberg JJM, Marsan NA, Kaandorp TAM, Reiber JHC, Zeppenfeld K, Lamb HJ, de Roos A (2009) Infarct Tissue Heterogeneity Assessed With Contrast-Enhanced MRI Predicts Spontaneous Ventricular Arrhythmia in Patients With Ischemic Cardiomyopathy and Implantable Cardioverter-Defibrillator. Circulation: Cardiovascular Imaging;2(3):183.

(19) Kannel WB (1985) Lipids, diabetes, and coronary heart disease: insights from the Framingham Study. Am Heart J;110(5):1100-7.

(20) Schomig A, Ndrepepa G, Mehilli J, Schwaiger M, Schuhlen H, Nekolla S, Pache J, Martinoff S, Bollwein H, Kastrati A (2003) Therapy-dependent influence of time-to-treatment interval on myocardial salvage in patients with acute myocardial infarction treated with coronary artery stenting or thrombolysis. Circulation;108(9):1084-8.

(21) Schomig A, Mehilli J, Antoniucci D, Ndrepepa G, Markwardt C, Di PF, Nekolla SG, Schlotterbeck K, Schuhlen H, Pache J, Seyfarth M, Martinoff S, Benzer W, Schmitt C, Dirschinger J, Schwaiger M, Kastrati A (2005) Mechanical reperfusion in patients with acute myocardial infarction presenting more than 12 hours from symptom onset: a randomized controlled trial. JAMA;293(23):2865-72.

(22) Heidary S, Patel H, Chung J, Yokota H, Gupta SN, Bennett MV, Katikireddy C, Nguyen P, Pauly JM, Terashima M, McConnell MV, Yang PC (2010) Quantitative tissue characterization of infarct core and border zone in patients with ischemic cardiomyopathy by magnetic resonance is associated with future cardiovascular events. J Am Coll Cardiol15;55(24):2762-8.

(23) ACE Inhibitor Myocardial Infarction Collaborative Group (1998) Indications for ACE inhibitors in the early treatment of acute myocardial infarction: systematic overview of individual data from 100,000 patients in randomized trials. Circulation;97(22):2202-12.

(24) Wijnmaalen AP, Schalij MJ, von der Thusen JH, Klautz RJ, Zeppenfeld K (2010) Early Reperfusion During Acute Myocardial Infarction Affects Ventricular Tachycardia Characteristics and the Chronic Electroanatomic and Histological Substrate. Circulation;4;121(17):1881-3

(25) Yokota T, Osanai T, Hanada K, Kushibiki M, Abe N, Oikawa K, Tomita H, Higuma T, Yokoyama J, Hanada H, Okumura K (210) Effects of telmisartan on markers of ventricular remodeling in patients with acute myocardial infarction: comparison with enalapril. Heart Vessels;25(6):460-8

(26) Mollema SA, Liem SS, Suffoletto MS, Bleeker GB, van der Hoeven BL, van d, V, Boersma E, Holman ER, van der Wall EE, Schalij MJ, Gorcsan J, III, Bax JJ (2007) Left ventricular dyssynchrony acutely after myocardial infarction predicts left ventricular remodeling. J Am Coll Cardiol;50(16):1532-40.

(27) Chareonthaitawee P, Christian TF, Hirose K, Gibbons RJ, Rumberger JA (1995) Relation of initial infarct size to extent of left ventricular remodeling in the year after acute myocardial infarction. J Am Coll Cardiol;25(3):567-73.

(28) Tarantini G, Razzolini R, Cacciavillani L, Bilato C, Sarais C, Corbetti F, Marra MP, Napodano M, Ramondo A, Iliceto S (2006) Influence of transmurality, infarct size, and severe microvascular obstruction on left ventricular remodeling and function after primary coronary angioplasty. Am J Cardiol;98(8):1033-40.

(29) Hirayama A, Adachi T, Asada S, Mishima M, Nanto S, Kusuoka H, Yamamoto K, Matsumura Y, Hori M, Inoue M (1993) Late reperfusion for acute myocardial infarction limits the dilatation of left ventricle without the reduction of infarct size. Circulation;88(6):2565-74.

(30) Pfeffer MA, Braunwald E (1990) Ventricular remodeling after myocardial infarction. Experimental observations and clinical implications. Circulation;81(4):1161-72.

(31) Ramos LW, Murad N, Goto E, Antonio EL, Silva JA, Jr., Tucci PF, Carvalho AC (2009) Ischemia/reperfusion is an independent trigger for increasing myocardial content of mRNA B-type natriuretic peptide. Heart Vessels;24(6):454-9.

Chapter 3

Relationship between Infarct tissue characteristics and left ventricular remodeling in patients with versus without early revascularization for acute myocardial infarction as assessed with contrast-enhanced cardiovascular magnetic resonance imaging

Olimulder MA, Galjee MA, Wagenaar LJ,
van Es J, van der Palen J, von Birgelen C.

Abstract

Purpose: Left ventricular (LV) remodeling following myocardial infarction (MI) is the result of complex interactions between various factors, including presence or absence of early revascularization. The impact of early revascularization on the relationship between infarct tissue characteristics and LV remodeling is incompletely known. Therefore, we investigated in patients with versus without succesful early revascularization for acute MI potential relations between infarct tissue characteristics and LV remodeling with contrast-enhanced (CE) cardiovascular magnetic resonance (CMR).

Methods: Patients with versus without successful early revascularization underwent CE-CMR for tissue characterization and assessment of LV remodeling including end-diastolic and end-systolic volumes, LV ejection fraction, and wall motion score index (WMSI). CE-CMR images were analyzed for infarct tissue characteristics including core-, peri- and total-infarct size, transmural extent, and regional scar scores.

Results: In early revascularized patients (n=46), a larger area of infarct tissue correlated significantly with larger LV dimensions and a more reduced LV function (r=0.39-0.68; all p≤0.01). Multivariate analyses identified peri-infarct size as the best predictor of LV remodeling parameters (R2=0.44-0.62). In patients without successful early revascularization (n=47), there was no correlation between infarct area and remodeling parameters; only peri-infarct size versus WMSI (r=0.33;p=0.03) and transmural extent versus LVEF (r=-0.27;p=0.07) tended to be related.

Conclusion: Only in patients with early successful revascularization, a correlation between infarct tissue characteristics and LV remodeling was found. Peri-infarct size was found to be the best determinant of LV remodeling. Our findings stress the importance of taking into account infarct tissue characteristics and success of revascularization when LV remodeling is studied.

Keywords: Early revascularization, Infarct tissue characterization, Left ventricular remodeling, Cardiovascular magnetic resonance imaging.

Introduction

In the initial clinical and postmortem studies of patients with acute myocardial infarction (MI), infarct size was found to predict LV dilatation and functional impairment,[1,2] while the introduction of novel non-invasive imaging techniques provided further insights (e.g. in vivo tissue characterization) and partly contradictory results.[3-9] Discrepancies between observations with different diagnostic techniques may reflect the fact that LV geometry and function after the MI result from a complex interaction of various factors, including successful early revascularization[10] which may limit unfavorable adaptive changes of the myocardium.[11-13] The effect of successful early revascularization on the relationship between infarct tissue characteristics versus LV remodeling is not completely known. While some investigators found significant correlations between infarct tissue characteristics and LV remodeling in patients with succesful early revascularization,[2;4;5;14-16] others found conflicting results in more heterogeneous study populations (Table 1).[3;6;8;9;17-19]

Cardiovascular magnetic resonance (CMR) imaging in combination with the contrast enhancement (CE) technique allows accurate assessment of LV geometry and function as well as tissue characteristics such as size, heterogeneity, and transmurality of the myocardial scar.[20-22] In the present study, we investigated the relation between infarct tissue characteristics and LV remodeling in patients with versus without successful early revascularization in a population of consecutive patients who underwent CE-CMR examination.

Table 1. Literature overview on studies that address the relationships between infarct tissue characteristics and LV remodeling

Study population	Imaging method(s)	Early Revascula-rization	Time between MI and imaging	Correlation IS vs. remodeling	References
1 st MI (n=20)	Radionuclide imaging	+	initial, 6 weeks, 1 year	+	*Christian(2)*
1 st MI (n=20)	Radionucide imaging/CT	+	initial, 6 weeks, 6 months, 1 year	+	*Chareonthai taee(4)*
1 st MI (n=76)	CMR / echocardio-graphy	+	6 ± 2 days 6 ± 1 months	+	*Tarantini(5)*
1 st MI (n=122)	CMR	+	1 week, 4 months	+	*Wu(14)*
1 st MI (n=76)	CMR	+	1 week, > 3 months	+	*Rubenstein(16)*
1 st MI (n=78)	CMR	+	3 months	+	*Pride(15)*
Previous MI (n=86)	CMR	0/-	-	0	*Yokota(6)*
CAD (n=48)	CMR	0/-	Within 32±6 days of EPS	+	*Bello(3)*
Previous MI (n=70)	CMR	0/-	-	0	*Heidary(17)*
1 st MI (12 pigs)	CMR	0/-	4 weeks, 13 weeks	+	*Wu(8)*
1 st MI (n=29)	CMR	0/-	1 week 9 months	+	*Kaandorp(18)*
Previous MI (n=57)	CMR	0/-	4.4 ± 0.4 years	+	*Orn(19)*
Previous MI (n=144)	CMR	0/-	-	+	*Yan(9)*

MI= myocardial infarction, CT= computed tomography, IS= infarct size, CAD=coronary artery disease, CMR=cardiovascular magnetic resonance, NA=not applicable, EPS= electrophysiologic study.
Early revascularization + = patients with successful early revascularization, Early revascularization 0 = patients without successful early revascularization, Early revascularization - = data concerning early revascularization not applicable, or a heterogeneous study population consisting of patients with and without successful early revascularization.

Methods

Patient population

We conducted this study between October 2007 and March 2010 at Thoraxcentrum Twente in consecutive patients with CE-CMR examination for various clinical reasons (e.g. eligibility for coronary artery bypass grafting, selection for implantable cardiac defibrillator therapy) and a

history of MI. Patients were included in the study if (1) the MI occurred at least one month prior to CMR ((according to the definition of a healed MI), therefore, patients with CE-CMR within one month after MI were not included),[23] (2) complete CE-CMR data were obtained, and (3) a positive infarct pattern of CE was found. To reduce the change of having an impaired function of the LV that was not mainly due to the MI, patients with cardiomyopathy (i.e idiopathic dilated, hyperthrophic) and/or other relevant concomitant disease (e.g myocarditis, tachycardiomyopathy) were excluded from this study.

The clinical charts, electrocardiograms, and angiographies of included MI patients were carefully examined to classify patients into two groups: patients with versus without successful early revascularization. The early revascularization group consisted of patients who underwent successful (vessel patency and/or resolution of ST-segment elevation and symptoms) early revascularization (percutaneous coronary intervention or thrombolysis in the thrombolytic era) within 12 hours after the start of symptoms.[24] Patients without early revascularization fulfilled at least one of these criteria: (1) presentation of MI > 12 hours after the onset of symptoms, (2) conservative treatment, or (3) failed revascularization procedure (narrowed culprit artery).

CMR data acquisition

CMR examination was performed on a 1.5-T whole body scanner (Achieva Scan, Philips Medical System, Best, Netherlands) using commercially available cardiac CMR software. For signal-reception a five-element cardiac synergy coil was used. Electrocardiogram triggering was performed with a vector-electrocardiogram set-up. Subjects were examined in the supine position. Cine (morphologic) images in the cardiac short-axis, four chamber, three chamber, and two chamber long-axis, and left ventricular outflow tract views were acquired by using fast field echo cine images (slice thickness 8.0mm, repetition time 3.4ms; echo time 1.7ms; flip angle 60°; matrix 256×256). Myocardial scar was assessed on CE multislice short- axis, two chamber long-axis, and four chamber long-axis views, obtained approximately 10 minutes after intravenous bolus injection of 0.1 mmol gadolinium/kg body weight (Dotarem 0.5 mmol/ml). A three-dimensional Turbo Field Echo-inversion recovery T1-weighted sequence was used with the following parameters: repetition time 4.0ms; echo time 1.3ms; flip angle 15°; inversion time individually optimized to null myocardial signal (usually between 180-250ms); matrix 157; and slice thickness 10 mm.

CMR data analysis and definitions

CMR data were analyzed on a workstation using dedicated software for cardiac analysis (Philips MR workspace, Release 2.5.3.0 2007-12-03; Philips, The Netherlands).

LV geometry and function: Left ventricular end-diastolic and end-systolic volumes; ml, left ventricular ejection fraction (LVEF; %), and end-diastolic wall mass; g were calculated from contiguous short-axis loops by segmentation of endocardial and epicardial borders on each frame. Papillary muscles were regarded as part of the ventricular cavity.

The left ventricular wall regions were further divided into 17 segments according to a standardized myocardial segmentation model. Wall motion was assigned the following scores: normal wall motion was 0, hyokinesia 1, severe hypokinesia 2, akinesia 3, and dyskinesia 4. The wall motion score index (WMSI) was calculated by dividing the sum of scores in each segment by the total number of segments (17 segments). WMSI of 0 was considered as normal, 0-1 as moderate, 1-2 as poor, and >2 as bad.

Infarct tissue characteristics: The infarcted myocardium was defined as the zone of hyper-enhancement on the CE images, in contrast with the dark-gray signal of the normal myocardium. As it was shown that pathological assessment of infarct size can be better approximated by the use of the full width at half maximum criteria than simple intensity thresholding based on the standard deviation of normal myocardial signal intensities, we used this semi-automatic thresholding technique to measure infarct size.[25] After outlining the myocardial segment containing the region with high signal intensity, the maximum signal intensity region was determined. Scar was divided into an infarct core zone and a heterogeneous zone (i.e. peri-infarct zone). Infarct core was then defined as myocardium with a signal intensity ≥50% of the maximal signal intensity. The heterogeneous zone was defined as myocardium with a signal intensity ≥35% of the maximal signal intensity and <50% of maximal signal intensity.[21] Total scar was defined as the sum of infarct core plus heterogeneous zone (figure 1). By the use of planimetry, the extent of CE was first determined on contiguous short-axis images, then summed up to a volume, and finally expressed as a percentage of the total myocardial volume.

Scar tissue characteristics were further quantified according to localization by use of a 17 segmental model.[26] Each segment was scored as follows: a scar score of 0 was considered as normal, 1 as 1-25% scar, 2 as 25-50% scar, 3 as 50-75% scar, and 4 as 75-100% scar.

The *transmural extent* of myocardial scar was defined as the number of segments with a scar score 3 or 4. In addition, a segmental *regional scar score* was calculated in order to relate scar size to the territories of the 3 major coronary arteries (i.e. left anterior descending, left circumflex, and right coronary artery according as previously described in detail.[26]
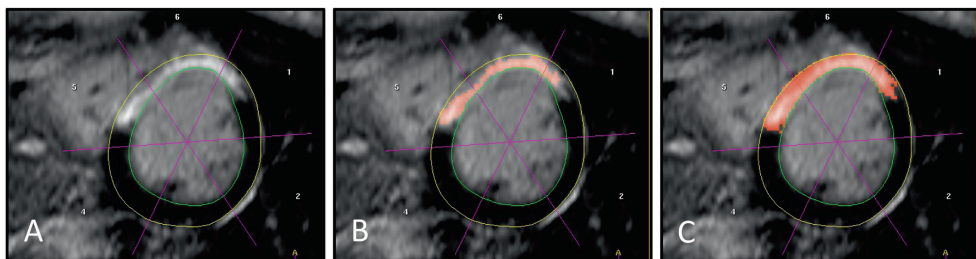
Figure 1. Assessment of myocardial infarct size.
A: myocardial scar colors white 10 minutes after administration of contrast agent and is representative for the infarction area. **B**: the infarct core zone is defined as all pixels in the myocardium with a signal intensity greater then or 50% of the maximal SI (orange in B). The peri infarct zone is defined as all pixels with a SI in the range of greater then or 35% and<50%. **C**: total infarct size is then the summation of both core and peri infarct zone (orange in C).

Statistical analysis

Continuous variables were presented as mean±SD; categorical data were summarized as frequencies and percentages. Differences in baseline characteristics between patients with versus without early revascularization were analyzed using Student's t-test and Mann-Whitney U test, as appropriate, if continuous, or chi-square or Fisher exact test if categorical. A P value <0.05 was considered statistically significant.

Univariable and multivariable linear regression models were constructed to study the relationship between infarct tissue characteristics and parameters of LV remodeling in subgroups of patients with prior MI with successful early revascularization versus without successful early revascularization. Univariate correlations were calculated using Spearman's rho or Pearson's correlation, as appropriate. Because of the large number of data- correlations performed in a relatively low number of patients and the presence of interrelationships, a P value ≤0.01 was considered as statistically significant. Only infarct tissue characteristics that appeared to be associated with parameters of LV remodeling at P<0.10 in univariate analysis were included in the multivariate analyses then. Total infarct size and peri-infarct size, as well as total infarct size and core-infarct size however, could not be included simultaneously in one multivariable linear regression model because these variables were strongly interrelated (Pearson correlation, 0.90; P<0.01 and 0.95; P<0.01). Therefore, separate multivariate models were constructed to determine the strongest predictor of LV remodelig. While no statistical difference was found due to variation of infarct age in each group, the median of infarct age was substantially different between early revascularization group (6 months) and no early revascularization group (37 months). Infarct age was therefore also incorporated when assessing the relation between infarct size and LV remodeling.

Regression coefficients (β) in the multivariate model reflected the estimated changes in LV remodeling outcome parameters. A priori we expected a difference in the relationship between infarct tissue characteristics and LV remodeling according to the success of early revascularization. Therefore, in all multivariate analyses, effect modification by revascularization status was formally tested by adding revascularization status as an interaction term. When effect modification was present, analyses were presented for early successful revascularization separately.

Results

Study patients

From October 2007 to March 2010 1004 patients underwent CE-CMR. A total of f 93 patients (61±11 years old; 77 men) with a median of 11 (range: 1-425) months after MI were examined in this study. Almost half of the patients (n=46, 49%) had undergone successful early revascularization by means of percutaneous coronary intervention (n= 33) or intravenous thrombolysis (n=13).

Patients without early revascularization (n=47, 51%) suffered from silent MI (n=22), had a late presentation >12 hours after onset of symptoms (n=16), or failed revascularization therapy (n=9). There was no significant difference in infarct age (time between onset of MI and CMR imgaging) between both groups. All patients with early successful revascularization demonstrated ST-elevation on the ECG. In patients without early revascularization, 15 patients demonstrated ST-elevation, and 32 patients had q waves on the ECG. Demographics and baseline characteristics did not significantly differ between groups. See also Table 2.

Table 2. Patient characteristics

	All patients (n=93)	Early revascularization (n=46)	No early revascularization (n=47)	P
Male sex, n	77 (83)	37 (80)	40 (85)	0.59
Age, y	61±11	60±10	61±11	0.55
Hypertension, n	42 (45)	22 (48)	20 (42)	0.67
Diabetes, n	16 (17)	4 (9)	12 (26)	0.08
Alcohol, n	43 (46)	23 (50)	20 (43)	0.68
Current smoking, n	36 (39)	19 (41)	17 (37)	
Medication				
- B-blocker, n	74 (80)	37 (80)	37 (79)	1.00
- Ace inhibitor, n	56 (60)	25 (54)	31 (66)	0.29
- Diuretic, n	46 (49)	19 (41)	27 (57)	0.14
- Statin, n	85 (91)	43 (93)	42 (89)	1.00
Infarct localization				0.82
- anterior, n	31	17	14	
- nonanterior, n	47	24	23	
- both, n	15	5	10	
Infarct age, m	11 (1-425)	6 (1-361)	37 (1-425)	0.31

Continuous data are expressed as mean ± standard deviation or median with range if appropriate; and categorical data as frequencies and percentage.

CMR results

LV geometry and function: In the early revascularization group, LV geometry (i.e. LV dimensions and mass) tended to be more preserved, (P=0.05-0.12) and LV function (i.e. LVEF and WMSI) was significantly better (P<0.05) (Table 3).

Infarct tissue characteristics: There were no significant differences with respect to core-, peri-, and total infarct size, as well as transmural extent and regional scar scores of the MI (P0.19-0.84). (Table 4).

Table 3. Cine CMR results for patients with versus without early revascularization during acute MI.

	Overall study population (n=93)	Early Revascularization (n =46)	No early revascularization (n=47)	P
LV geometry and function				
EDV, ml	240±76	226±68	255±81	0.07
ESV, ml	162±86	144±79	180±90	0.045
EDWM, g	139±33	134±32	145±34	0.12
LVEF, %	36±16	40±18	33±13	0.03
WMSI	1.26±0.79	1.09±0.86	1.43±0.69	0.04

Continuous data are expressed as mean ± standard deviation or median with range if appropriate; and categorical data as frequencies and percentage. EDV = end-diastolic volume, ESV = end-systolic volume, EDWM = end-diastolic wall mass, LVEF = left ventricular ejection fraction, WMSI = wall motion score index.

Table 4. CE CMR results for patients with versus without early revascularization during acute MI

	Overall study population (n=93)	Early Revascularization (n =46)	No early revascularization (n=47)	P
Infarct characteristics				
Infarct size – core, %	10±6	10±7	10±6	0.78
Infarct size – peri, %	10±4	10±4	10±4	0.84
Infarct size – total, %	20±9	20±10	20±9	0.79
Infarct localization				
- LAD score	1.00 (0.14-3.00)	1.00 (0.14-2.71)	1.00 (0.14-3.00)	0.58
- RCA score	1.40±0.77	1.30±0.72	1.51±0.81	0.19
- LCX score	1.28±0.87	1.26±0.89	1.30±0.87	0.85
Transmural extent	2.97±2.20	2.67±2.09	3.27±2.29	0.20

Data are presented as mean ± SD or median with range if appropriate. Categorical data are presented as frequencies and percentages. LAD = left anterior descending, RCA = right coronary artery, LCX= left circumflex.

Infarct tissue characteristics and relation with LV dimensions and function

Because of a significant interaction of revascularization status for the outcome parameters end-systolic volume(p=0.04) and LVEF (p=0.02), and a near significant interaction for end-diastolic volume (p=0.07) and WMSI (p=0.07), the results were presented separately for patients with versus without succesful early revascularization.

In univariate models, in patients with successful early revascularization, infarct tissue characteristics (i.e. core-, peri-, and total infarct size, transmural extent, left anterior descending location) correlated significantly with all parameters of cardiac remodeling (i.e.LV dimensions, mass, LVEF and WMSI) (r=0.39-0.68; p≤0.01) (Table 5 and Figure 2). The strongest significant

relationship between total infarct size and LVEF (r=-0.79) was observed in a subgroup of patients (n=10) with infarct size ≥15%.

No such correlations between infarct tissue characteristics and LV remodeling were observed in patients without early revascularization except for a weak but nonsignificant correlation between peri- infarct size versus WMSI (r=0.33; p=0.03) and transmural extent versus LVEF (r=-0.27; p=0.07). Table 5 and Figure 2.

Table 5. Univariate correlations between infarct tissue characteristics and LV remodeling in patients with (n=46) and without early revascularization (n=47)

	Successful early revascularization / *No early revascualarization*							
Variable	EDV, ml		ESV, ml		LVEF,%		WMSI	
Infarct size - core, %	r=0.51 P=<0.01	*r=-0.14 P=0.36*	r=0.60 P=<0.01	*r=-0.97 P=0.52*	r=-0.63 P=<0.01	*r=-0.13 P=0.37*	r=0.56 P=<0.01	*r=0.13 P=0.41*
Infarct size - peri, %	r=0.62 P=<0.01	*r=0.15 P=0.31*	r=0.68 P=<0.01	*r=0.18 P=0.22*	r=-0.63 P=<0.01	*r=-0.26 P=0.16*	r=0.63 P=<0.01	*r=0.33 P=0.03*
Infarct size - total, %	r=0.59 P=<0.01	*r=-0.03 P=0.87*	r=0.68 P=<0.01	*r=0.02 P=0.92*	r=-0.68 P=<0.01	*r=-0.21 P=0.16*	r=0.63 P=<0.01	*r=0.23 P=0.12*
Transmural extent	r=0.39 P=0.01	*r=0.09 P=0.54*	r=0.44 P=<0.01	*r=0.11 P=0.47*	r=-0.46 P=<0.01	*r=-0.27 P=0.07*	r=0.43 P=0.01	*r=0.24 P=0.11*
LAD score	r=0.44 P=<0.01	*r=0.02 P=0.92*	r=0.49 P=<0.01	*r=0.09 P=0.58*	r=-0.51 P=<0.01	*r=-0.16 P=0.31*	r=0.41 P=<0.01	*r=0.19 P=0.22*
RCA score	r=-0.03 P=0.83	*r=0.14 P=0.38*	r=-0.26 P=0.87	*r=0.16 P=0.34*	r=0.01 P=0.94	*r=-0.12 P=0.48*	r=-0.11 P=0.95	*r=0.11 P=0.51*
LCX score	r=0.15 P=0.38	*r=0.14 P=0.43*	r=0.20 P=0.26	*r=0.05 P=0.79*	r=-0.23 P=0.19	*r=-0.02 P=0.91*	r=0.24 P=0.16	*r=-0.06 P=0.72*

Data in the subgroup of patients without early revascularization (n=47) are presented in italic. EDV = end diastolic volume, ESV = end-systolic volume, EDWM = end-diastolic wall mass, LVEF = left ventricular ejection fraction, WMSI = wall motion score index, LAD = left anterior descending, RCA = right coronary artery, LCX= left circumflex.
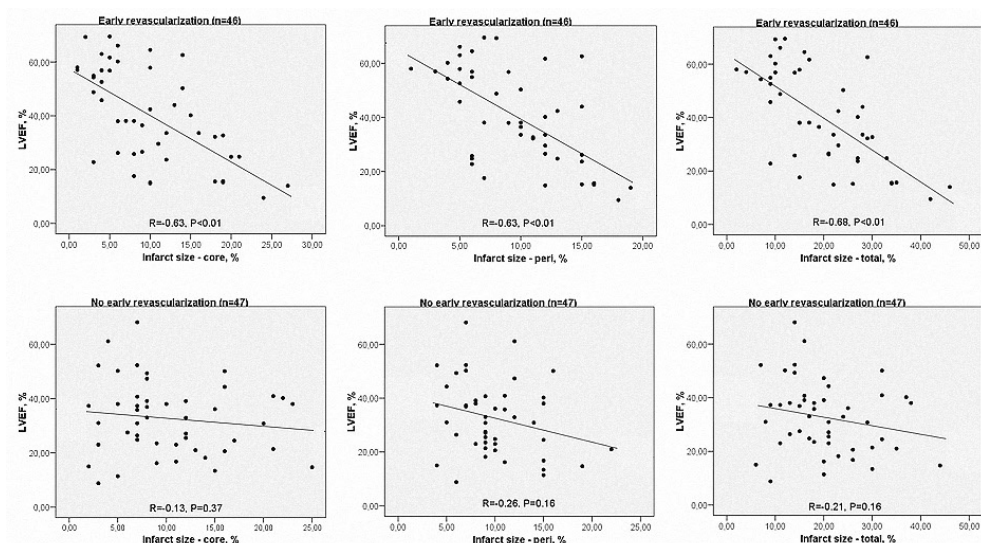
Figure 2. Univariate correlations between parameters of LV remodeling and infarct tissue characteristics in patients with (n=46) versus patients without (n=47) early revascularization.
LVEF= left ventricular ejection fraction, r= correlation coefficient

Multivariate regression analyses in patients with early revascularization identified peri- infarct size as the most important predictor of parameters of LV remodeling (i.e. end-diastolic volume, end-systolic volume, LVEF and WMSI) (R^2= 0.44-0.62). See also Table 6.

We also assessed relationships in a subgroup of patients with an infarct age >3 and ≤24 months, while the process of remodeling continues beyond >1 month after MI, whereas other factors can affect the relationship with an increasing infarct age. In patients with successful early revascularization (n=21), infarct tissue characteristics (i.e., core-, peri-, and total infarct size,) correlated significantly with parameters of cardiac remodeling (i.e. LVEF and end-systolic volume) (r=0.48-0.66). No significant correlations between infarct tissue characteristics and LV remodeling were observed in the subgroup of patients without early revascularization (n=10).

Table 6. Multivariate regression analysis for prediction of LV remodeling in patients with successful early revascularization (n=46) *

Variable	EDV, ml			ESV, ml			LVEF, %			WMSI		
	ß	R^2	P	ß	R^2	P	ß	R^2	P	ß	R^2	P
Infarct size – core, %	0.19		0.94	1.70		0.46	-0.68		0.17	0.01		0.68
Infarct size – peri, %	8.06	0.44	<0.01	9.25	0.59	<0.01	-1.41	0.62	0.02	0.08	0.53	0.02
Transmural extent	-0.94		0.88	-2.99		0.62	0.62		0.62	0.01		0.85
LAD score	21.77		0.09	26.23		0.04	-6.62		0.02	0.28		0.06

* Analyses were corrected for infarct age. ß = Regression coefficients, R^2 = explained variance EDV = end-diastolic volume, ESV = end-systolic volume, LVEF = left ventricular ejection fraction, WMSI = wall motion score index, LAD-left anterior descending.

Discussion

The main finding of the present study is that only in the subgroup of MI patients with successful early revascularization a larger area of infarct tissue was related to larger LV dimension and a more reduced LV function, with peri-infarct size being the best determinant of LV remodeling. The LAD score tended to predict remodeling.

Peri-infarct zone as predictor of LV remodeling
With the introduction of CE-CMR assessed tissue characterization , a more quantitative evaluation of the infarcted myocardium can be performed by analyzing the size of the infarct core and border zone (i.e. peri-infarct zone). There is increasing interest in quantification of this peri-infarct zone because (mechanical) characteristics of this area may serve as a substrate for life-threatening ventricular arrhythmia.[9;21;22;27] According to Yan et al., identification of a distinct infarct core and border zone may also provide prognostic insights into post-MI remodeling.[9] However, most previous CE-CMR studies that investigated the relationship between infarct size and cardiac remodeling did not measure the size of the peri- infarct zone.[2-6;8;9;14-16;18;19] The only exception was a study by Heidary et al.,[17] who found in a population of patients with ischemic cardiomyopathy no significant relation between infarct tissue characteristics (including peri-infarct size) and both LV geometry and function.

The definition of peri-infarct zone or heterogeneous zone is still controversial. Center-dependent, several formulas have been used and described, which can be used to analyze infarct tissue characteristics including the heterogeneous zone, while there is currently no consensus on a definite gold standard. We used a formula in which infarct tissue characteristics are defined based on the maximum signal intensity of the infarct area (in accordance with Roes et al. and Schmidt et al.),[21;22] whereas others use a formula in which infarct tissue characteristics are defined as having a signal intensity >2 SD (up to >6 SD) above the signal intensity of a normal area of interest (e.g. Bello et al).[3] With current clinically applied CE-CMR technology, spatial resolution imposes constraints on what type of tissue is concealed within the peri-infarct zone, characterized by intermediate signal intensities. High-resolution CE-CMR imaging with 1000-fold higher resolution than clinical scans, may bear the potential to obtain further insights.

The population of the present study consisted of long-term survivors of MI. In the subgroup of our patients with early revascularization, multivariate regression analysis identified the peri-infarct size as the most important predictor of LV remodeling. A similar multivariable model with total infarct size instead of peri-infarct size demonstrated nearly simular results, whereas core-infarct size in this model was not an important predictor of LV remodeling. Therefore, it may be assumed that total infarct size as predictor of LV remodeling is mainly attributed to the peri-infarct size.

Recent studies have indicated that biophysical and neurohormonal characteristics within this peri-infarct zone may contribute to the process of LV remodeling.[27-29] Our findings suggest that CE-CMR examination of the heterogeneity of the infarct zone may provide valuable insights into the process of LV remodeling.

Effect of early revascularization on correlation infarct characteristics and LV remodeling
Our observation, that there is a significant correlation between infarct tissue size and LV remodeling only in patients with successful early revascularization, corresponds with earlier studies that reported similar relations in patients with successful early revascularization for MI.[2;4;5;14-16]

In our study population, the strongest relationship between total infarct size and LVEF (r=-0.79, p<0.01) was found in early revascularized patients (n=10) with an infarct size ≥15% of the LV mass. This was also recently shown by Pride et al., who found a similar relationship in MI patients with an infarct size ≥ 15% (r=-0.81, p<0.001).[15]

The absence of a significant relationship between infarct size and LV remodeling in our MI population without early revascularization is consistent with the findings of previous post-MI studies with heterogeneous populations regarding early revascularization.[3;6;8;9;17-19] Our finding and the results of these studies may imply that in patients without early revascularization LV remodeling is mainly dependent on factors beyond infarct tissue characteristics. Such factors include persistent or recurrent ischaemia, pressure and volume overload hypertrophy, neurohormonal and biophysical factors, and genetic mechanisms such as adapted gene expression in the setting of heart failure.[10;28;30-35] Thus, based on our findings, we emphasize the importance of taking into account the success of early revascularization when investigating the various mechanisms that are involved in the process of LV remodeling, both in experimental and clinical studies.

Limitations

Our study population represents long-term survivors of MI which has the potential risk of selecting patients with a more favorable clinical course. Therefore, large prospective studies, in which also the impact of multivessel disease and residual ischaemia has to be investigated, are necessary to confirm our results.

Conclusion

Only in patients with early successful revascularization, a correlation between infarct tissue characteristics and LV remodeling was found. Peri-infarct size was found to be the best determinant of LV remodeling. Our findings stress the importance of taking into account the infarct tissue characteristics and success of revascularization when LV remodeling is studied.

References

(1)   Pfeffer MA, Pfeffer JM, Fishbein MC, Fletcher PJ, Spadaro J, Kloner RA, Braunwald E. Myocardial infarct size and ventricular function in rats. Circ Res 1979;44:503-12.

(2)   Christian TF, Behrenbeck T, Gersh BJ, Gibbons RJ. Relation of left ventricular volume and function over one year after acute myocardial infarction to infarct size determined by technetium-99m sestamibi. Am J Cardiol 1991;68:21-6.

(3)   Bello D, Fieno DS, Kim RJ, Pereles FS, Passman R, Song G, Kadish AH et al. Infarct morphology identifies patients with substrate for sustained ventricular tachycardia. J Am Coll Cardiol 2005;45:1104-8.

(4)   Chareonthaitawee P, Christian TF, Hirose K, Gibbons RJ, Rumberger JA. Relation of initial infarct size to extent of left ventricular remodeling in the year after acute myocardial infarction. J Am Coll Cardiol 1995;25:567-73.

(5)   Tarantini G, Razzolini R, Cacciavillani L, Bilato C, Sarais C, Corbetti F, Marra MP, et al. Influence of transmurality, infarct size, and severe microvascular obstruction on left ventricular remodeling and function after primary coronary angioplasty. Am J Cardiol 2006;98:1033-40.

(6)   Yokota H, Heidary S, Katikireddy CK, Nguyen P, Pauly JM, McConnell MV, Yang PC. Quantitative characterization of myocardial infarction by cardiovascular magnetic resonance predicts future cardiovascular events in patients with ischemic cardiomyopathy. J Cardiovasc Magn Reson 2008;10:17.

(7)   Chareonthaitawee P, Christian TF, Miller TD, Hodge DO, Gibbons RJ. Correlation of resting first-pass left ventricular ejection fraction and resting myocardial infarct size. Am J Cardiol 1998;81:1281-5.

(8)   Wu Y, Chan CW, Nicholls JM, Liao S, Tse HF, Wu EX. MR study of the effect of infarct size and location on left ventricular functional and microstructural alterations in porcine models. J Magn Reson Imaging 2009;29:305-12.

(9)   Yan AT, Shayne AJ, Brown KA, Gupta SN, Chan CW, Luu TM, Di Carli MF, et al. Characterization of the peri-infarct zone by contrast-enhanced cardiac magnetic resonance imaging is a powerful predictor of post-myocardial infarction mortality. Circulation 2006;114:32-9.

(10)   Pfeffer MA, Braunwald E. Ventricular remodeling after myocardial infarction. Experimental observations and clinical implications. Circulation 1990;81:1161-72.

(11)   Eitel I, Desch S, Sareban M, Fuernau G, Gutberlet M, Schuler G, Thiele H. Prognostic significance and magnetic resonance imaging findings in aborted myocardial infarction after primary angioplasty. Am Heart J 2009;158:806-13.

(12)   Karagueuzian HS, Fenoglio JJ, Jr., Weiss MB, Wit AL. Protracted ventricular tachcardia induced by premature stimulation of the canine heart after coronary artery occlusion and reperfusion. Circ Res 1979;44:833-46.

(13)   Michelson EL, Spear JF, Moore EN. Electrophysiologic and anatomic correlates of sustained ventricular tachyarrhythmias in a model of chronic myocardial infarction. Am J Cardiol 1980;45:583-90.

(14)   Wu E, Ortiz JT, Tejedor P, Lee DC, Bucciarelli-Ducci C, Kansal P, Carr JC, et al. Infarct size by contrast enhanced cardiac magnetic resonance is a stronger predictor of outcomes than left ventricular ejection fraction or end-systolic volume index: prospective cohort study. Heart 2008;94:730-6.

(15)   Pride YB, Giuseffi JL, Mohanavelu S, Harrigan CJ, Manning WJ, Gibson CM, Appelbaum E. Relation between infarct size in ST-segment elevation myocardial infarction treated successfully by percutaneous coronary intervention and left ventricular ejection fraction three months after the infarct. Am J Cardiol 2010;106:635-40.

(16)   Rubenstein JC, Ortiz JT, Wu E, Kadish A, Passman R, Bonow RO, Goldberger JJ. The use of periinfarct contrast-enhanced cardiac magnetic resonance imaging for the prediction of late postmyocardial infarction ventricular dysfunction. Am Heart J 2008;156:498-505.

(17)   Heidary S, Patel H, Chung J, Yokota H, Gupta SN, Bennett MV, Katikireddy C, et al. Quantitative tissue characterization of infarct core and border zone in patients with ischemic cardiomyopathy by magnetic resonance is associated with future cardiovascular events. J Am Coll Cardiol 2010;55:2762-8.

(18)   Kaandorp TA, Lamb HJ, Viergever EP, Poldermans D, Boersma E, van der Wall EE, de RA, et al. Scar tissue on contrast-enhanced MRI predicts left ventricular remodelling after acute infarction. Heart 2007;93:375-6.

(19) Orn S, Manhenke C, Anand IS, Squire I, Nagel E, Edvardsen T, Dickstein K. Effect of left ventricular scar size, location, and transmurality on left ventricular remodeling with healed myocardial infarction. Am J Cardiol 2007;99:1109-14.

(20) Baks T, van Geuns RJ, Biagini E, Wielopolski P, Mollet NR, Cademartiri F, van der Giessen WJ, et al. Effects of primary angioplasty for acute myocardial infarction on early and late infarct size and left ventricular wall characteristics. J Am Coll Cardiol 2006;47:40-4.

(21) Roes SD, Borleffs C, van der Geest RJ, Westenberg JJM, Marsan NA, Kaandorp TAM, Reiber JHC, et al. Infarct Tissue Heterogeneity Assessed With Contrast-Enhanced MRI Predicts Spontaneous Ventricular Arrhythmia in Patients With Ischemic Cardiomyopathy and Implantable Cardioverter-Defibrillator. Circulation: Cardiovascular Imaging 2009;2:183.

(22) Schmidt A, Azevedo CF, Cheng A, Gupta SN, Bluemke DA, Foo TK, Gerstenblith G, et al. Infarct tissue heterogeneity by magnetic resonance imaging identifies enhanced cardiac arrhythmia susceptibility in patients with left ventricular dysfunction. Circulation 2007;115:2006-14.

(23) Thygesen K, Alpert JS, White HD. Universal definition of myocardial infarction. Eur Heart J 2007;28:2525-38.

(24) Van de Werf, Bax J, Betriu A, Blomstrom-Lundqvist C, Crea F, Falk V, Filippatos G, et al. Management of acute myocardial infarction in patients presenting with persistent ST-segment elevation: the Task Force on the Management of ST-Segment Elevation Acute Myocardial Infarction of the European Society of Cardiology. Eur Heart J 2008;29:2909-45.

(25) Hsu LY, Natanzon A, Kellman P, Hirsch GA, Aletras AH, Arai AE. Quantitative myocardial infarction on delayed enhancement MRI. Part I: Animal validation of an automated feature analysis and combined thresholding infarct sizing algorithm. J Magn Reson Imaging 2006;23:298-308.

(26) Cerqueira MD, Weissman NJ, Dilsizian V, Jacobs AK, Kaul S, Laskey WK, Pennell DJ, et al. Standardized myocardial segmentation and nomenclature for tomographic imaging of the heart: a statement for healthcare professionals from the Cardiac Imaging Committee of the Council on Clinical Cardiology of the American Heart Association. Circulation 2002;105(4):539-42.

(27) Inoue Y, Yang X, Nagao M, Higashino H, Hosokawa K, Kido T, Kurata A, et al. Peri-infarct dysfunction in post-myocardial infarction: assessment of 3-T tagged and late enhancement MRI. Eur Radiol 2010;20(5):1139-48.

(28) Dixon JA, Spinale FG. Pathophysiology of myocardial injury and remodeling: implications for molecular imaging. J Nucl Med 2010;51 Suppl 1:102S-106S. Epub;%2010 Apr 15.:102S-6S.

(29) Nishioka T, Onishi K, Shimojo N, Nagano Y, Matsusaka H, Ikeuchi M, Ide T, et al. Tenascin-C may aggravate left ventricular remodeling and function after myocardial infarction in mice. Am J Physiol Heart Circ Physiol 2010;298:1072-1078.

(30) Bogaert J, Bosmans H, Maes A, Suetens P, Marchal G, Rademakers FE. Remote myocardial dysfunction after acute anterior myocardial infarction: impact of left ventricular shape on regional function: a magnetic resonance myocardial tagging study. J Am Coll Cardiol 2000;35:1525-34.

(31) Boyle MP, Weisman HF. Limitation of infarct expansion and ventricular remodeling by late reperfusion. Study of time course and mechanism in a rat model. Circulation 1993;88:2872-83.

(32) Cohn JN, Ferrari R, Sharpe N. Cardiac remodeling--concepts and clinical implications: a consensus paper from an international forum on cardiac remodeling. Behalf of an International Forum on Cardiac Remodeling. J Am Coll Cardiol 2000;35:569-82.

(33) Larose E, Rodes-Cabau J, Pibarot P, Rinfret S, Proulx G, Nguyen CM, Dery JP, et al. Predicting late myocardial recovery and outcomes in the early hours of ST-segment elevation myocardial infarction traditional measures compared with microvascular obstruction, salvaged myocardium, and necrosis characteristics by cardiovascular magnetic resonance. J Am Coll Cardiol 2010 June 1;55(22):2459-69.

(34) Tarantini G, Napodano M, Gasparetto N, Favaretto E, Marra MP, Cacciavillani L, Bilato C, et al. Impact of multivessel coronary artery disease on early ischemic injury, late clinical outcome, and remodeling in patients with acute myocardial infarction treated by primary coronary angioplasty. Coron Artery Dis 2010;21:78-86.

(35) Ugander M, Ekmehag B, Arheden H. The relationship between left ventricular ejection fraction and infarct size assessed by MRI. Scand Cardiovasc J 2008;42:137-45.
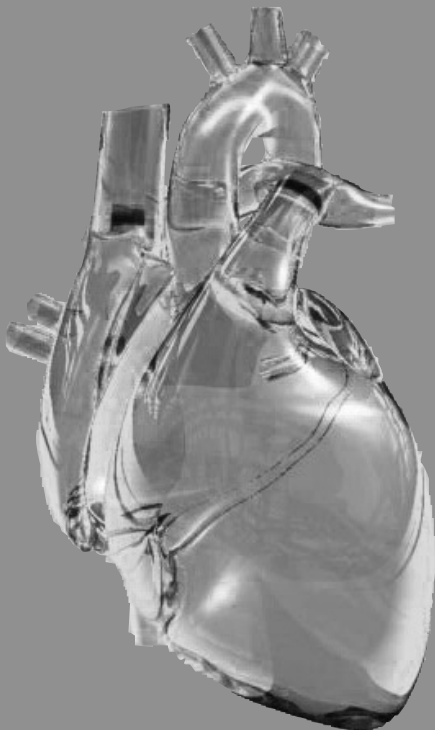
Chapter 4

Relationship between Framingham Risk Score and left ventricular remodeling after successful primary percutaneous coronary intervention in patients with first myocardial infarction and single-vessel disease

Olimulder MA, Galjee MA, van Es J, Wagenaar LJ, Stoel MG, van Houwelingen GK, Louwerenburg HW, de Man FH, van der Palen J, von Birgelen C.

Abstract

Background: Limited data is available on the potential value of estimated cardiovascular event risk for prediction of left ventricular (LV) remodeling and size of infarcted tissue after ST-elevation myocardial infarction (STEMI).

Methods: Therefore, we assessed in a consecutive series of patients with first STEMI, successful primary percutaneous coronary intervention (PCI), and single-vessel disease the potential relationship between the Framingham Risk Score and parameters of both LV remodeling and infarct tissue characteristics, as determined with contrast-enhanced (CE) cardiovascular magnetic resonance (CMR) 6 months after the index event. Parameters of LV remodeling were end-diastolic and end-systolic volumes, ejection fraction, and wall motion score index; infarct tissue characteristics comprised core, peri, and total infarct size, and transmural extent.

Results: A total of 25 patients (21 men, 56±10 years) were studied, and the mean Framingham Risk Score was 14.1±5.8%. There was a significant relation between Framingham Risk Score and multiple parameters of LV remodeling: LV ejection fraction, end-diastolic volume, end-systolic volume, and wall motion score index after 6 months (r=-0.55-0.76;p=0.000 for all). Framingham Risk Score showed no relation with various infarct tissue characteristics (ns). Male gender was the only component of the Framingham Risk Score that correlated *individually* with a few parameters of LV remodeling: LV end-diastolic volume and end-systolic volume (p=0.000 for both).

Conclusion: In a series of consecutive patients with first STEMI, successful primary PCI, and single-vessel coronary artery disease, we observed a significant relation between the Framingham Risk Score and several CMR-based parameters of LV remodeling.
The results of our small hypothesis-generating study underline the supremacy of multifactorial risk scores as tools for prediction of unfavorable cardiovascular outcome. Additionally, the data support the hypothesis that there might be a future role for a *novel and specific* multifactorial risk score in predicting unfavorable LV remodeling*,* which finally could trigger risk-adjusted preventive measures.

Introduction

Major determinants of poor outcome following ST-elevation myocardial infarction (STEMI) are, left ventricular (LV) remodeling, as well as size, location, transmurality, and heterogeneity of the infarcted tissue as assessed by (histo)pathologic analyses.[1;2] The best strategy to limit LV remodeling and infarct size is a successful early revascularization of the culprit artery.[3](3) In addition, chronic medical therapy has been shown to reduce the extent of LV remodeling during follow-up.[4-6] Both LV remodeling and infarct tissue characteristics can be assessed with cardiovascular magnetic resonance (CMR) imaging in combination with the contrast enhancement (CE) technique.[7-10] There is no such thing as a "single cause" of LV remodeling, which can even be observed following successful revascularization procedures. In fact, there is growing evidence that multiple factors are involved in the process of LV remodeling,[2;11-16] and for that reason there is increasing interest in the impact of various cardiovascular risk factors on LV remodeling.[17;18] Identification of patients with a particularly high risk of developing LV remodeling is warranted, as it may represent a first step towards further targeted treatment of patients at risk. It has recently been shown that the Framingham Risk Score, an established cardiovascular event risk score for primary prevention,[19] predicts the likelihood of certain adaptive changes in LV structure and function during lifetime within a general population.[20] Therefore, we hypothesized that the Framingham Risk Score may also be related to LV remodeling and/or tissue characteristics following STEMI. We used CE-CMR in a consecutive series of patients with first STEMI, successful primary percutaneous coronary intervention (PCI), and single-vessel disease to assess the potential relationship between the Framingham Risk Score and parameters of LV remodeling and infarct tissue characteristics at 6-month follow-up.

Methods

Study population. Patients were included from March 2009 until December 2011. Patients were selected from a larger database of patients (n=36) with a MI in which remodeling after MI was investigated with a six-months CMR follow up. Of these 36 patients, 26 had one-vessel disease; one patient was excluded because of blurred CE-images. Patients met the following inclusion criteria: (1) STEMI with successful early revascularization within 12 hours after the start of symptoms and TIMI 3 flow at the end of the procedure, defined as complete perfusion (normal flow which fills the distal coronary bed completely), (2) single-vessel disease at coronary angiogram (only patients with single-vessel disease were assessed in order to investigate a homogeneous patient population without potential confounding ischemia that could otherwise have been caused by coronary lesions in non-culprit vessels), (3) complete CE-CMR data available 6 months after STEMI. After PCI, all patients were treated according to the present guidelines

with acetylsalicylic clopidogrel, betablocker, ACE-inhibitor, and statin (unless contra-indicated). This study complied with the Declaration of Helsinki for investigation in human beings and was approved by the institutional ethics committee of Medisch Spectrum Twente and the Dutch Central Committee on Research Involving Human Subjects. All patients provided informed written consent for participation in this study.

For all patients, traditional cardiovascular risk factors and laboratory results were recorded at the time of the index MI: sex, age, systolic and diastolic blood pressure, (hypertension defined as systolic pressure > 140 mm Hg and/or diastolic pressure > 90 mm Hg), total cholesterol level, serum high density lipoproteins (HDL) cholesterol level, serum low density lipoprotein cholesterol level, triglyceride level, current smoking, family history for coronary artery disease (MI of first-degree family member <60 years of age), diabetes mellitus (known diabetes or repeated fasting glucose levels >120 mg/dl), hypercholesterolemia (medication dependent, total serum cholesterol >200 mg/dl, or low density lipoprotein cholesterol >160 mg/dl). Current cardiovascular medication was also recorded.

The cardiovascular event risk was calculated using the Framingham Risk Score. The Framingham score was calculated by use of an algorithm previously described.(19) The score considers sex, age, total cholesterol, HDL cholesterol, systolic blood pressure, and smoking. It was used to predict the 10-year risk of cardiovascular events (fatal/non-fatal MI or sudden death).

CMR examination was performed on a 1.5-T whole body scanner (Achieva Scan, Philips Medical System, Best, the Netherlands) using commercially available cardiac CMR software. For signal-reception a five-element cardiac synergy coil was used. Electrocardiogram triggering was performed with a vector-electrocardiogram set-up. Subjects were examined in the supine position. Cine (morphologic) images in the cardiac short-axis, four-chamber, three-chamber, and two-chamber long axis, and LV outflow tract views were acquired by using fast field echo cine images (slice thickness 8.0mm, repetition time 3.4ms; echo time 1.7ms; flip angle 60°; matrix 256×256). Myocardial scar was assessed on CE multislice short- axis, two-chamber long-axis, and four-chamber views, obtained approximately 10 minutes after intravenous bolus injection of 0.2 mmol gadolinium/kg-1 body weight (Shering AG, Berlin, Germany). A three-dimensional Turbo Field Echo-inversion recovery T1-weighted sequence was used with the following parameters: repetition time 4.0 ms; echo time 1.3 ms; flip angle 15°; inversion time individually optimized to null myocardial signal (usually between 180-250 ms); matrix 157; and slice thickness 10 mm. CMR data were analyzed on a workstation, using dedicated software for cardiac analysis (Philips MR workspace, Release 2.5.3.0 2007-12-03; Philips, the Netherlands).

LV geometry and function: LV end-diastolic and end-systolic volumes (mL), LV ejection fraction (%), and end-diastolic wall mass (g) were calculated from contiguous short-axis loops by segmentation of endocardial and epicardial borders on each frame. Papillary muscles were regarded as part of the ventricular cavity. The LV wall regions were further divided into 17 segments according to a standardized myocardial segmentation model. Wall motion was assigned the following scores:

normal wall motion was 0, mild hypokinesia 1, severe hypokinesia 2, akinesia 3, and dyskinesia 4. The wall motion score index was calculated by dividing the sum of scores in each segment by the total number of observed segments.[9]

Infarct tissue characteristics: The infarcted myocardium was defined as the zone of hyper-enhancement on the CE images, in contrast with the dark-gray signal of the normal myocardium. We used a semi-automatic thresholding technique, in which infarct size was approximated by use of the full width at half maximum criteria.[21] After outlining the myocardial segment containing the region with high signal intensity, the maximum signal intensity region was determined. Scar was divided into an infarct core zone and a heterogeneous zone (i.e. peri-infarct zone). Infarct core was then defined as myocardium with a signal intensity ≥50% of the maximal signal intensity. The heterogeneous zone was defined as myocardium with a signal intensity ≥35% of the maximal signal intensity and <50% of maximal signal intensity.[21] Total scar was defined as the sum of infarct core plus heterogeneous zone. By use of planimetry, the extent of CE was first determined on contiguous short-axis images, then summed up to a volume, and finally expressed as a percentage of the total myocardial volume.

Scar tissue characteristics were further quantified according to localization by use of a 17 segmental model. Each segment was scored as follows: a scar score of 0 (0% of segmental myocardial volume is scarred) was considered as normal, 1 as 1-25% scar, 2 as 26-50% scar, 3 as 51-75% scar, and 4 as 76-100% scar.[22] The *transmural extent* of myocardial scar was defined as the number of segments with a scar score 3 or 4. See also figure 1. which represents one of the study patients who fulfilled a complete CE-CMR examination.

Statistical analyses were performed with SPSS 15.0 (SPSS INC., Chicago IL, USA). Dichotomous variables are presented as frequencies and percentages. Quantitative data are presented as mean ± SD. Correlations between the Framingham risk score (or individual parameters of the risk score) and CE-CMR imaging parameters were calculated using Spearman's rho or Pearson correlations. A two-sided p-value <0.05 was considered significant.
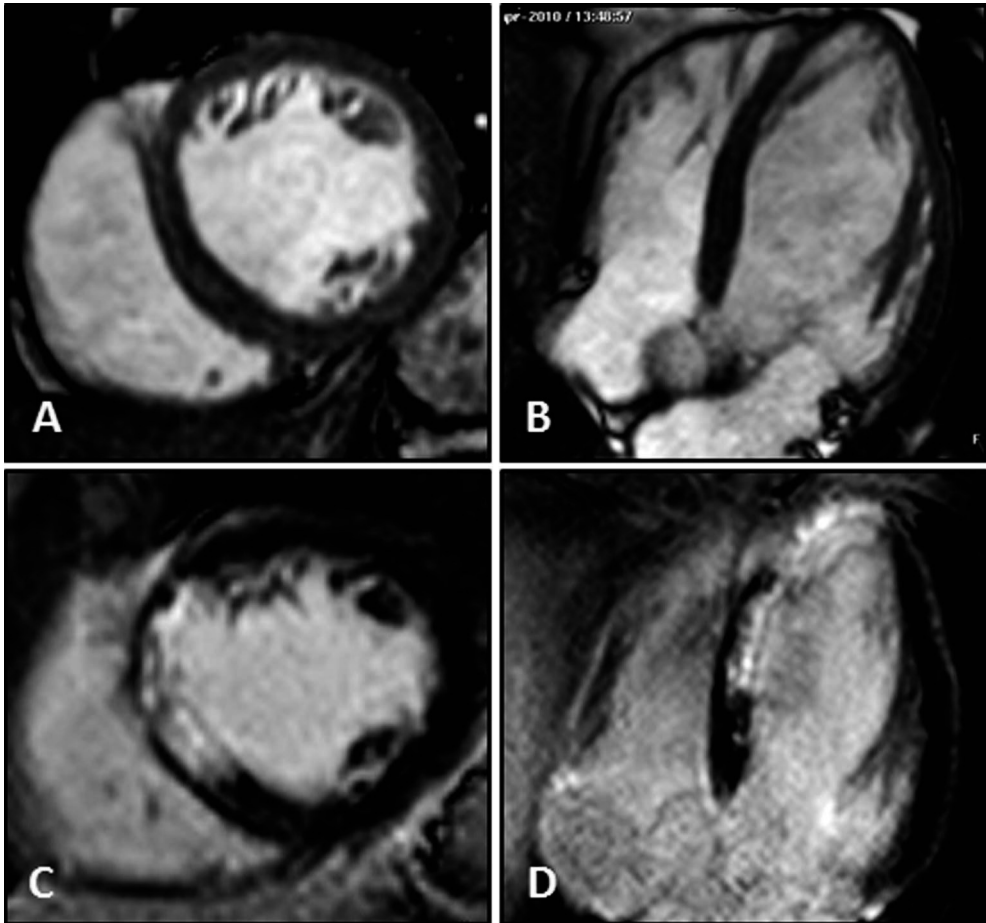
Figure 1. Example of cine- and CE-CMR images of a STEMI patient at the 6 month follow-up. Example of a patient with a Framingham Risk Score of 17.57%, LVEF 55%, and total infarct size 12%. **A, B**: Cine short-axis and four-chamber image; on this images parameters of remodeling are assessed. **C, D**: Short-axis and four-chamber image with contrast enhancement in the anteroseptal, inferoseptal, and apical region; on this images extent of infarction is assessed.

Results

A total of 25 patients with single-vessel disease (age 56±10 years; 21 men) were examined in this study. All patients demonstrated ST-elevation on the electrocardiogram; none of the patients had electrocardiographic signs of LV hypertrophy. All patients had undergone successful early revascularization by means of primary PCI in 9 left anterior descending, 3 left circumflex, and 13 right coronary arteries as the culprit vessel. Baseline patient characteristics are shown in Table 1. *Data on LV geometry and function after 6 months*: LV ejection fraction was 56±9%, wall motion

score index was 0.34±0.26, end-diastolic volume was 195±44mL, and end-systolic volume was 89±39mL. The *infarct tissue characteristics* core, peri, total infarct size, and transmural extent were 5.7±3.8%, 7.2±4.4%, 12.9±7.7%, and 2.1±2.0, respectively.

Table 1. Patient baseline characteristics.

	All patients (n=25)
Male sex	21 (84%)
Age (years)	56±10
Hypertension	10 (40%)
- Systolic blood pressure (mmHg)	137±23
- Diastolic blood pressure (mmHg)	78±13
Diabetes	2 (8%)
Hypercholesterolemia (mmol/l)	4 (16%)
- Total cholesterol	5.6±0.9
- HDL cholesterol	1.4±1.3
- LDL cholesterol	3.6±1.0
- Triglycerides	2.0±1.5
Current smoking	10 (40%)
Positive family history of CAD	16 (64%)
Cardiovascular medication at admission	
- Betablocker	1 (4%)
- Calcium antagonist	1 (4%)
- Ace-/Angiontension inhibitor	0 (0%)
- Statin	2 (8%)
- Diuretic	1 (4%)
Culprit lesion	
- LAD	9 (36%)
- LCX	3 (12%)
- RCA	13 (52%)
Time to revascularization (hours)	3.7±1.5
CK max (U/l)	1026 (176-8074)
LV hypertrophy on ECG	0 (0%)
Infarct age (months)	5.6±0.6
Framingham Risk Score	14.1±5.8

Continuous data are expressed as mean ± standard deviation or median with range if appropriate; and categorical data as frequencies and percentage. HDL = high density lipoprotein, LDL = low density lipoprotein, CAD = coronary artery disease, LAD = left anterior descending, LCX = left circumflex, RCA = right coronary artery, CK = creatine kinase, LV = left ventricle, ECG = electrocardiogram.

The Framingham Risk Score was 14.1±5.8%. There was a significant relation between the Framingham risk score versus left ventricular ejection fraction (r=-0.76; p=0.000), end-diastolic volume, (r=0.70; p=0.000), end-systolic volume (r=0.76; p=0.000), and WMSI (r=0.54; p=0.000; Figure 2). Even after excluding a single outlier, there were still significant relationships between the Framingham risk score versus parameters of remodeling (r=0.55-0.66; p=0.000). No significant correlations were observed between the Framingham risk score versus various CE-

CMR tissue characteristics. There were significant relations between the Framingham risk score and various parameters of LV remodeling (left ventricular ejection fraction, wall motion score index, end-diastolic volume, and end-systolic volume). When assessing the potential relation between individual risk factors as components of the Framingham risk versus LV remodeling, only male gender was related with a greater extent of LV remodeling (i.e. larger end-diastolic and end-systolic volumes; p=0.000 for both, Table 2). In addition, current smoking showed a significant relation with transmural extent of scar (p=0.04, Table 2).
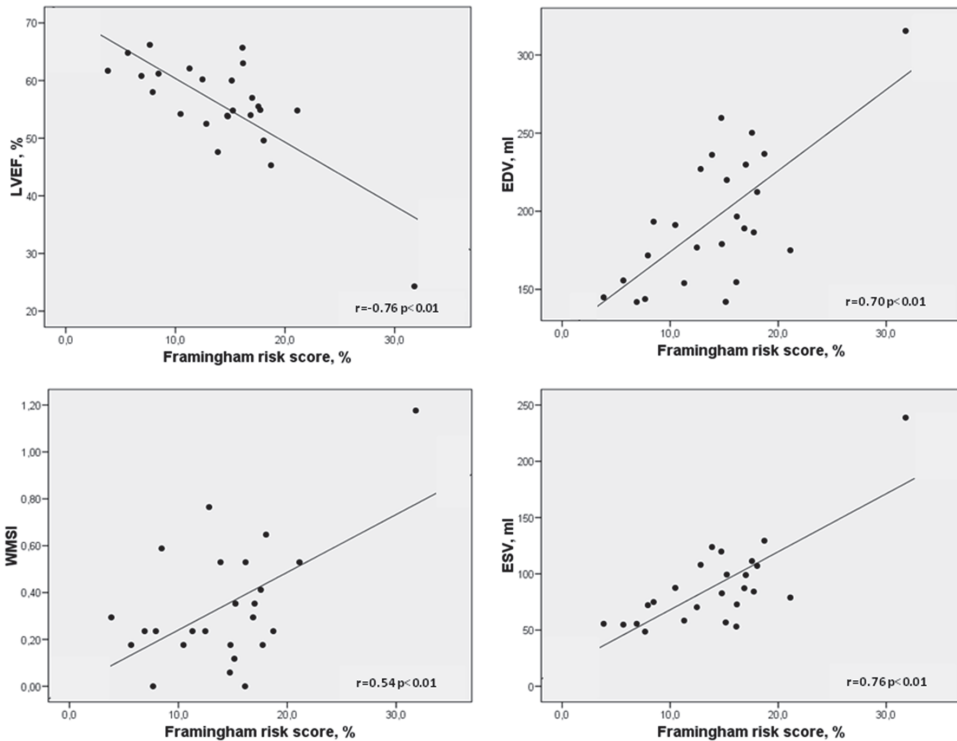
Figure 2. Univariate correlations between parameters of LV remodeling 6 months after STEMI versus the Framingham Risk Score

Table 2. Correlations between individual risk factors versus parameters of LV remodeling and infarct tissue characteristics.

Framingham Risk Score parameters	LVEF%	WMSI	EDV,mL	ESV,mL	Infarct size core, %	Infarct size peri, %	Infarct size total, %	Trans-mural extent
Male sex	p=0.13	p=0.27	p=0.000	p=0.000	p=0.28	p=0.48	p=0.34	p=0.26
Age	r=-0.25; p=0.23	r=0.10; p=0.63	r=0.16; p=0.45	r=0.22; p=0.29	r=-0.13; p=0.55	r=-0.11; p=0.60	r=-0.13; p=0.55	r=-0.19; p=0.36
Total cholesterol	r=-0.29; p=0.16	r=0.17; p=0.41	r=0.14; p=0.50	r=0.20; p=0.34	r=-0.13; p=0.54	r=0.16; p=0.45	r=0.16; p=0.45	r=0.26; p=0.20
HDL-cholesterol, mmol/l	r=-0.07; p=0.73	r=0.18; p=0.38	r=-0.11; p=0.60	r=-0.04; p=0.84	r=-0.10; p=0.96	r=-0.02; p=0.92	r=-0.02; p=0.94	r=-0.06; p=0.77
Systolic blood pressure, mmHg	r=-0.19; p=0.36	r=0.20; p=0.33	r=0.20; p=0.35	r=0.20; p=0.35	r=-0.33; p=0.53	r=-0.22; p=0.30	r=-0.19; p=0.36	r=-0.13; p=0.55
Diabetes Mellitus	r=0.36; p=0.73	r=0.33; p=0.59	r=0.35; p=0.91	r=0.35; p=0.99	r=0.53; p=0.41	r=0.30; p=0.37	r=0.36; p=0.36	r=0.55; p=0.96
Current smoking	p=0.58	p=0.76	p=0.77	p=0.56	p=0.10	p=0.09	p=0.09	p=0.04
LV hypertrophy on ECG	NA	NA	NA	NA	NA	NA	NA	NA

HDL=high density lipoprotein, ECG=electrocardiogram, LVEF=left ventricular ejection fraction, WMSI=wall motion score index, EDV=end-diastolic volume, ESV=end-systolic volume, NA=not applicable.

Discussion

In this relatively small but homogeneous series of consecutive patients with first STEMI, successful primary PCI, and single-vessel coronary artery disease, we observed a significant relation between the Framingham Risk Score and several parameters of LV remodeling as assessed with CE-CMR six months after the event. Of the individual risk factors that form the Framingham Risk Score, only male gender was individually related to some CE-CMR parameters that indicate LV remodeling. This may be explained by the fact that the process of LV remodeling is multifactorial, which is better reflected by a comprehensive risk score than by a single, individual risk factor. Nevertheless, the individual risk factor male gender has contributed to the calculated risk score and to the significant relations observed between the Framingham Risk Score and CE-CMR parameters of LV remodeling following acute MI.

In the present study, many patients suffered from arterial hypertension. Nevertheless, only a minority of them was on antihypertensive drugs as many of these patients had been symptom-free prior to the STEMI and their arterial hypertension had been undetected. During follow-up, all patients were treated according to current guidelines, which included the prescription of a betablocker and an ACE inhibitor.

In our study, women had a more favorable course of LV remodeling following STEMI, which could be related to gender differences in levels of sex hormones.[23] Cavasin et al. have demonstrated that estrogen and testosterone play different and opposing roles in the development of heart failure and long-term LV remodeling following MI. In particular, high testosterone levels enhance acute myocardial inflammation, and adversely affect myocardial healing and early remodeling, which may result in worsening LV function following MI.[24;25] In addition, we cannot completely exclude that gender differences in normal LV end-diastolic and end-systolic volumes (with generally higher LV volumes in men, as was earlier reported by others)[18] may to some extent have exaggerated the outcome of a favorable post-STEMI course of LV dimensions in women.

Other studies also reported relations between cardiovascular risk factors and LV remodeling.[17;26-28] Kenchaiah et al. found hypertension to be associated with subsequent LV dilatation following acute MI.[26] However, that study investigated only MI patients with LV dysfunction (i.e. ejection fraction ≤ 40%), whereas in our study of consecutive first MI patients with single-vessel disease the LV ejection fraction was on average preserved, which may explain the difference in findings of both studies. In our study, no relation was found between age and parameters of remodeling. This is in contrast with an echocardiography-based study by Carabba et al., who found a relation with age, as acute MI patients ≥ 70 years had a higher prevalence of LV remodeling than younger patients. [17]

In the absence of a validated risk score for secondary prevention, established primary-event risk scores have already been used to assess the relations between predicted cardiovascular risk and (1) the extent of plaque progression as assessed with serial intravascular ultrasound,[29] and (2)

the extent of coronary calcifications in patients with a first MI.[30] Notably, in the latter study by Pohle et al., which also investigated patients with a first MI, the estimated 10-year event risk as calculated by the Framingham Risk Score (14.3±4.4%) was similar to that of our study (14.1±5.8% ((i.e. <10%; low risk, 10-20%; intermediate, and >=20%; high risk)).

Our present study also assessed potential relationships between the Framingham Risk Score and various infarct tissue characteristics as determined by CE-CMR 6 months after a first STEMI, but we found no such relation. Only smoking as an individual risk factor correlated with a single infarct tissue parameter – the transmural extent of infarction. Similar to our finding, Todt et al. also previously reported a relation between smoking and infarct size.[28]

Conflicting results were reported regarding the question of whether individual risk factors other than smoking might affect the size of infarct tissue characteristics. As in the present study, other groups previously demonstrated the absence of a relation between both total cholesterol and arterial hypertension versus infarct size.[26;27] In our study population, there were only two diabetic patients, which actually prevents meaningful analyses of this risk factor, but Donnino et al. recently found no difference in the extent of mycardial scar between diabetics and non-diabetic patients.[31] On the other hand, Mather et al. recently observed with CE-CMR that MI patients with hyperglycemia or diabetes mellitus had larger infarct sizes than normoglycemic patients.[18]

In clinical practice, the prediction of unfavorable LV remodeling remains difficult, while there is much interest in this field.[2;11-16;32] The results of our small hypothesis-generating study underline the supremacy of multifactorial risk scores as tools for the prediction of unfavorable cardiovascular outcome. In addition, the data support the hypothesis that there might be a future role for a *novel and specific* multifactorial risk score in predicting unfavorable LV remodeling*, which finally could trigger risk-adjusted preventive measures. Nevertheless, such risk sore could only be derived from data of prospective studies with longer-term follow-up of a much larger patient population than assessed in our present study.

Limitations

The study population is relatively small and the findings should be considered as hypothesis generating. Nevertheless, the population is very homogeneous as it consists only of patients with first STEMI, single-vessel disease, and a complete CMR examination including the assessment of CE. In the absence of a generally accepted, validated risk score for secondary prevention, we used the Framingham-algorithm that was initially developed for risk estimation in the context of primary prevention(19) and predicts both fatal and non-fatal adverse cardiovascular events, which we felt to be most appropriate for the assessment of potential relations with LV remodeling. The high number of the relationships examined may have inreased the likelihood of finding a statistically significant relation due to chance. On the other hand, significant relationships were already found with a relatively small-sized but homogeneous study population.

Conclusions

In a series of consecutive patients with first STEMI, successful primary PCI, and single-vessel coronary artery disease, we observed a significant relation between the Framingham Risk Score and several parameters of LV remodeling, as assessed by CMR.

References

(1) Burns RJ, Gibbons RJ, Yi Q, Roberts RS, Miller TD, et al. (2002) The relationships of left ventricular ejection fraction, end-systolic volume index and infarct size to six-month mortality after hospital discharge following myocardial infarction treated by thrombolysis. J Am Coll Cardiol 39:30-6.

(2) Pfeffer MA, Pfeffer JM, Fishbein MC, Fletcher PJ, Spadaro J, et al. (1979) Myocardial infarct size and ventricular function in rats. Circ Res 44:503-12.

(3) Kloner RA, Rezkalla SH (2004) Cardiac protection during acute myocardial infarction: where do we stand in 2004? J Am Coll Cardiol 44:276-86.

(4) Lee SH, Yoon SB, Cho JR, Choi S, Jung JH, et al. (2008) The effects of different beta-blockers on left-ventricular volume and function after primary coronary stenting in acute myocardial infarction. Angiology 59:676-81.

(5) St John SM, Pfeffer MA, Plappert T, Rouleau JL, Moye LA, et al. (1994) Quantitative two-dimensional echocardiographic measurements are major predictors of adverse cardiovascular events after acute myocardial infarction. The protective effects of captopril. Circulation 89:68-75.

(6) Doughty RN, Whalley GA, Walsh HA, Gamble GD, Lopez-Sendon J, et al. (2004) Effects of carvedilol on left ventricular remodeling after acute myocardial infarction: the CAPRICORN Echo Substudy. Circulation 109:201-6.

(7) Friedrich MG (2008) Tissue characterization of acute myocardial infarction and myocarditis by cardiac magnetic resonance. JACC Cardiovasc Imaging 1:652-62.

(8) Roes SD, Kelle S, Kaandorp TA, Kokocinski T, Poldermans D, et al. (2007) Comparison of myocardial infarct size assessed with contrast-enhanced magnetic resonance imaging and left ventricular function and volumes to predict mortality in patients with healed myocardial infarction. Am J Cardiol 15:930-6.

(9) Olimulder MA, Galjee MA, Wagenaar LJ, van Es J, van der Palen J, et al. (2012) Relationship between infarct tissue characteristics and left ventricular remodeling in patients with versus without early revascularization for acute myocardial infarction as assessed with contrast-enhanced cardiovascular magnetic resonance imaging. Int Heart J 53:263-9.

(10) Olimulder MA, Galjee MA, van Es J, Wagenaar LJ, von Birgelen C (2011) Contrast-enhancement cardiac magnetic resonance imaging beyond the scope of viability. Neth Heart J 19:236-45.

(11) Bello D, Fieno DS, Kim RJ, Pereles FS, Passman R, et al. (2005) Infarct morphology identifies patients with substrate for sustained ventricular tachycardia. J Am Coll Cardiol 45:1104-8.

(12) Chareonthaitawee P, Christian TF, Hirose K, Gibbons RJ, Rumberger JA (1995) Relation of initial infarct size to extent of left ventricular remodeling in the year after acute myocardial infarction. J Am Coll Cardiol 25:567-73.

(13) Christian TF, Behrenbeck T, Gersh BJ, Gibbons RJ (1991) Relation of left ventricular volume and function over one year after acute myocardial infarction to infarct size determined by technetium-99m sestamibi. Am J Cardiol 68:21-6.

(14) Pfeffer MA, Braunwald E (1990) Ventricular remodeling after myocardial infarction. Experimental observations and clinical implications. Circulation 81:1161-72.

(15) Tarantini G, Napodano M, Gasparetto N, Favaretto E, Marra MP, et al. (2010) Impact of multivessel coronary artery disease on early ischemic injury, late clinical outcome, and remodeling in patients with acute myocardial infarction treated by primary coronary angioplasty. Coron Artery Dis 21:78-86.

(16) Wu Y, Chan CW, Nicholls JM, Liao S, Tse HF, et al. (2009) MR study of the effect of infarct size and location on left ventricular functional and microstructural alterations in porcine models. J Magn Reson Imaging 29:305-12.

(17) Carrabba N, Parodi G, Valenti R, Migliorini A, Antoniucci D (2009) Comparison of effects of primary coronary angioplasty on left ventricular remodeling and heart failure in patients <70 versus > or =70 years with acute myocardial infarction. Am J Cardiol 104:926-31.

(18) Mather AN, Crean A, Abidin N, Worthy G, Ball SG, et al. (2010) Relationship of dysglycemia to acute myocardial infarct size and cardiovascular outcome as determined by cardiovascular magnetic resonance. J Cardiovasc Magn Reson 12:61.:61.

(19) Anderson KM, Wilson PW, Odell PM, Kannel WB (1991) An updated coronary risk profile. A statement for health professionals. Circulation 83:356-62.

(20) Cheng S, Xanthakis V, Sullivan LM, Lieb W, Massaro J, et al. (2010) Correlates of echocardiographic indices of cardiac remodeling over the adult life course: longitudinal observations from the Framingham Heart Study. Circulation 122:570-8.

(21) Roes SD, Borleffs C, van der Geest RJ, Westenberg JJM, Marsan NA, et al. (2009) Infarct Tissue Heterogeneity Assessed With Contrast-Enhanced MRI Predicts Spontaneous Ventricular Arrhythmia in Patients With Ischemic Cardiomyopathy and Implantable Cardioverter-Defibrillator. Circulation: Cardiovascular Imaging 2:183.

(22) Schmidt A, Azevedo CF, Cheng A, Gupta SN, Bluemke DA, et al. (2007) Infarct tissue heterogeneity by magnetic resonance imaging identifies enhanced cardiac arrhythmia susceptibility in patients with left ventricular dysfunction. Circulation 115:2006-14.

(23) Piro M, Della BR, Abbate A, Biasucci LM, Crea F (2010) Sex-related differences in myocardial remodeling. J Am Coll Cardiol 55:1057-65.

(24) Cavasin MA, Sankey SS, Yu AL, Menon S, Yang XP (2003) Estrogen and testosterone have opposing effects on chronic cardiac remodeling and function in mice with myocardial infarction. Am J Physiol Heart Circ Physiol 284:H1560-H1569.

(25) Cavasin MA, Tao ZY, Yu AL, Yang XP (2006) Testosterone enhances early cardiac remodeling after myocardial infarction, causing rupture and degrading cardiac function. Am J Physiol Heart Circ Physiol 290:H2043-H2050.

(26) Kenchaiah S, Pfeffer MA, St John SM, Plappert T, Rouleau JL et al. (2004) Effect of antecedent systemic hypertension on subsequent left ventricular dilation after acute myocardial infarction (from the Survival and Ventricular Enlargement trial). Am J Cardiol 94:1-8.

(27) Becker RC, Corrao JM, Lew R, Bradley J, Queenan J (1992) Relationship between serum total cholesterol, infarct size, and early clinical outcome following acute myocardial infarction. Cardiology 80:65-70.

(28) Todt T, Maret E, Alfredsson J, Janzon M, Engvall J, et al. (2012) Relationship between treatment delay and final infarct size in STEMI patients treated with abciximab and primary PCI. BMC Cardiovasc Disord 12:9.

(29) von Birgelen C, Hartmann M, Mintz GS, van Houwelingen KG, Deppermann N, et al. (2004) Relationship between cardiovascular risk as predicted by established risk scores versus plaque progression as measured by serial intravascular ultrasound in left main coronary arteries. Circulation 110:1579-85.

(30) Pohle K, Ropers D, Geitner P, Regenfus M, Daniel WG, et al. (2006) Analysis of coronary calcifications versus Framingham and PROCAM risk assessment in patients with a first myocardial infarction. Int J Cardiol 110:231-6.

(31) Donnino R, Patel S, Nguyen AH, Sedlis SP, Babb JS, et al. (2011) Comparison of quantity of left ventricular scarring and remodeling by magnetic resonance imaging in patients with versus without diabetes mellitus and with coronary artery disease. Am J Cardiol 107:1575-8.

(32) Olimulder MA, Kraaier K, Galjee MA, Scholten MF, van Es J, et al. (2012) Infarct tissue characteristics of patients with versus without early revascularization for acute myocardial infarction: a contrast-enhancement cardiovascular magnetic resonance imaging study. Heart Vessels 27:250-7.

Chapter 5

Infarct tissue characterization in implantable cardioverter-defibrillator recipients for primary versus secondary prevention following myocardial infarction: a study with contrast-enhancement cardiovascular magnetic resonance imaging

Olimulder MA, Kraaier K, Galjee MA, Scholten MF, van Es J, Wagenaar LJ, van der Palen J, von Birgelen C.
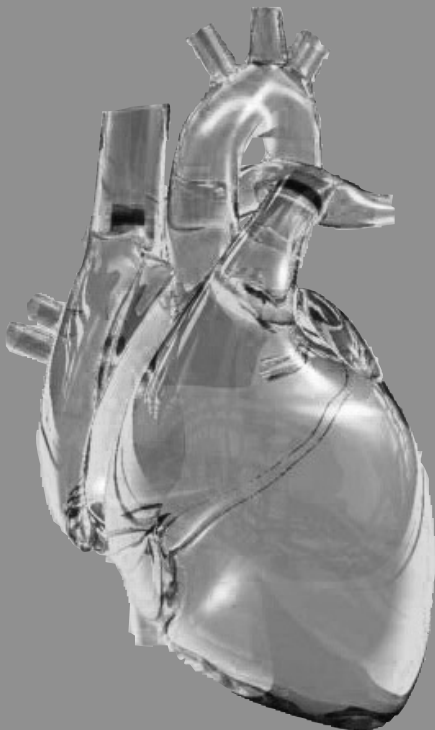
Abstract

Purpose: Knowledge about potential differences in infarct tissue characteristics between patients with prior life-threatening ventricular arrhythmia vs. patients receiving prophylactic implantable cardioverter-defibrillator (ICD) might help to improve the current risk stratification in myocardial infarction (MI) patients who are considered for ICD implantation. In a consecutive series of (ICD) recipients for primary and secondary prevention following myocardial infarction (MI), we used contrast-enhanced (CE) cardiovascular magnetic resonance (CMR) imaging to evaluate differences in infarct tissue characteristics.

Methods: Cine-CMR measurements included left ventricular (LV) end-diastolic and end-systolic volumes (EDV, ESV), ejection fraction (LVEF), wall motion score index (WMSI), and mass. CE-CMR images were analyzed for core, peri, and total infarct size, infarct localization (according to coronary artery territory), and transmural extent.

Results: In this study, 95 ICD recipients were included. In the primary prevention group (n=66), LVEF was lower (23±9 vs.31±14%; P<0.01), ESV and WMSI were higher (223±75 vs.184±97ml, P=0.04, and 1.89±0.52 vs.1.47±0.68; P<0.01), and anterior infarct localization was more frequent (P=0.02) than in the secondary prevention group (n=29). There were no differences in infarct tissue characteristics between patients treated for primary vs. secondary prevention (p>0.6 for all). During 21±9 months of follow-up, 3 (5%) patients in the primary prevention group and 9 (31%) in the secondary prevention group experienced appropriate ICD therapy for treatment of ventricular arrhythmia (P<0.01).

Conclusion: There was no difference in infarct tissue characteristics between recipients of ICD for primary vs. secondary prevention, while the secondary prevention group showed a higher frequency of applied ICD therapy for ventricular arrhythmia.

Introduction

Ventricular arrhythmia (VA) is a major cause of sudden cardiac death (SCD) in patients with prior myocardial infarction (MI).[1] Several randomized trials have shown a beneficial effect of implantable cardioverter-defibrillator (ICD) therapy among MI patients with prior life-threatening VA (secondary prevention).[2-4] In the setting of prophylactic ICD therapy (primary prevention), left ventricular ejection fraction (LVEF) below 35% is considered an indication for ICD implantation. However, less than 25% of these ICD recipients actually experience a life-threatening VA requiring shock therapy during median follow-up of 45.5 months.(5) Current guidelines consider a low LVEF post-MI as the most important criterion to determine a patient's eligibility. Therefore, these guidelines appear to be suboptimal.(1) Better risk stratification is warranted to reduce the number of unnecessary device implantations, especially in the setting of primary prevention.[3;5-7]

Cardiovascular magnetic resonance (CMR) imaging in combination with the contrast-enhancement (CE) technique allows the accurate assessment of LV geometry and function as well as tissue characteristics. This permits accurate assessment of size, heterogeneity, and transmurality of the myocardial scar.[8;9] Infarct tissue characteristics (e.g. localization, heterogeneity) (10-13) are considered potential predictors of life-threatening VAs, and could play a role in risk stratification before implantable cardioverter-defibrillator (ICD) implantation.[8;9;14]

Previous studies demonstrated a higher occurrence of VA (and thus a higher incidence of appropriate ICD therapy) in ICD recipients for secondary prevention compared to patients who received an ICD in the setting of primary prevention.[2;15-18] Insight into potential differences in infarct tissue characteristics between ICD recipients for primary vs. secondary prevention may potentially help to improve the current practice of risk stratification in MI patients considered for ICD implantation, specifically in the primary prevention group.

Therefore, in a consecutive series of ICD recipients for primary and secondary prevention following MI, we used CE-CMR to evaluate potential differences in infarct tissue characteristics.

Methods

Patient population

The study was conducted at Medisch Spectrum Twente, Enschede, the Netherlands. A consecutive series of patients with prior MI, who received an ICD for primary or secondary prevention following current guidelines of the Dutch (NVVC) and European society of Cardiology (ESC) in which the LVEF was determined based on echocardiographic findings, was assessed. The referring physicians had no access to the CMR report before defining therapeutic management. Prior to ICD implantation, these patients were referred for CMR to assess left ventricular (LV) dimension

and function, and after intravenous injection of gadolinium, characterization of the infarcted tissue. According to current guidelines, the patients who received ICD treatment for primary prevention had an indication based on a LVEF ≤ 35% (majority of patients) or the presence of spontaneous ventricular tachycardia, even with a somewhat more preserved LV function. Patients were only included in the study if the MI occurred at least one month prior to CMR (according to the definition of a healed MI(19) and a positive infarct pattern on CE imaging was found. The study was approved by the local ethics committee and informed consent was obtained.

As the secondary prevention group (dissimilar to the primary prevention group) was not selected based on a particularly low ejection fraction, the mean LVEF of this group may be expected to be higher. To correct for this potential confounder, ICD recipients from both groups with a LVEF ≤35% were separately compared. A comparable subgroup analysis in ICD recipients with a LVEF >35% was not performed as the limited number of patients did not permit a meaningful analysis.

CMR data acquisition

CMR examination was performed on a 1.5-T whole body scanner (Achieva scan, Philips Medical System, Best, the Netherlands) using commercially available software. For signal-reception a five-element cardiac synergy coil was used. Electrocardiogram triggering was performed with a vector-electrocardiogram set-up. Subjects were examined in the supine position. Cine (morphologic) images in the cardiac short-axis, four-chamber, three-chamber, two-chamber long-axis, and LV outflow tract views were acquired by using fast field echo cine images. (Slice thickness 8.0 mm, repetition time 3.4ms; echo time 1.7ms; flip angle 60°; matrix 256×256).

Myocardial scar was assessed on CE multislice short- axis, long-axis and four-chamber views, obtained 10 minutes after intravenous bolus injection of 0.2mmol gadolinium/kg body weight (Shering AG, Berlin, Germany). A three-dimensional Turbo Field Echo-inversion recovery T1-weighted sequence was used with the following parameters: repetition time 4.0ms; echo time 1.3ms; flip angle 15°; inversion time individually optimized to null myocardial signal (usually between 180-250ms); matrix 157; and slice thickness 10 mm.

CMR data analysis and definitions

CMR data were analyzed on a workstation using dedicated software (Philips MR workspace, Release 2.5.3.0; the Netherlands). Analysis was performed by reviewers blinded to clinical information.

LV geometry and function: Left ventricular end-diastolic and end-systolic volumes (EDV and ESV; ml), left ventricular ejection fraction (LVEF; %), and end-diastolic wall mass (EDWM; g) were calculated from contiguous short-axis loops by segmentation of endocardial and epicardial borders on each frame. Body surface area adjusted EDV (EDVi), ESV (ESVi) and EDWM (EDWMi) were also calculated.

The left ventricular wall regions were further divided into 17 segments according to a standardized myocardial segmentation model.[19] Normal wall motion was assigned a score 0, hypokinesia 1, severe hypokinesia 2, akinesia 3, and dyskinesia 4. The wall motion score index (WMSI) was calculated by dividing the sum of scores in each segment by the total number of observed segments.

Infarct tissue characteristics. Infarcted myocardium was defined as the zone of hyperenhancement on the CE images, in contrast with the dark-gray signal of normal myocardium (figure 1). Infarct size was quantified by a semi-automatic thresholding technique with the full width at half maximum approach as previously validated.[20] After outlining the myocardial segment containing the region with high signal intensity, the maximum signal intensity region was determined. Scar was divided into an infarct core zone and a heterogeneous zone (i.e peri-infarct zone). Infarct core was then defined as myocardium with a signal intensity ≥50% of the maximal signal intensity. The heterogeneous zone was defined as myocardium with a signal intensity between ≥35% and <50% of maximal signal intenstiy. Total scar was defined as the sum of infarct core plus heterogenous zone.

Scar tissue characteristics were further quantified according to location by use of a 17 segmental model.[19] Each segment was scored as follows: a scar score of 0 was defined normal, 1 as 1-25% scar, 2 as 26-50% scar, 3 as 51-75% scar, and 4 as 76-100% scar of the segmental area.

The *transmural extent* of myocardial scar was defined as the number of segments with a scar score 3 or 4.[21] In addition, a segmental *regional scar score* was calculated in order to relate scar size to the territories of the three major coronary arteries as previously described in detail.[19]
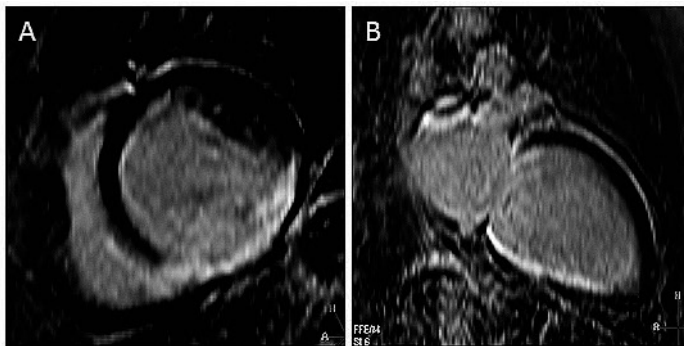
Figure 1. CE-CMR of a secondary prevention patient with a previous MI.
A: Short-axis view showing contrast-enhancement inferoseptal, inferior and inferolateral. **B**: long-axis view showing contrast-enhancement inferior.

Follow-up and definition of events

Follow-up was performed by our outpatient clinic, including registration of the occurrence of events and survival status. Regular device interrogation was scheduled every 3 to 6 months. In case of any experienced event, an additional device interrogation was performed. Device therapy was classified as appropriate or inappropriate. Appropriate ICD therapy was defined as anti-tachycardia pacing and/or appropriate shock in response to ventricular tachycardia or ventricular fibrillation. For the purpose of this study, only appropriate device therapies were considered as arrhythmic events. Mortality was reported and causes of death were scored as follows: (1) myocardial infarction, (2) heart failure, (3) cerebrovascular accident, (4) carcinoma, or (5) other causes of death.

A major cardiovascular event (MACE) was defined as appropriate ICD therapy and/or death.

Statistical analysis

Continuous variables had a normal distribution and were expressed as mean±standard deviation. Categorical data were expressed as frequencies and percentages. To compare the primary and secondary prevention groups, Student's t-test and Mann-Whitney U test were used to compare continuous variables, and chi-square test and Fisher exact test were used to compare categorical variables. A survival analysis was performed to investigate if the association between infarct tissue characteristics with MACE is different among groups (ICD for primary preventions vs. ICD for secondary prevention). A P value <0.05 was considered statistically significant.

Results

Study patients

In this study, 95 patients (64±10 years old; 79 men) with a median of 141 (1-434) months after MI were examined. A total of 66 patients received an ICD for primary prevention and 29 patients for secondary prevention. Indication for secondary prevention by ICD implantation was (1) sudden cardiac death in 14 patients (48%) or (2) VT episodes in 15 patients (52%). Time between events and ICD implantation was on average 2 weeks (median). (25th percentile 1 week, 50th percentile 2 weeks, 75th percentile 4 weeks). In general, ICD implantation was performed shortly after CE-CMR assessment; the average (median) within 1 week, the 75th percentile within 1 week and the 90th percentile within 5.4 weeks. Demographics and baseline characteristics did not differ between groups except for diuretic usage (80%vs.45%; P<0.01;). Patient demographics are presented in Table 1, which also shows a subgroup of patients with LVEF≤35%.

Table 1. Patient characteristics

	All patients			Patients with LVEF ≤ 35%		
	Primary prevention (n=66)	Secondary prevention (n=29)	P	Primary prevention (n=60)	Secondary prevention (n=20)	P
Male sex, n	56 (85)	23 (79)	0.56	52 (87)	16 (80)	0.48
Age, y	65±9	61±11	0.09	66±8	62±9	0.08
Hypertension	24 (36)	11 (38)	1.00	22 (37)	8 (40)	1.00
Diabetes	18 (27)	5 (17)	0.43	17 (28)	3 (15)	0.25
Medication						
- B-blocker	59 (89)	23 (79)	0.21	53 (88)	16 (80)	0.45
- Ace inhibitor	50 (76)	20 (69)	0.62	43 (72)	16 (80)	0.57
- Diuretic	53 (80)	13 (45)	<0.01	48 (80)	12 (60)	0.13
- Statin	58 (88)	28 (97)	0.27	54 (90)	20 (100)	0.33
Infarct						
Single	56 (84)	24 (83)	0.87	51 (85)	17 (85)	0.67
Multiple	5 (8)	2 (7)		5 (8)	2 (10)	
Unknown	5 (8)	3 (10)		4 (7)	1 (5)	
Infarct localization			0.08			0.15
- anterior	33 (50)	10 (35)		28 (47)	6 (30)	
- nonanterior	18 (27)	14 (48)		17 (28)	9 (45)	
- both	15 (23)	5 (17)		15 (25)	5 (25)	
Infarct age, months	133 (1-434)	166 (1-426)	0.24	155 (1-434)	209 (13-426)	0.07

Continuous data are expressed as mean±standard deviation or median with range; and categorical data as frequencies and percentage.

CMR results

LV geometry and function: In the primary prevention group, LVEF (23±9 vs. 31±14%; P<0.01) was significantly lower while ESVi (113±39 vs. 91±49ml; P0.03) and WMSI (1.89±0.52 vs.1.47±0.68; P<0.01) were significantly higher than in the secondary prevention group (Table 2).

Infarct characteristics: There were no significant differences between size of the infarct core (12±7 vs. 11±9%; P0.62), size of the peri-infarct (10±4 vs.10±5%; P0.70), total infarct size (24±10 vs.21±12%; P0.62) and transmural extent (3.19±2.41 vs. 2.97±2.76; P0.70) of the infarct (Figure 2). According to the regional scar score, left anterior descending scar score (1.55±0.81 vs.1.08±0.84; P0.02) was significantly higher in the primary prevention group. (Table 2.)

Table 2. CMR characteristics in all patients and in the subgroup of patients with LVEF ≤35%.

	All patients			Patients with LVEF ≤ 35		
	Primary prevention (n=66)	Secondary prevention (n=29)	P	Primary Prevention (n=60)	Secondary Prevention (n=20)	P
LV geometry and function						
EDV	284±72	259±91	0.16	293±68	288±95	0.81
EDVi	144±38	129±45	0.09	150±34	144±45	0.53
ESV	222±75	184±97	0.04	231±69	225±63	0.54
ESVi	113±39	91±49	0.03	119±35	111±47	0.43
EDWM	145±37	143±34	0.79	148±37	141±32	0.46
EDWMi	37±10	36±9	0.66	75±18	73±17	0.63
LVEF	23±9	31±14	<0.01	22±7	23±7	0.31
WMSI	1.89±0.52	1.47±0.68	<0.01	1.96±0.48	1.76±0.47	0.11
Infarct characteristis						
Infarct size-core%	12±7	11±9	0.62	12±7	13±9	0.58
Infarct size-peri %	10±4	10±5	0.70	10±4	11±5	0.53
Infarct size-total%	24±10	21±12	0.62	23±10	24±13	0.52
Infarct localization						
- **LAD score**	1.55±0.81	1.08±0.84	0.02	1.54±0.82	1.25±0.86	0.23
- **RCA score**	1.30±0.86	1.53±0.97	0.28	1.30±0.85	1.62±1.01	0.19
- **RCX score**	1.10±0.89	1.07±0.76	0.92	1.07±0.85	1.14±0.86	0.80
Transmural extent	3.19±2.41	2.97±2.76	0.70	3.11±2.46	3.55±2.91	0.52

Data are presented as mean±standerd deviation or median with range. Categorical data are presented as frequencies and percentages. EDV = end diastolic volume, ESV = end systolic volume, EDWM = end diastolic wall mass, LVEF = left ventricular ejection fraction, WMSI = wall motion score index, LAD = left anterior descending, RCA = right coronary artery, LCX= left circumflex.

CMR results in subgroup of patients with LVEF ≤35%

In order to correct for the difference in LVEF between the primary and secondary prevention group (Table 2), patients with an LVEF ≤35% were included in a subanalysis.There was no difference in demographics and baseline characteristics of the remaining 60 and 20 patients, respectively. According to LV geometry and function as well as CE-CMR assessed infarct tissue characterization, no significant differences were observed between primary and secondary prevention patients with an LVEF ≤35% (Table 2).
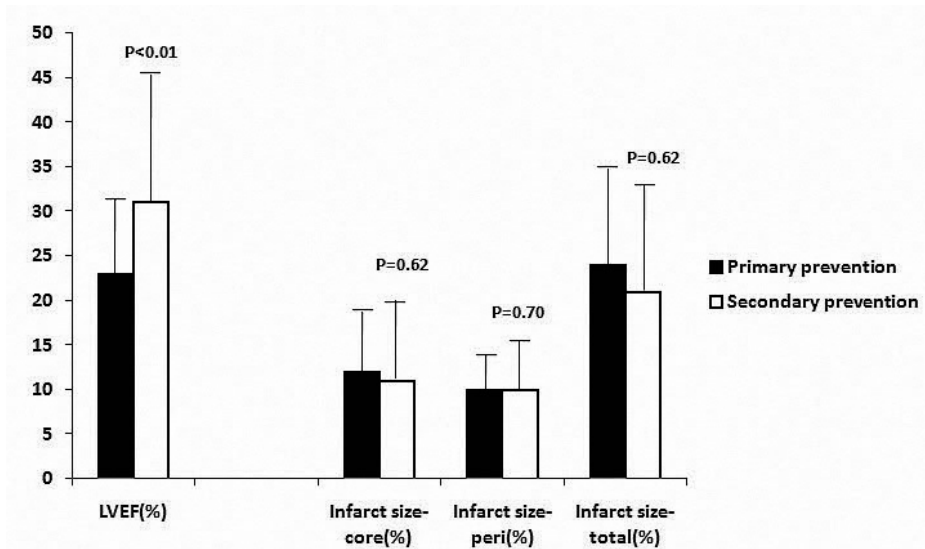
Figure 2. LVEF and infarct tissue characteristics (mean±SD) in primary and secondary prevention patients. While in primary vs. secondary prevention patients LVEF differed significantly, there were no significant differences in infarct tissue characteristics.

CMR results according to infarct localization

As infarct localization differed between the primary and secondary prevention group (Tables 1 and 2), patients were stratified according to infarct localization. Between the 33 and 10 patients with anterior wall MI, respectively, there was no significant difference in LV dimensions, LV function, or infarct tissue characteristics (Table 3). Among patients with non-anterior infarct localization, the primary prevention group (n=18) showed a lower LVEF (22±9 vs. 31±14%; P0.04) and a higher WMSI (2.10±0.52vs.1.47±0.50; P<0.01) than the secondary prevention group (n=14); but there was no significant difference in infarct tissue characteristics (Table 3).

Table 3. CMR characteristics in all patients stratified according to infarct localization.

	Anterior infarction			Nonanterior infarction		
	Primary prevention (n=33)	Secondary prevention (n=10)	P	Primary Prevention (n=18)	Secondary Prevention (n=14)	P
LV geometry and function						
EDV	282±79	275±106	0.83	286±67	250±90	0.20
EDVi	144±40	135±50	0.56	149±35	126±48	0.17
ESV	218±81	192±119	0.43	225±75	180±99	0.15
ESVi	111±41	95±58	0.31	117±40	90±53	0.15
EDWM	137±42	140±34	0.83	158±29	145±32	0.24
EDWMi	71±21	69±15	0.81	82±14	75±19	0.26
LVEF	25±9	32±17	0.22	22±9	31±14	0.04
WMSI	1.73±0.52	1.51±0.89	0.32	2.04±0.56	1.36±0.62	<0.01
Infarct characteristics						
Infarct size-core%	12±6	11±9	0.47	11±6	10±7	0.62
Infarct size-peri%	11±4	11±6	0.77	9±3	9±5	0.80
Infarct size-total%	23±9	22±14	0.71	21±9	19±11	0.65
Transmural extent	3.29±2.22	2.80±2.90	0.58	3.60±0.47	2.79±2.69	0.40

See legend of Table 2 for details

Follow-up

During 21±9 months of follow–up, 4 patients in the primary prevention group and 4 patients in the secondary prevention group died, respectively. All 8 patients died on heart failure. The frequency of appropriate ICD therapy differed significantly between the primary and secondary prevention group (3/66 (5%) vs. 9/29 (31%); p<0.01). In the primary prevention group, only appropriate shock therapy (2 on VF, 1 on VT) was delivered, while in the secondary prevention group both appropriate shock therapy (n=3; all on VT) and antitachycardia pacing (n=6) were delivered. All but 2 patients with appropriate ICD therapy (both secondary prevention) had a LVEF ≤35%.

Patients with appropriate ICD therapy did not differ from patients without event in per-infarct size (8.83 ± 3.20% versus 10.51 ± 4.39%; p=0.20), but core infarct size was smaller in patients with events (8.00 ± 4.93%, versus 12.58 ± 7.37%; p=0.040).

The association between infarct tissue characteristics with MACE did not significantly differ among groups (ICD for primary prevention vs. ICD for secondary prevention) (p=0.25–0.91).

Discussion

The implantation of ICD in MI patients provides protection from SCD following VA. When current guidelines are followed, less than 1 out of 4 primary prevention ICD recipients experiences actual life-threatening VA requiring shock therapy during a follow-up period of almost 4 years.[5] This shows that there may be some room for improvement in the selection of ICD candidates in the setting of primary prevention.

The infarct core and heterogeneous zone, as well as presence of transmural infarction may serve as an anatomic pathway for reentry, and consequently, the occurrence of VA.(10-13;23;24) In this respect, it has recently been demonstrated that a larger size of infarct heterogeneity is related to increased ventricular irritability by programmed electrical stimulation as well as spontaneous VA.[8;9]

While there was a difference in frequency of applied ICD therapy between primary and secondary prevention patients in our study, there was no difference in the size of the infarct tissue characteristics between these two subpopulations of patients. These findings may question the importance of the size of infarct tissue characteristics as a predictor of life-threatening VA.[25] However, size of infarct tissue characteristics is not really all that matters, as it has been demonstrated that a substantial portion of tachycardia originates from reentry occurring in a very small circuit extending just over a few millimeters.[26] Other factors than anatomic substrate may interfere with the risk of VA in the setting of MI; an example may be genetic factors. In this respect, recently, a genome-wide association study identified in patients with a first MI a gene locus prone for ventricular fibrillation.[27]

In the primary prevention group, we found a substantially larger amount of MI tissue in the anterior wall of the LV during CMR assessment. Several clinical studies observed that patients with anterior MI usually have a worse LVEF.[28] The larger amount of anterior MI in the primary prevention group may thus actually be expected, as LVEF below 35% is used as a major risk stratifier for primary prevention with ICD, according to current guidelines. In addition, in our primary prevention group (P<0.01) there was a higher use of diuretics for symptomatic treatment of heart failure. On the other hand, secondary prevention patients – patients who already had a life-threatening VA in the past – showed more appropriate ICD therapies during follow-up, as may be expected based on the difference in indication. Thus, there must be other factors than the studied CMR characteristics involved to make the myocardium prone to the development of life-threatening VA.

With current clinically applied CE-CMR technology, spatial resolution imposes constraints on what type of tissue is concealed within the peri-infarct zone, characterized by intermediate signal intensities.[29] High-resolution CE-CMR imaging with 1000-fold higher resolution than clinical scans may bear the potential to obtain further insights in an experimental setting.[30] There is a lack of well-defined gold standard formula for the assessment of infarcted myocardium. Partial

volume effects and blurred images by cardiac motion during image acquisition may lead to a relative increase of signal intensity in pixels of the border zone of infarcted compared to remote myocardium, which may lead to an overestimation of the total scar score. Initial visual assessment, manual tracing of endo and epicardial contours, visual identification of the region of interest with maximum signal intensity, and visual check for erroneous inclusion of other regions with high signal intensity (e.g. in/folding or motion artefacts, fat, or pericardial effusion)[31] require experience and involve a certain degree of interpretation. The subjectivity involved can only be minimized by an optimized training of experienced analysts. Finally, signal intensity analysis with current CE-CMR techniques do not incorporate areas of microvascular obstruction, which are hypo-enhanced in CE-CMR,[32] which may lead to underestimation of infarct size. As only one patient of the present patient population showed microvascular obstruction, the microvascular obstruction area was not incorporated to the infarct core.

While CMR is the gold standard for the assessment of LV function, myocardial viability, extent and transmurality of scar, our findings suggest that infarct tissue analysis with the CE-CMR technique that is currently applied in clinical practice does not appear to have the potential to improve the current practice of risk stratification in MI patients considered for ICD implantation.

Limitations

Our study comprises a limited number of patients; nevertheless, this represents a consecutive series of patients examined with CE-CMR for that indication. While the secondary outcome of defibrillator shocks was prospectively collected and analyzed, the primary comparison of CE-CMR image characteristics was based on a cross-sectional approach. In the light of the duration of clinical follow-up of 21 ± 9 months, event rates in subgroups should be interpreted carefully. In addition, primary aim of the present study was the assessment of potential differences in infarct tissue characteristics between ICD recipients for primary vs. secondary prevention.

Conclusion

There was no difference in infarct tissue characteristics between recipients of ICD for primary versus secondary prevention, while the secondary prevention group showed a higher frequency of applied ICD therapy for ventricular arrhythmia.

References

(1)   Zipes DP, Camm AJ, Borggrefe M, Buxton AE, Chaitman B, Fromer M, et al. ACC/AHA/ESC 2006 Guidelines for Management of Patients With Ventricular Arrhythmias and the Prevention of Sudden Cardiac Death: a report of the American College of Cardiology/American Heart Association Task Force and the European Society of Cardiology Committee for Practice Guidelines (writing committee to develop Guidelines for Management of Patients With Ventricular Arrhythmias and the Prevention of Sudden Cardiac Death): developed in collaboration with the European Heart Rhythm Association and the Heart Rhythm Society. Circulation 2006 Sep 5;114(10):e385-e484.

(2)   A comparison of antiarrhythmic-drug therapy with implantable defibrillators in patients resuscitated from near-fatal ventricular arrhythmias. The Antiarrhythmics versus Implantable Defibrillators (AVID) Investigators. N Engl J Med 1997 Nov 27;337(22):1576-83.

(3)   Bardy GH, Lee KL, Mark DB, Poole JE, Packer DL, Boineau R, et al. Amiodarone or an implantable cardioverter-defibrillator for congestive heart failure. N Engl J Med 2005 Jan 20;352(3):225-37.

(4)   Kuck KH, Cappato R, Siebels J, Ruppel R. Randomized comparison of antiarrhythmic drug therapy with implantable defibrillators in patients resuscitated from cardiac arrest : the Cardiac Arrest Study Hamburg (CASH). Circulation 2000 Aug 15;102(7):748-54.

(5)   Strauss DG, Selvester RH, Lima JA, Arheden H, Miller JM, Gerstenblith G, et al. ECG quantification of myocardial scar in cardiomyopathy patients with or without conduction defects: correlation with cardiac magnetic resonance and arrhythmogenesis. Circ Arrhythm Electrophysiol 2008 Dec;1(5):327-36.

(6)   Kraaier K, Verhorst PM, VAN Dessel PF, Wilde AA, Scholten MF. Towards a better risk stratification for sudden cardiac death in patients with structural heart disease. Neth Heart J 2009 Mar;17(3):101-6.

(7)   Kraaier K, VAN Dessel PF, VAN DER PJ, Wilde AA, Scholten MF. ECG Quantification of Myocardial Scar Does Not Differ between Primary and Secondary Prevention ICD Recipients with Ischemic Heart Disease. Pacing Clin Electrophysiol 2009 Nov 4.

(8)   Roes SD, Borleffs CJ, van der Geest RJ, Westenberg JJ, Marsan NA, Kaandorp TA, et al. Infarct tissue heterogeneity assessed with contrast-enhanced MRI predicts spontaneous ventricular arrhythmia in patients with ischemic cardiomyopathy and implantable cardioverter-defibrillator. Circ Cardiovasc Imaging 2009 May;2(3):183-90.

(9)   Schmidt A, Azevedo CF, Cheng A, Gupta SN, Bluemke DA, Foo TK, et al. Infarct tissue heterogeneity by magnetic resonance imaging identifies enhanced cardiac arrhythmia susceptibility in patients with left ventricular dysfunction. Circulation 2007 Apr 17;115(15):2006-14.

(10) Bolick DR, Hackel DB, Reimer KA, Ideker RE. Quantitative analysis of myocardial infarct structure in patients with ventricular tachycardia. Circulation 1986 Dec;74(6):1266-79.

(11) Cardinal R, Vermeulen M, Shenasa M, Roberge F, Page P, Helie F, et al. Anisotropic conduction and functional dissociation of ischemic tissue during reentrant ventricular tachycardia in canine myocardial infarction. Circulation 1988 May;77(5):1162-76.

(12) Karagueuzian HS, Fenoglio JJ, Jr., Weiss MB, Wit AL. Protracted ventricular tachcardia induced by premature stimulation of the canine heart after coronary artery occlusion and reperfusion. Circ Res 1979 Jun;44(6):833-46.

(13) Saeed M, Bremerich J, Wendland MF, Wyttenbach R, Weinmann HJ, Higgins CB. Reperfused myocardial infarction as seen with use of necrosis-specific versus standard extracellular MR contrast media in rats. Radiology 1999 Oct;213(1):247-57.

(14) Pascale P, Schlaepfer J, Oddo M, Schaller MD, Vogt P, Fromer M. Ventricular arrhythmia in coronary artery disease: limits of a risk stratification strategy based on the ejection fraction alone and impact of infarct localization. Europace 2009 Dec;11(12):1639-46.

(15) Raitt MH, Klein RC, Wyse DG, Wilkoff BL, Beckman K, Epstein AE, et al. Comparison of arrhythmia recurrence in patients presenting with ventricular fibrillation versus ventricular tachycardia in the Antiarrhythmics Versus Implantable Defibrillators (AVID) trial. Am J Cardiol 2003 Apr 1;91(7):812-6.

(16) Moss AJ, Zareba W, Hall WJ, Klein H, Wilber DJ, Cannom DS, et al. Prophylactic implantation of a defibrillator in patients with myocardial infarction and reduced ejection fraction. N Engl J Med 2002 Mar 21;346(12):877-83.

(17)   Moss AJ, Greenberg H, Case RB, Zareba W, Hall WJ, Brown MW, et al. Long-term clinical course of patients after termination of ventricular tachyarrhythmia by an implanted defibrillator. Circulation 2004 Dec 21;110(25):3760-5.

(18)   van Welsenes GH, van Rees JB, Borleffs CJ, Cannegieter SC, Bax JJ, van EL, et al. Long-term follow-up of primary and secondary prevention implantable cardioverter defibrillator patients. Europace 2011 Jan 5.

(19)   Thygesen K, Alpert JS, White HD, On behalf of the Joint ESC/ACCF/AHA/WHF Task Force for the Redefinition of Myocardial Infarction (2007) Universal definition of myocardial infarction. Eur Heart J 28:2525-2538

(20)   Cerqueira MD, Weissman NJ, Dilsizian V, Jacobs AK, Kaul S, Laskey WK, et al. Standardized myocardial segmentation and nomenclature for tomographic imaging of the heart: a statement for healthcare professionals from the Cardiac Imaging Committee of the Council on Clinical Cardiology of the American Heart Association. Circulation 2002 Jan 29;105(4):539-42.

(21)   Amado LC, Gerber BL, Gupta SN, Rettmann DW, Szarf G, Schock R, et al. Accurate and objective infarct sizing by contrast-enhanced magnetic resonance imaging in a canine myocardial infarction model. J Am Coll Cardiol 2004 Dec 21;44(12):2383-9.

(22)   Roes SD, Kelle S, Kaandorp TA, Kokocinski T, Poldermans D, Lamb HJ, et al. Comparison of myocardial infarct size assessed with contrast-enhanced magnetic resonance imaging and left ventricular function and volumes to predict mortality in patients with healed myocardial infarction. Am J Cardiol 2007 Sep 15;100(6):930-6.

(23)   Tarantini G, Razzolini R, Cacciavillani L, Bilato C, Sarais C, Corbetti F, et al. Influence of transmurality, infarct size, and severe microvascular obstruction on left ventricular remodeling and function after primary coronary angioplasty. Am J Cardiol 2006 Oct 15;98(8):1033-40.

(24)   Yokota H, Heidary S, Katikireddy CK, Nguyen P, Pauly JM, McConnell MV, et al. Quantitative characterization of myocardial infarction by cardiovascular magnetic resonance predicts future cardiovascular events in patients with ischemic cardiomyopathy. J Cardiovasc Magn Reson 2008;10(1):17.

(25)   Bello D, Fieno DS, Kim RJ, Pereles FS, Passman R, Song G, et al. Infarct morphology identifies patients with substrate for sustained ventricular tachycardia. J Am Coll Cardiol 2005 Apr 5;45(7):1104-8.

(26)   de Bakker JM, van Capelle FJ, Janse MJ, Wilde AA, Coronel R, Becker AE, et al. Reentry as a cause of ventricular tachycardia in patients with chronic ischemic heart disease: electrophysiologic and anatomic correlation. Circulation 1988 Mar;77(3):589-606.

(27)   Bezzina CR, Pazoki R, Bardai A, Marsman RF, de Jong JS, Blom MT, et al. Genome-wide association study identifies a susceptibility locus at 21q21 for ventricular fibrillation in acute myocardial infarction. Nat Genet 2010 Aug;42(8):688-91.

(28)   Wu Y, Chan CW, Nicholls JM, Liao S, Tse HF, Wu EX. MR study of the effect of infarct size and location on left ventricular functional and microstructural alterations in porcine models. J Magn Reson Imaging 2009 Feb;29(2):305-12.

(29)   Zeppenfeld K, van der Geest RJ. The infarct characteristics on magnetic resonance imaging and ventricular tachycardia: do we see what we need to see? Europace 2011 Jun;13(6):770-2.

(30)   Schelbert EB, Hsu LY, Anderson SA, Mohanty BD, Karim SM, Kellman P, et al. Late gadolinium-enhancement cardiac magnetic resonance identifies postinfarction myocardial fibrosis and the border zone at the near cellular level in ex vivo rat heart. Circ Cardiovasc Imaging 2010 Nov;3(6):743-52.

(31)   Bondarenko O, Beek AM, Hofman MB, Kuhl HP, Twisk JW, van Dockum WG, et al. Standardizing the definition of hyperenhancement in the quantitative assessment of infarct size and myocardial viability using delayed contrast-enhanced CMR. J Cardiovasc Magn Reson 2005;7(2):481-5.

(32)   Wong DT, Leung MC, Richardson JD, Puri R, Bertaso AG, Williams K, et al. Cardiac magnetic resonance derived late microvascular obstruction assessment post ST-segment elevation myocardial infarction is the best predictor of left ventricular function: a comparison of angiographic and cardiac magnetic resonance derived measurements. Int J Cardiovasc Imaging 2012 Feb 5.

Chapter 6

Scar tissue and microvolt T-wave alternans

Kraaier K, Olimulder MA, Galjee MA, Van Dessel P.F,
van der Palen J, Wilde AM, Scholten MF.
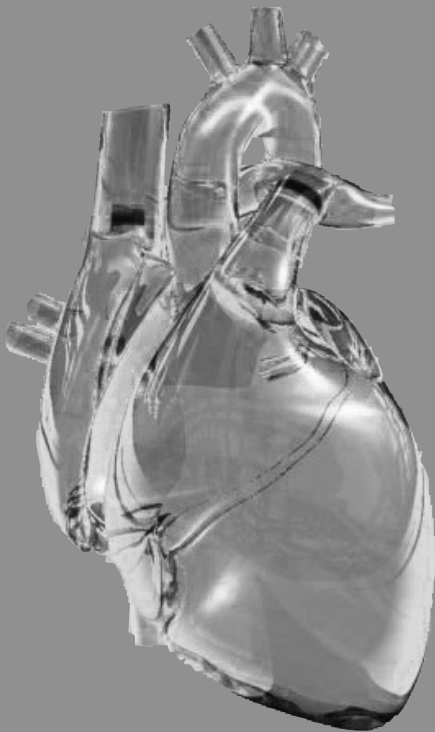
Abstract

Purpose: Microvolt T-wave Alternans (MTWA) is an electrocardiographic marker for predicting sudden cardiac death. In this study, we aimed to study the relation between MTWA and scar assessed with cardiac magnetic resonance imaging (CMR) in patients with ischemic (ICM) or dilated cardiomyopathy (DCM).

Methods: Sixty-eight patients with positive or negative MTWA and analysable CMR examination were included. Using CMR and the delayed enhancement technique, ejection fraction (LVEF), volumes, wall motion and scar characteristics were assessed.

Results: Overall, positive MTWA (n=40) was related to male gender (p=0.04), lower LVEF (p=0.04) and increased LVEDV (p<0.01). After multivariate analysis, male gender (p=0.01) and lower LVEF remained significant (p=0.02). Scar characteristics (presence, transmurality, and scar score) were not related to MTWA (all p>0.5). In the patients with ICM (n=40) scar was detected in 38. Positive MTWA (n=18) was related to higher left ventricular end-diastolic volume (p=0.05). In patients with DCM (n=28), scar was detected in 11. Trends were found between positive MTWA (n=15) and male gender (p=0.10), lower LVEF (p=0.10), and higher LVEDV (p=0.09). In both subgroups, the presence, transmurality or extent of scar was not related to MTWA (all p>0.45).

Conclusion: In this small study, neither in patients with ICM or DCM a relation was found between the occurrence of MTWA and the presence, transmurality or extent of myocardial scar. Overall there was a significant relation between heart failure remodeling parameters and positive MTWA.

Introduction

Microvolt T-wave alternans (MTWA) is a promising electrocardiographic risk marker for predicting sudden cardiac death (SCD) and life threatening ventricular arrhythmia (VA). Previous studies have demonstrated that MTWA screening in patients with ischemic and dilated cardiomyopathy is effective in identifying patients the level of risk for SCD or all cause mortality.[1;2] In the current and ACC/AHA/ESC guidelines for management of patients with VA and prevention of SCD, there is a class IIa indication for MTWA testing to improve the diagnosis and risk stratification in patients with ischemic and non-ischemic dilated cardiomyopathy.[3]

MTWA is a phenomenon of beat-to-beat change in amplitude of the T-wave. This reflects temporal heterogeneity or dispersion in the ventricular repolarization. The exact cellular pathophysiological mechanism underlying MTWA remains unclear. At this moment, there are two hypothesis: 1) the action potential duration restitution hypothesis, and 2) the calcium cycling hypothesis.[4;2] Recently it has been suggested that MTWA could also be related to an anatomic fibrotic substrate.[5;6;7] Experimental models have shown the influence of structural barriers on the occurrence of MTWA.[6]In clinical research, the relation between myocardial disarray, fibrosis and MTWA was demonstrated by Kon-No et al, in a group of patients with hypertrophic cardiomyopathy.[5] Recently Narayan et al. demonstrated a spatial correlation between MTWA and wall motion abnormalities due to myocardial infarct.[7] Using cardiac magnetic resonance imaging (CMR) and the late gadolineum enhancement (LGE) technique, it is possible to identify and characterize areas of scar or fibrosis in both patients with ischemic and non-ischemic cardiomyopathy.[8;9;10]

The purpose of this study is to evaluate the influence of scar tissue on MTWA in patients with ischemic (ICMP) or non-ischemic dilated cardiomyopathy (DCM).

Methods

Study population

The study was conducted at the Medisch Spectrum Twente (Enschede, The Netherlands) as part of the Twente ICD Cohort Study (NL13939.044.06). In this study, the role of several non-invasive risk markers in predicting SCD and life threatening VA in patients with an ICD are studied. All patients received an ICD following current guidelines for primary and secondary prevention.[3] LVEF was measured using echocardiography or nuclear imaging. After obtaining informed consent, MTWA testing and CMR were performed before implantation, both test were performed within a month. In this analysis, patients with DCMP or ICMP who received an ICD following current guidelines for primary and secondary prevention were included. Patients with indeterminate MTWA results, or poor image quality were excluded from analysis. Ischemic

origin of cardiomyopathy was defined as a history of prior myocardial infarction, or coronary abnormalities >70% and/or coronary interventions.

Microvolt T-Wave Alternans

All MTWA tests were performed with the HearTWave system II (Cambridge Heart Inc., Bedford, Massachusetts, USA) using the spectral analysis method and an exercise protocol. After gradually increasing the workload to achieve a constant heart rate, a target heart rate between 100 and 110 beats per minute was attained and kept stable for 2.5 minutes. Subsequently during 1.5 minutes, a target heart rate between 110 and 120 beats per minute was attained. The MTWA tests were read and interpreted by two trained physicians and in case of disagreement a third physician was consulted. Each MTWA report was classified as positive, indeterminate, or negative using accepted criteria.[11] A test was defined positive if the MTWA voltage was ≥1.9μV for at least 1 minute with an onset heart rate <110 bpm or at rest in any of three orthogonal leads (X, Y or Z), or in two adjacent precordial leads. If the recording did not prove positive and the heart rate was >105 bpm for at least one minute, the MTWA test was defined negative (figure 1). A MTWA test was considered indeterminate if the test did not meet the criteria for being classified as positive or negative. Patients continued their medication, including beta blocking agents and amiodarone, and therefore represent a real life population.
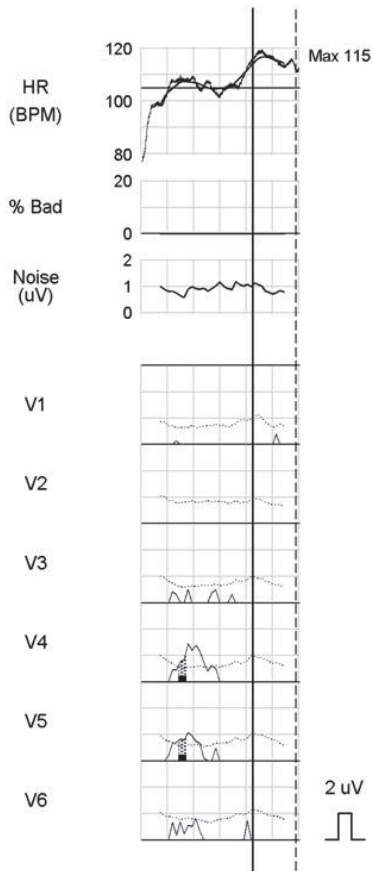
Figure 1. Example of MTWA
From top till bottom: heart rate (HR) profile, ectopy (% bad beats), noise level and alternans magnitude
magnitude (microvolts µV) in the precordial leads (V1-V6) demonstrates no significant sustained alternans.

Cardiac Magnetic Resonance Imaging

CMR examination was performed on a 1.5-T whole body scanner (Achieva scan, Philips Medical System, Best, The Netherlands) using commercially available cardiac CMR software. For signal-reception a five-element cardiac synergy coil was used. Electrocardiogram (ECG) triggering was done with a vector-ECG set-up. Subjects were examined in the supine position. Morphologic images in the cardiac short axis, four chamber long axis, three chamber, and two chamber long axis, and left ventricular outflow tract views were acquired by using fast field echo cine images. Myocardial scar and/or fibrosis was assessed on LGE multislice (without interslice gap) short-axis, long-axis and 4 -chamber views, obtained approximately 10 minutes after the peripheral bolus injection of gadolinium (Shering AG, Berlin, Germany; 0.2 mmol/kg of body weight). All CMR data were analyzed on a workstation using dedicated software for cardiac analysis (Philips

MR workspace. Release 2.5.3.0 2007-12-03). All analyses were performed by two trained investigators who were blinded from the MTWA test results, in case of disagreement, a third investigator was asked.

Left ventricular end-diastolic volume (LVEDV), end systolic volume, stroke volume, ejection fraction (LVEF), cardiac output and cardiac mass were calculated from contiguous short-axis loops by segmentation of endocardial and epicardial borders on each frame. Papillary muscles were regarded as part of the ventricular cavity. As an internal control for estimation of stroke volume and LVEF, the stroke volume over the aortic valve was estimated (on condition that no mitral insufficiency is present).

Scar was defined as the zone of hyper enhancement on the late gadolinium-enhanced images, in contrast with the dark-gray signal of the normal myocardium. Since scar patterns differ between patients with ICM and DCM (figure 2),[8] different definitions of scar were used. In patients with ICM, scar was divided into an infarct core and - border zone. After outlining thye myocardiale segment containing the region with high signal intensity, the maximum signal intensity (SI) within the infarct region was determined. Infarct core was defined as myocardium with SI ≥50% of the maximal SI.[12] The border zone was defined as myocardium with SI ≥35% of the maximal SI and <50% of maximal SI. Total scar was defined as the summation of infarct core and border zone.[13] In patients with DCM, no difference was made between core and border zone. In these patients, scar was defined as myocardium with SI >50% of the maximal SI.

After qualitative assessment of scar, the wall motion score in the left ventricular wall regions were scored quantitatively using a standardized 17 segment model. Wall motion of all 17 separate segments was assigned the following scores: normal wall motion was 0, hypokinesia 1, severe hypokinesia 2, akinesia 3, and dyskinesia 4. The wall motion score index (WMSI) was calculated by dividing the sum of scores in each segment by the total number of segments (17 segments). WMSI of 0 was considered as normal, 0–1 as moderate, 1–2 as poor, and >2 as bad.

Statistical analysis

Continuous variables are presented as mean±SD, categorical data are summarized as frequencies and percentages. Differences in baseline characteristics between MTWA positive and negative patients were analyzed using Students t-test or Mann-Whitney U-test, as appropriate, if continuous, or chi-square or Fisher exact test if categorical. All variables that were significant at $p<0.15$ were entered in a multivariate logistic regression analysis. Subsequently, non-significant variables were removed from the model, based on -2 log likelihood tests. All tests were 2-sided, p-values of 0.05 were considered statistically significant.
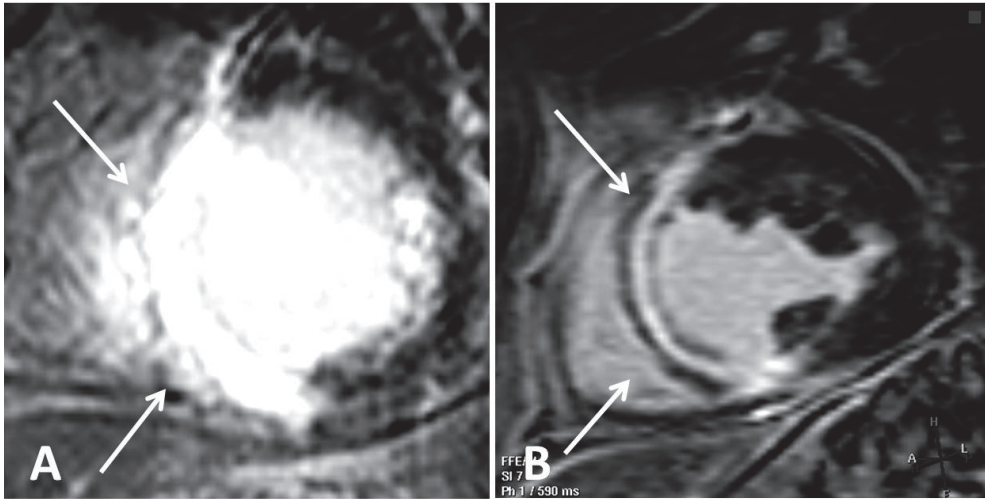
Figure 2. Example of delayed enhancement magnetic resonance image.
A: Example of a patient with an ischemic cardiomyopathy **B:** and non-ischemic dilated cardiomyopathy. In patient A, transmural enhancement is seen in the anteroseptal, septal and inferoseptal area with a high signal intensity (arrow). In patient B, midwall enhancement with a lower signal intensity (arrow), without transmurality, is seen in the anteroseptal, septal and inferoseptal area.

Results

From our TICS-database, 68 patients were included. All these patients had a positive or negative MTWA-test and a good quality CMR prior to implantation. Baseline characteristics of the 68 included patients are listed in table 1. The mean age was 60 years, 79% were men and the average LVEF was 26%. Fiftyfive patients received an ICD as primary prevention therapy; the remaining 13 patients as secondary prevention therapy.

Patients with positive MTWA were predominantly male, had lower LVEF, higher LVEDV, and used more often aldosteron antagonists. Scar was identified in 43 patients, with different patterns in patients with ICM and DCM. Overall, no relation was found between the presence of scar, its transmurality, and scar score (Table 1). In the multivariate analysis, only male gender and lower LVEF remained significant predictors of a positive MTWA.

Table 1. Patient characteristics

	Overall	MTWA positive	MTWA negative	p_{uni}	p_{multi}
Patients, n	68	33	35		
Men	54 (79)	30 (91)	24 (69)	0.02	0.01
Age, years (±SD)	60±11	61±10	59±13	0.35	
Etiology					
Ischemic	40 (59)	18 (54)	22 (63)	0.49	
Dilated	28 (41)	15 (46)	13 (37)		
Indication ICD					
Primary	55 (81)	28 (85)	27 (77)	0.42	
Secondary	13 (19)	5 (15)	8 (23)		
NYHA ≥3	14 (21)	7 (21)	7 (20)	0.90	
LVEF, % (±SD)	26±13	23±10	29±14	0.04	0.02
LVEDV, ml/m² (±SD)	137±39	146±41	128±37	<0.01	NS
QRS >120ms	45 (66)	21 (64)	24 (69)	0.67	
Co morbidity					
Hypertension	17 (25)	8 (24)	9 (26)	0.89	
COPD	3 (4)	2 (6)	1 (3)	0.52	
DM	9 (13)	3 (9)	6 917)	0.33	
Medication					
Beta-blocker	56 (82)	26 (79)	30 (86)	0.45	
Diuretics	49 (72)	27 (82)	22 (63)	0.08	NS
ACE-i/ AT-II antagonist	58 (85)	29 (88)	29 (83)	0.56	
Scar Characteristics					
Scar	49 (73)	22 (67)	27 (79)	0.24	
Transmural	20 (29)	9 (24)	12 (34)	0.36	

All values are numbers (percentage) unless otherwise specified. * - median (range). ICD – implantable cardioverter defibrillator, LVEF – left ventricular ejection fraction, LVEDV – left ventricular end diastolic volume, COPD – chronic obstructive pulmonary disease, DM – diabetes mellitus, ACE-I – Ace-inhibitor, AT-II ant – Angiotensin-II antagonist.

Patients with ischemic heart disease

There were 40 patients with ICM included in the analysis (table 2). MTWA was positive in 18 patients. In 38 patients scar was identified. In the 2 patients without scar, no clinical myocardial infarction had been documented but revascularization had been performed due to angina pectoris with significant stenosis in the coronary arteries. Including or excluding these patients from analyses did not influence the results. There was no relation between presence of scar and MTWA (p=0.27). Transmural scar was identified in 50% of the patients, with no statistical difference between MTWA positive and negative patients (p=0.53). Total infarct size was 20.4 gram in the MTWA positive patients and 21.0 gram in the MTWA negative patients (ns, p=0.88). There was also no difference in core size (11.2 vs 11.4; p=0.94), border zone size (9.3 vs 9.5, p=0.84) or wall motion score (1.9 vs 1.8, p=0.56). LVEDV was significantly higher in MTWA positive patients (140 vs 124 ml/m², p=0.05).

Table 2. Ischemic heart disease

	MTWA test result		p_{uni}
Positive			
	Negative		
Patients	18	22	
Men	17 (94)	17 (77)	0.13
Age, years (±SD)	64±9	63±11	0.69
Indication ICD			
Primary	14 (78)	17 (77)	0.97
Secondary	4 (22)	5 (23)	
NYHA ≥3	15 (83)	18 (82)	0.90
LVEF, % (±SD)	24±8	28±13	0.23
LVEDV, ml/m^2 (±SD)	140±33	124±35	0.05
EDWM, g (±SD)	149±41	138±37	0.37
QRS >120ms	11 (61)	17 (77)	0.27
Co morbidity			
Hypertension	5 (28)	6 (27)	0.97
COPD	0 (0)	1 (5)	0.36
DM	2 (11)	5 (23)	0.34
Medication			
Beta-blocker	13 (72)	20 (91)	0.12
Diuretics	14 (78)	15 (68)	0.50
ACE-i/AT-II antagonist	16 (89)	19 (86)	0.81
Scar Characteristics			
Scar	17 (95)	21 (100)	0.27
Infarct age, years (range)	12.5±10.0	7.5±7.8	0.14
Transmural	8 (44)	12 (55)	0.53
Total infarct	20.4±12.9	21.0±7.5	0.88
Core	11.2±8.1	11.4±6.2	0.92
Border zone	9.3±5.6	9.5±3.3	0.84
Wall motion score	1.9±0.6	1.8±0.5	0.56

All values are numbers (percentage) unless otherwise specified. * - median (range). ICD – implantable cardioverter defibrillator, LVEF – left ventricular ejection fraction, LVEDV – left ventricular end diastolic volume, COPD – chronic obstructive pulmonary disease, DM – diabetes mellitus, ACE-I – Ace-inhibitor, AT-II ant – Angiotensin-II antagonist.

Patients with dilated cardiomyopathy

Twenty-eight patients were included in the analysis (table 3). Positive MTWA was found in 15 patients. In 11 patients, scar was detected on the LGE-CMR, which predominantly showed a midwall enhancement pattern and more diffuse spread. In none of the patients transmurality was seen. There were no statistically significant differences between the positive tested and negative tested group regarding presence of scar. There was a trend for larger scar size in patients with a positive MTWA test (10.3 vs 2.3 g; p=0.09) There was also trends for higher LVEDV (155 vs 137 ml/m^2; p=0.09), lower LVEF (22 vs 31%; p=0.10) and more male gender (67 vs 54%; p=0.10) in the MTWA positive patients. After the multivariate analysis, male gender was associated with MTWA positivity, and a trend was seen for a association between lower EF and positive MTWA.

Table 3. Dilated Cardiomyopathy

| | MTWA test result | | p_{uni} | p_{multi} |
	Positive	Negative		
Patients	15	13		
Men	13 (67)	7 (54)	0.10	0.04
Age, years (±SD)	58±10	52±13		
Indication ICD				
Primary	14 (93)	10 (77)	0.31	
Secondary	1 (7)	3 (23)		
NYHA ≥3	4 (27)	3 (23)	1.00	
LVEF, % (±SD)	22±12	31±17	0.10	0.06
LVEDV, ml/m² (±SD)	155±50	134±41	0.09	NS
EDWM, g (±SD)	188±71	154±75	0.23	
QRS >120ms	10 (67)	7 (54)	0.70	
Co morbidity				
Hypertension	3 (20)	3 (23)	1.00	
COPD	2 (13)	0 (0)	0.48	
Diabetes	1 (7)	1 (8)	1.00	
Medication				
Beta-blocker	13 (87)	10 (77)	0.64	
Diuretics	13 (87)	7 (54)	0.10	
ACE-i/AT-II antagonist	13 (87)	10 (77)	0.64	
Scar Characteristics				
Scar	5 (33)	6 (46)	0.70	
Transmural	0 (0)	0 (0)	1.00	
Total scar size	10.3±15.9	2.3±4.44	0.09	NS

All values are numbers (percentage) unless otherwise specified. * - median (range). ICD – implantable cardioverter defibrillator, LVEF – left ventricular ejection fraction, LVEDV – left ventricular end diastolic volume, COPD – chronic obstructive pulmonary disease, DM – diabetes mellitus, ACE-I – Ace-inhibitor, AT-II ant – Angiotensin-II antagonist.

Discussion

This is the first study aimed to relate MTWA to the presence and extent of myocardial scar and/or fibrosis using LGE-CMR. Neither in patients with ICM or DCM a relationship was found between MTWA result and the presence, transmurality or extent of myocardial scar as assessed by LGE-CMR.

Both in patients with ischemic and non-ischemic CMP, myocardial scar can act as an anatomical substrate for re-entry tachycardia which can lead to potentially lethal arrhythmias. Using LGE-CMR, it is possible to visualize these scars. The patterns of scar differ between ICM and DCM.[8] In patients with ICM, areas of scar involve the subendocardium and extend up to the epicardium, resulting in a transmural scar. In contrast, in patients with DCM, scar has a more diffuse pattern,

is most commonly located in the midwall, and is unrelated to a coronary artery territory. The relation between scar size and the spontaneous occurrence of SCD or potential life-threatening VA was shown in several CMR studies. The relation was both found in patients with ICM and DCM.[13;14;15]

In the past years, MTWA has been associated with susceptibility to VA and SCD. However, its exact pathophysiological mechanism remains unknown. Besides the action potential duration restitution hypothesis and the calcium cycling hypothesis it has been suggested that MTWA might be relate to the extent of fibrosis or scar tissue.[5-7] Our present study does not support this last hypothesis, since we were not able to find a relation between the presence, transmurality or extent of myocardial scar and MTWA. However, MTWA appears to have a relation with heart failure remodelling parameters (low LVEF, large LVEDV). Male gender was also related to positive MTWA, this can be explained by higher incidence of SCD in male patients.[16]

In our study, older infarct age was related to presence of MTWA in patients with prior myocardial infarction. This is supported by earlier studies which showed increased arrhythmogenesis of myocardial scar with a peak 4-12 years after the index myocardial infarction.[17;18]

Limitations

An important limitation of this study is its small study size. Caution is required when interpreting the results and present conclusions require confirmation in larger study groups. Patients with DCM have smaller scars with lower signal intensities; therefore, utilization of the semi-automatic thresholding technique can lead to overestimating of scar score due to difficulties to differentiate scar from remote myocardium and artifacts.[19] The question whether MTWA, CMR or its combination have additional value in predicting SCD or potentially life threatening arrhythmia can only be answered after sufficient follow up data have been obtained.

Conclusion

In this relatively small study, no relation was found between the occurrence of MTWA and the presence, extent or characteristics of myocardial scar as assessed by LGE-CMR in patients with ICM and DCM. Overall there was a relation between heart failure remodeling parameters and positive MTWA.

References

(1)   Gehi AK, Stein RH, Metz LD, and Gomes JA (2005) Microvolt T-wave alternans for the risk stratification of ventricular tachyarrhythmic events: a meta-analysis. J Am Coll Cardiol 46(1):75-82.

(2)   Verrier RL, Klingenheben T, Malik M, El-Sherif N, Exner DV, Hohnloser SH, Ikeda T, Martinez JP, Narayan SM, Nieminen T, and Rosenbaum DS (2011) Microvolt T-wave alternans physiological basis, methods of measurement, and clinical utility--consensus guideline by International Society for Holter and Noninvasive Electrocardiology. J Am Coll Cardiol 58(13):1309-1324.

(3)   Zipes DP, Camm AJ, Borggrefe M, Buxton AE, Chaitman B, Fromer M, Gregoratos G, Klein G, Moss AJ, Myerburg RJ, Priori SG, Quinones MA, Roden DM, Silka MJ, Tracy C, Smith SC, Jr., Jacobs AK, Adams CD, Antman EM, Anderson JL, Hunt SA, Halperin JL, Nishimura R, Ornato JP, Page RL, Riegel B, Blanc JJ, Budaj A, Dean V, Deckers JW, Despres C, Dickstein K, Lekakis J, McGregor K, Metra M, Morais J, Osterspey A, Tamargo JL, and Zamorano JL (2006) ACC/AHA/ESC 2006 Guidelines for Management of Patients With Ventricular Arrhythmias and the Prevention of Sudden Cardiac Death: a report of the American College of Cardiology/American Heart Association Task Force and the European Society of Cardiology Committee for Practice Guidelines (writing committee to develop Guidelines for Management of Patients With Ventricular Arrhythmias and the Prevention of Sudden Cardiac Death): developed in collaboration with the European Heart Rhythm Association and the Heart Rhythm Society. Circulation 114(10):e385-e484.

(4)   Cutler MJ and Rosenbaum DS (2009) Explaining the clinical manifestations of T wave alternans in patients at risk for sudden cardiac death. Heart Rhythm 6(3 Suppl):S22-S28.

(5)   Kon-No Y, Watanabe J, Koseki Y, Koyama J, Yamada A, Toda S, Shinozaki T, Fukuchi M, Miura M, Kagaya Y, and Shirato K (2001) Microvolt T wave alternans in human cardiac hypertrophy: electrical instability and abnormal myocardial arrangement. J Cardiovasc Electrophysiol 12(7):759-763.

(6)   Pastore JM and Rosenbaum DS (2000) Role of structural barriers in the mechanism of alternans-induced reentry. Circ Res 87(12):1157-1163.

(7)   Narayan SM, Smith JM, Lindsay BD, Cain ME, and vila-Roman VG (2006) Relation of T-wave alternans to regional left ventricular dysfunction and eccentric hypertrophy secondary to coronary heart disease. Am J Cardiol 97(6):775-780.

(8)   McCrohon JA, Moon JC, Prasad SK, McKenna WJ, Lorenz CH, Coats AJ, and Pennell DJ (2003) Differentiation of heart failure related to dilated cardiomyopathy and coronary artery disease using gadolinium-enhanced cardiovascular magnetic resonance. Circulation 108(1):54-59.

(9)   Gottlieb I, Macedo R, Bluemke DA, and Lima JA (2006) Magnetic resonance imaging in the evaluation of non-ischemic cardiomyopathies: current applications and future perspectives. Heart Fail Rev 11(4):313-323.

(10)   Lim RP, Srichai MB, and Lee VS (2007) Non-ischemic causes of delayed myocardial hyperenhancement on MRI. AJR Am J Roentgenol 188(6):1675-1681.

(11)   Richter S, Duray G, and Hohnloser SH (2005) How to analyze T-wave alternans. Heart Rhythm 2(11):1268-1271.

(12)   Amado LC, Gerber BL, Gupta SN, Rettmann DW, Szarf G, Schock R, Nasir K, Kraitchman DL, and Lima JA (2004) Accurate and objective infarct sizing by contrast-enhanced magnetic resonance imaging in a canine myocardial infarction model. J Am Coll Cardiol 44(12):2383-2389.

(13)   Roes SD, Borleffs CJ, van der Geest RJ, Westenberg JJ, Marsan NA, Kaandorp TA, Reiber JH, Zeppenfeld K, Lamb HJ, de RA, Schalij MJ, and Bax JJ (2009) Infarct tissue heterogeneity assessed with contrast-enhanced MRI predicts spontaneous ventricular arrhythmia in patients with ischemic cardiomyopathy and implantable cardioverter-defibrillator. Circ Cardiovasc Imaging 2(3):183-190.

(14)   Yan AT, Shayne AJ, Brown KA, Gupta SN, Chan CW, Luu TM, Di Carli MF, Reynolds HG, Stevenson WG, and Kwong RY (2006) Characterization of the peri-infarct zone by contrast-enhanced cardiac magnetic resonance imaging is a powerful predictor of post-myocardial infarction mortality. Circulation 114(1):32-39.

(15)   Yokokawa M, Tada H, Koyama K, Naito S, Oshima S, and Taniguchi K (2009) Nontransmural scar detected by magnetic resonance imaging and origin of ventricular tachycardia in structural heart disease. Pacing Clin Electrophysiol 32 Suppl 1:S52-S56.

(16)   Rivero A and Curtis AB (2010) Sex differences in arrhythmias. Curr Opin Cardiol 25(1):8-15.

(17)   Huikuri HV, Tapanainen JM, Lindgren K, Raatikainen P, Makikallio TH, Juhani Airaksinen KE, and Myerburg RJ (2003) Prediction of sudden cardiac death after myocardial infarction in the beta-blocking era. J Am Coll Cardiol 42(4):652-658.

(18)   Pascale P, Schlaepfer J, Oddo M, Schaller MD, Vogt P, and Fromer M (2009) Ventricular arrhythmia in coronary artery disease: limits of a risk stratification strategy based on the ejection fraction alone and impact of infarct localization. Europace 11(12):1639-1646.

(19)   Neilan TG, Coelho-Filho OR, Danik SB, Shah RV, Dodson JA, Verdini DJ, Tokuda M, Daly CA, Tedrow UB, Stevenson WG, Jerosch-Herold M, Ghoshhajra BB, Kwong RY (2013) Quantification of myocardial scar provides additive prognostic information in nonischemic cardiomyopathy JACC; cardiovascular imaging 6(9):944-954.
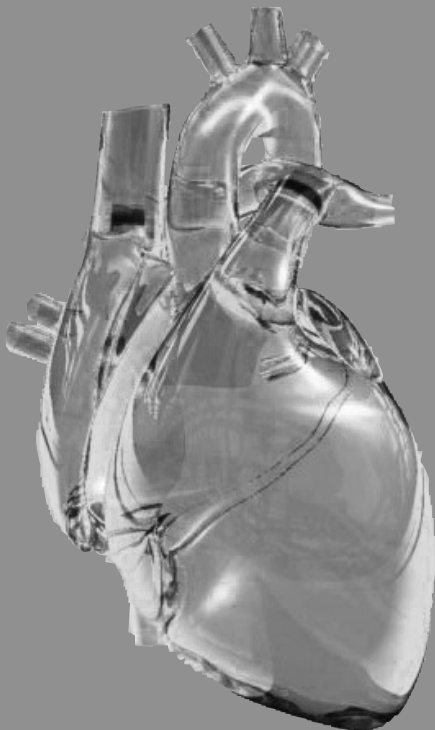
Chapter 7

The importance of cardiac MRI as a diagnostic tool in

viral myocarditis-induced cardiomyopathy

Olimulder MA, van Es J, Galjee MA.

Abstract

Myocarditis is an acute or chronic inflammatory disease of the myocardium which can be viral, post-infectious immune or primarily organ-specific autoimmune. Clinical manifestations of acute and chronic myocarditis are extremely various ranging from mild to severe. Affected patients may recover or develop (dilated) cardiomyopathy (DCM) with life threatening symptoms including heart failure, conduction disturbances, arrhythmias, cardiogenic shock or sudden cardiac death.

The diagnosis of myocarditis is a challenging process and not only because of a diverse presentation; other problems are limited sensitivity of endomyocardial biopsies (EMB) and overlapping symptoms. Furthermore, the diagnosis is not well defined. However, early diagnosis is mandatory to address specific aetiology-directed therapeutic management in myocarditis that influences patient morbidity and mortality.

Currently, EMB remains the only way to confirm the presence of viral genome and other histopathological findings allowing proper treatment to be implemented in case of myocarditis. Increased recognition of the role of myocardial inflammatory changes have given rise to interest in non-invasive imaging as a diagnostic tool, especially cardiovascular magnetic resonance imaging (CMR). In this review we discuss the current role of CMR in the evaluation of myocarditi- induced inflammatory cardiomyopathies.

Introduction

Myocarditis is a cardiac disease associated with inflammation and injury of the myocardium.[1] The term myocarditis was first introduced in the 19th century. In 1986, in an effort to standardize the diagnostic criteria, a panel consisting of eight cardiac pathologists proposed the Dallas criteria and provided a histopathological categorization by which the diagnosis of myocarditis could be established.[2] However, this classification had several pitfalls, being susceptible to variation in pathological interpretation, sampling error and not considering the exact cause of pathological findings. A clinicopathologic classification utilizing both histologic and clinical features in which four distinct subgroups were subdivided was provided in 1991 and adjusted in 2001 but it has received only limited acceptance. Acute myocarditis (AM) was categorized into a common and fulminant type depending on whether or not patients received mechanical circulatory support in the management of heart failure. Chronic myocarditis (CM) was subdivided into chronic active and chronic persistent myocarditis. There is consensus that viral infection is responsible for the vast majority of cases in North America and Europe.[3;4] Coxsackievirus B3 (CBV3) is considered the dominant viral aetiological agent.[5] Other frequently detected viral genomes are enterovirus, adenovirus, Parvovirus B19 (PVB19), human herpes virus 6 (HHV6) and Epstein-barr virus (EBV).[6]

AM must be considered in patients presenting with recent-onset of cardiac failure or arrhythmia, though the onset of clinical symptoms may be vague and clinical features are heterogeneous, ranging from asymptomatic, generalised malaise, acute heart failure, dilated cardiomyopathy and even sudden cardiac death which accounts for up to 20% of cases in young adults.[4;7] Important clues to its epidemiology come from routine post-mortem examinations where it is identified in 1% to 9%.[8]

In contrast, fulminant myocarditis (FM) is characterized by a distinct viral prodrome, a rapid onset of symptoms, extensive haemodynamic compromise and marked myocardial inflammation.[9] The clinical course is related to the type of virus; with a benign course in PVB19, and a worse progression in the setting of HHV6 with a latent state after primary infection.[10] Prognosis in biopsy proven AM is also related to histological classification and biomarkers with a higher survival rate observed in patients with FM versus an AM group.[11] A high early mortality rate of patients with myocarditis varying from 22% in the acute fulminate group to 50% in the chronic recurrent group has been observed with a high prevalence of late deaths in patients with chronic latent myocarditis.[12]

Chronic myocarditis (CM) is a common evolution of AM.[13] AM recovers spontaneously within a few weeks to months in up to 50% of patients. Nevertheless, progression of AM to CM or DCM occurs in about 21% of cases by both viral persistence and /or autoimmune self-perpetration.[14;15] In CM, a viraemia is frequently absent and intramyocardial inflammation is considerably lower than in patients with AM and thus can be detected only by using sensitive immunohistologic

techniques and nested polymerase chain rather than histological Dallas criteria. CM can be divided in chronic active myocarditis and chronic persistent myocarditis. In active CM, symptoms of moderate left ventricular dysfunction, ongoing inflammation, myocardial damage and active scar tissue are present (active or borderline myocarditis). Persistent CM often has a normal left ventricular function, atypical chest pain and persistence of inflammation. On occasion, a viral genome can be detected in biopsy sampling. Therefore CM is mainly diagnosed clinically by symptoms of left-sided chronic heart failure, especially idiopathic DCM or myocardial fibrosis. Frequently detected viral genomes in endomyocardial biopsies from patients with clinically suspected myocarditis in the past and DCM are CVB3 and B4, echovirus, adenovirus, PVB19, EBV and HHV6.[16]

The current diagnostic gold standard for the detection of myocarditis is direct visualization by autopsy or endomyocardial biopsy with the histological Dallas criteria in conjunction with new tools of immunohistochemistry and viral polymerase chain reaction, according to the 1995 World Health Organisation classification of cardiomyopathies. Although, recent data suggest that current histopathological criteria for myocardial inflammation are not sensitive to identify the population with viral or autoimmune-related heart compromise.[2] Furthermore, interpretation of bioptic findings are subjective due to a considerable interobserver variability, occurrence of complications, and the lack of standardisation in performing the biopsy.[7] However, early diagnosis is mandatory to address specific aetiology-directed therapeutic management in AM and CM which influences patients morbidity and mortality. Further, early diagnosis of myocardial involvement may permit earlier onset of heart failure treatment and expand the life span in these patients.

New insights into the role of myocardial inflammatory changes have given rise to interest in non-invasive imaging as a diagnostic tool, especially cardiovascular magnetic resonance imaging (CMR). CMR provides the opportunity of anatomical imaging and an accurate assessment of functional parameters, but in this respect more important the ability to characterise tissue. Presence of contrast enhancement (CE) indicates myocardial injury (i.e. scar, fibrosis) and T2-weighted images mark interstitial oedema, known as an integral part of the inflammatory response.

The present review therefore focuses on the current role of CMR in the evaluation of myocarditis and myocarditis-induced cardiomyopathies.

Pathophysiology myocarditis
In order to better understand the often unpredictable clinical manifestations and progression of viral myocarditis, the pathophysiological process has to be elucidated. Important lessons come largely from studies in animals.[17]

The actual underlying pathological mechanism remains controversial, though three mechanisms have been proposed. During the first acute phase (days 0 to 3), direct excessive destruction of

the myocardium occurs by infiltrating immune cells targeting virus-infected cardiomyocytes, within 3 days after infection, frequently extending to the remote uninfected region. A high titre of virus is present in the blood. The initial phase frequently passes unnoticed since the initial damage is often prevented by the innate immune response. The second subactue phase (days 4 to 14) develops as a result of autoimmune-mediated destruction of cardiac cells by circulating autoantibodies and/or autoreactive immune cells or by immune-mediated obliteration of cardiomyocytes which is caused by mimicked epitopes shared between viral and cardiac antigens. Finally, in the third chronic phase (days 15 to 90), viral particles are typically absent in blood and peripheral tissues. Viral RNA persistence and immune infiltrates may contribute to long-term tissue degeneration and a typical picture of DCM, and congestive heart failure develops as a result of direct virus-induced cardiomyocyte injury.[5;18;19]

Myocarditis induced (dilated) cardiomyopathy

In 20% of cases, acute myocarditis progresses to DCM.[20] Evidence suggests that a viral mechanism not only contributes to the acute phase of myocarditis but also to the evolution of ongoing cardiac disease. The persistence of a higher incidence of neutralising antibodies to (coxsackie B) viruses in patients with cardiomyopathy than in age-, sex-, race-, and geographic-matched control subject pointed to the theory of a viral cause underlying the pathogenesis of cardiomyopathy.[19] A substantial proportion (10 to 34%) of DCM patients may in fact suffer from viral myocarditis.[9;17] DCM, a major cause of heart failure and cardiac transplantation, is characterised by dilatation and impaired contraction of the ventricles. The clinical manifestation of DCM and a history of acute viral myocarditis does not confirm a CM. Three possible mechanisms for the development of DCM as a consequence of an episode of CBV myocarditis have been described.[21] The first proven mechanism is developing of DCM in an acute or subacute timeframe as a direct cytotoxic effect subsequent to an episode of myocarditis. The second potential (hypothetical) mechanism comprises a slow, chronic and continuous destruction of cardiac myocytes or impairment of myocyte function. The third mechanistic possibility is that of DCM developing long after complete resolution of the initial episode of myocarditis. DCM develops as a result of an undefined process in which an episode of remote viral infection renders the healed myocardium more susceptible to the remote development of idiopathic DCM. Mutations in several genes encoding structural proteins of the myocyte can cause DCM, but the gene defects identified so far appear to account for a minority of cases. Recently, increasing evidence has emerged that a substantial portion of patients of myocarditis and DCM represents different stages of an organ-specific autoimmune disease in genetically predisposed individuals.[22]

CMR in the acute and chronic phase of myocarditis

Recent studies have demonstrated that CMR has shown promising results in the early diagnosis and the follow-up of AM and its subsequent stages. CMR includes several techniques that can be used in various combinations to assess left ventricular (LV) functional parameters, morphology, myocardial perfusion, and myocardial disorders within one examination.[23]

Besides significantly lower ejection fractions and wall motion abnormalities in patients with AM, two relevant contrast-enhancement CMR (CE-CMR) approaches have been found to be effective in identifying areas of myocardial damage in AM. Myocardial global relative enhancement (gRE) reflects myocardial hyperaemia and increased capillary permeability as features of present inflammation, whereas late CE-CMR mostly indicates irreversible myocardial injury. GRE (T1-weighted imaging pre- en post contrast, used to calculate gRE from the mean signal intensities (SI) within the manually outlined borders around the LV myocardium and right erector spinae muscle) has been observerd significantly more often in myocarditis patients compared with controls.[14;24] CE-CMR enables visualisation of myocardial damage in patients with myocarditis after intravenous injection of gadolinium. Due to different wash-in and wash-out kinetics, areas with myocardial changes, such as scarring, fibrosis and oedema retain gadolinium for prolonged periods. This provides an opportunity to visualise areas of myocarditis defined by histopathology, with a reported sensitivity of 100% and specificity of 90%.[25] Presence of late CE is reported in 44% - 95% of patients with myocarditis.[10;25] In acute myocarditis, CE is frequently located in the lateral wall originating from the epicardial quartile, though the pattern of myocardial injury is influenced by the virus type.[26] According to CE patterns, this technique is also capable of ruling out an ischaemic cause in the differential diagnosis of myocarditis because CE patterns in the setting of ischaemic infarction always includes the subendocardial layer of the myocardium (figure 1).[4] Enhancement patterns in myocarditis generally exclude the subendocardium with the exception of eosinophilic myocarditis frequently involving the endomyocardium (figure 2).[27;28] Further, the type of virus and pattern of myocardial damage are related. CE in the lateral free wall is found in the majority of PVB19 patients, whereas in HHV6 myocarditis, CE frequently is observed in the midwall of the interventricular septum (figure 3).[10] Thus CE not only differentiates between myocarditis or infarction, it can also differentiate between various viral origins.

Another interesting CMR approach in acute myocarditis is T2-weighted imaging, a pulse sequence sensitive to regional or global increases of myocardial water, a substantial feature of the inflammatory response in human myocarditis.[15;24] A combined CMR approach using blackblood T2-weighted imaging and CE-CMR showed a significantly higher T2 SI in patients with myocarditis.

An alternative acquisition mode for imaging oedema in myocarditis could be the T2-prepared steady state free precession (SSPF) technique which is more reliable in acute myocardial infarction. It provides fewer artifacts and has better diagnostic accuracy than convential dark blood acquisitions.[29] The parameters described above are also of utmost importance in the clinical follow-up and in the evaluation of the response to the initiated treatment.

MRI can also play an important role in the diagnosis of the chronic phase of myocarditis as the aetiology of DCM. As noted earlier, chronic myocarditis can be divided in chronic active myocarditis and chronic persistent myocarditis. In patients clinically suspected of CM, viraemia is often absent. Therefore, CM is mainly diagnosed clinically by the presence of chronic heart failure, especially idiopathic DCM or myocardial fibrosis. CMR is capable of accurate detection of myocardial fibrosis in DCM. Global relative enhancement (gRE) may be useful in the non-invasive detection of inflammatory processes of the myocardium. Beside increased oedema ratio (ER) from T2-weighted imaging, increased gRE was a common finding in suspected chronic myocarditis that could be confirmed at immunohistologic analysis.[14] CE-CMR confirmed areas of myocardial inflammation in 70% of patients with biopsy-proven CM presenting with heart failure or ventricular arrhythmias.[13] A frequent pattern of CM in CE-CMR is midwall- or subepicardial enhancement generally exluding the subendocardium. Evaluated CM subgroups (histologic evidence of active myocarditis and borderline myocarditis) reveal different enhancement patterns. In both groups, the group with histological evidence of active myocarditis and the group with with borderline myocarditis, a mid-wall pattern is a frequent finding (figure 4). Though, a pattern of subepicardial CE is only observed in patients with histological evidence of active myocarditis.[13] Enhancement patterns seen on CE-CMR may also serve as a map for the exact location to accomplish endomyocardial biopsy if necessary; thus enhancing the diagnostic accuracy of endomyocardial biopsy.
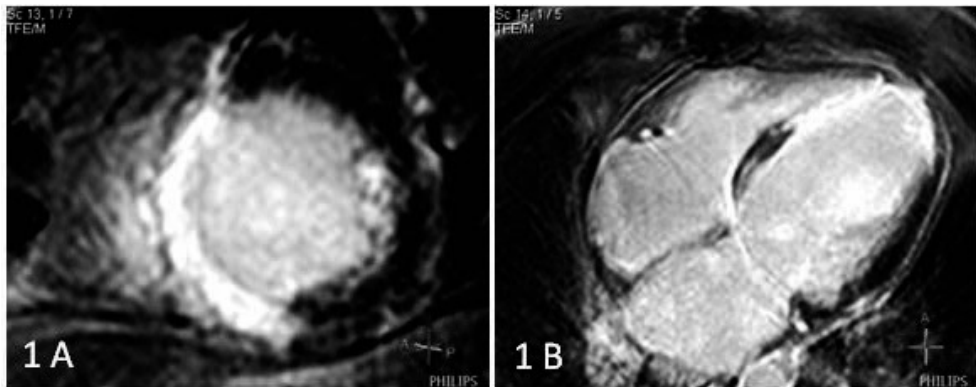

Figure 1. Ischemic anteroseptal infarction. **A:** Short axis view showing a transmural pattern of delayed enhancement in the anteroseptal wall. **B:** 4 chamber view showing a transmural pattern of delayed enhancement in the inferoseptal and apical wall.
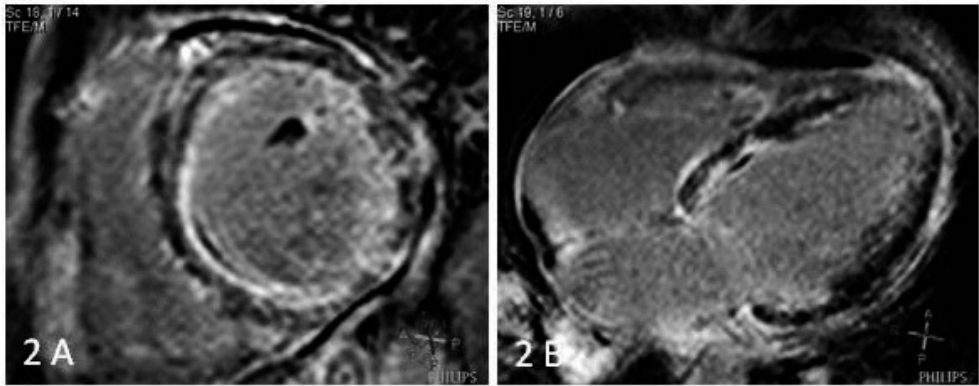
Figure 2. Eosinophilic myocarditis. **A:** Short axis view showing a pattern of subendocardial and midwall delayed enhancement in the anteroseptal and inferoseptal wall. **B**: 4 chamber view showing subendocardial and midwall delayed enhancement in the inferioseptal wall.
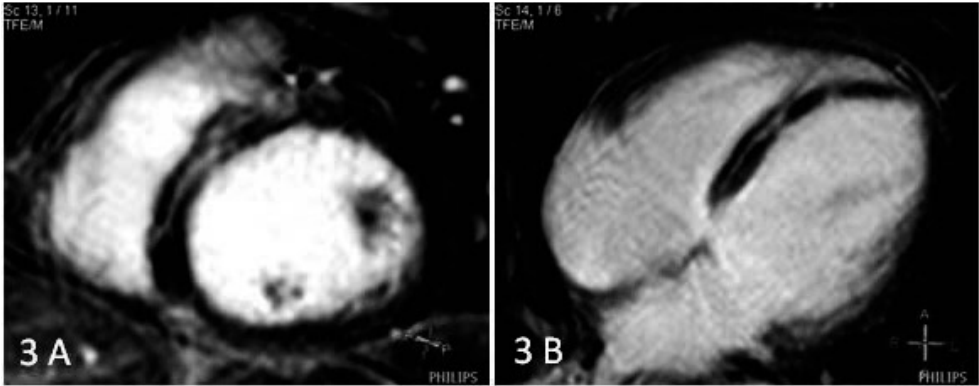
Figure 3. Myocarditis. **A:** Short axis view and 4 chamber view showing a pattern of midwall delayed enhancement in the septal wall. **B:** 4 chamber view showing a pattern of midwall delayed enhancement in the inferoseptal wall.
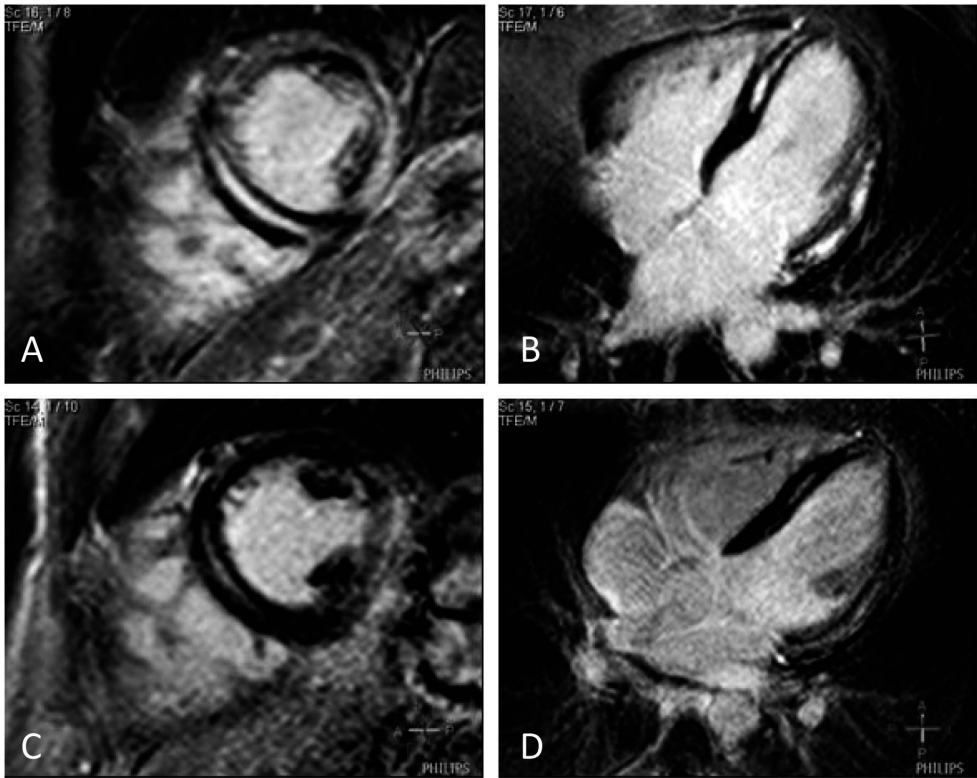
Figure 4. Acute and chronic phase of myocarditis in a patient. **A, B**: Acute myocarditis: short-axis view and four-chamber view showing an extensive pattern of midwall contrast enhancement. Only the basal septal wall and distal anterolateral wall are spared. **C,D**: Chronic myocarditis: short-axis and four-chamber view showing the same pattern of midwall delayed contrast enhancement with lower signal intensity.

Therapeutic management

The diagnosis of myocarditis has relevant therapeutic implications. Supportive care is the first-line therapy for patients with myocarditis. Treatment of myocarditis-induced cardiac failure includes the standard regimen (including diuretics to lower ventricular filling pressures, an angiontensin-converting-enzyme inhibitor to decrease vascular resistance, and a beta-blocker after achievement of clinical stability). Arrhythmias should be monitored and treated. Mechanical support with an intra-aortic balloon pump or LV assist device as a bridge to recovery or heart transplantation may be necessary in cases that fail to improve.[18]

Apart from symptomatic or supportive therapy, additional treatments are investigated for myocarditis because long-term consequences of myocarditis appear to be related to the activation of cellular and humoral autoimmunity.[19] A variety of immunosuppressive agents and intravenous imunoglobulins caused marked improvement. Interferon-B treatment resulted in elimination of viral genomes (22 of 22 patients) and improved left ventricular function (assessed

echocardiographically; 15 of 22 patients) in patients with enteroviral or adenoviral persistence.[30] In a serie of ten patients with new-onset DCM treated with high-dose immune globulin, echocardiographic left ventricular ejection fraction (LVEF) improved 17 EF units.[31] The Marburg registry also favors intravenous immunoglobulin treatment in biopsy-proven adenovirus and parvovirus B19 myocarditis combined with optimal conventional therapy to achieve virus clearance.[32] A subset of patients with CM, those expressing class I and II human lymphocyte antigen on cardiac myocytes may have a response to azathioprine and prednisone.[8]

Other results did not support routine treatment of myocarditis with immunosuppressive drugs. Additional treatments did not have a real advantage over standard treatment for heart failure; no beneficial effect on the primary endpoint, angiographically determined LVEF, was seen.[33] Actually, a mild negative influence on left ventricular dimensions was observed.[34]

There is evidence that intramyocardial viral persistence is associated with progressive ventricular dysfunction, whereas spontaneous viral elimination was associated with a significant improvement in LV function.[16] Though, another study showed that an advanced New York Heart Association functional class, immunohistological signs of inflammation, and lack of β-blocker therapy, but not histology (positive Dallas criteria) or viral genome detection, are related to poor outcome. With regard to as yet unestablished antiviral or immunosuppressive treatment strategies, according to these authors it is mandatory to differentiate chronic active viral myocarditis, (myocardial viral infection with cellular inflammation), from postviral autoimmunity and from harmless latent viral persistence without inflammatory infiltrates to address specific aetiology-directed therapeutic management.[7]

Unfortunately, randomized clinical trials highlighting the clinical importance of CMR visualising the extent of endomyocardial involvement and response of a therapeutic regimen have not been performed. However, a number of cases and case series have been reported, illustrating the usefulness of CE-CMR in the evaluation of the response to the initiated treatment in patients with myocarditis.[28;35-37]

Conclusion

With current insights into the knowledge of progression of AM to CM or DCM with life-threatening symptoms, we emphasise the importance of a correct diagnosis of myocarditis.

This can be done non-invasively with a high diagnostic accuracy, by using a combined approach with cine CMR, early and late CE-CMR and T2 acquisitions. Evidence of persisting inflammatory activity detected with CMR in AM and CM may have relevant prognostic implications and serve as a powerful tool to triage patients for appropriate treatment. CMR can also monitor the left ventricular functional parameters and the regression of myocardial inflammation in patients undergoing a therapeutic regimen.

We recommend this combined CMR approach in patients suspected of having myocarditis as a valuable non-invasive diagnostic imaging tool in identifying areas of myocardial damage that suggest a myocardial inflammatory process. CMR is also a valuable research tool. The conflicting results of specific treatment, such as antiviral or immunosuppressive medication, need at least randomised trials before a final statement can be made on the value of CMR data to visualise the improvement of left ventricular functional parameters and the extent of myocardial involvement.

References

(1)   Caforio AL, Mahon NJ, Tona F, McKenna WJ. Circulating cardiac autoantibodies in dilated cardiomyopathy and myocarditis: pathogenetic and clinical significance. Eur J Heart Fail 2002 August;4(4):411-7.

(2)   Baughman KL. Diagnosis of myocarditis: death of Dallas criteria. Circulation 2006 January 31;113(4):593-5.

(3)   Liu PP, Mason JW. Advances in the understanding of myocarditis. Circulation 2001 August 28;104(9):1076-82.

(4)   Kadalie CT. [MRI in chronic myocarditis]. Z Kardiol 2005;94 Suppl 4:IV/94-IV/96.

(5)   Esfandiarei M, McManus BM. Molecular biology and pathogenesis of viral myocarditis. Annu Rev Pathol 2008;3:127-55.

(6)   Caforio AL, Calabrese F, Angelini A et al. A prospective study of biopsy-proven myocarditis: prognostic relevance of clinical and aetiopathogenetic features at diagnosis. Eur Heart J 2007 June;28(11):1326-33.

(7)   Kindermann I, Kindermann M, Kandolf R et al. Predictors of outcome in patients with suspected myocarditis. Circulation 2008 August 5;118(6):639-48.

(8)   Skouri HN, Dec GW, Friedrich MG, Cooper LT. Noninvasive imaging in myocarditis. J Am Coll Cardiol 2006 November 21;48(10):2085-93.

(9)   Lieberman EB, Herskowitz A, Rose NR, Baughman KL. A clinicopathologic description of myocarditis. Clin Immunol Immunopathol 1993 August;68(2):191-6.

(10)   Mahrholdt H, Wagner A, Deluigi CC et al. Presentation, patterns of myocardial damage, and clinical course of viral myocarditis. Circulation 2006 October 10;114(15):1581-90.

(11)   McCarthy RE, III, Boehmer JP, Hruban RH et al. Long-term outcome of fulminant myocarditis as compared with acute (nonfulminant) myocarditis. N Engl J Med 2000 March 9;342(10):690-5.

(12)   Kodama M, Oda H, Okabe M, Aizawa Y, Izumi T. Early and long-term mortality of the clinical subtypes of myocarditis. Jpn Circ J 2001 November;65(11):961-4.

(13)   De CF, Pieroni M, Esposito A et al. Delayed gadolinium-enhanced cardiac magnetic resonance in patients with chronic myocarditis presenting with heart failure or recurrent arrhythmias. J Am Coll Cardiol 2006 April 18;47(8):1649-54.

(14)   Gutberlet M, Spors B, Thoma T et al. Suspected chronic myocarditis at cardiac MR: diagnostic accuracy and association with immunohistologically detected inflammation and viral persistence. Radiology 2008 February;246(2):401-9.

(15)   Zagrosek A, Wassmuth R, bdel-Aty H, Rudolph A, Dietz R, Schulz-Menger J. Relation between myocardial edema and myocardial mass during the acute and convalescent phase of myocarditis--a CMR study. J Cardiovasc Magn Reson 2008;10(1):19.

(16)   Kuhl U, Pauschinger M, Seeberg B et al. Viral persistence in the myocardium is associated with progressive cardiac dysfunction. Circulation 2005 September 27;112(13):1965-70.

(17)   Feldman AM, McNamara D. Myocarditis. N Engl J Med 2000 November 9;343(19):1388-98.

(18)   Dennert R, Crijns HJ, Heymans S. Acute viral myocarditis. Eur Heart J 2008 July 9.

(19)   Kawai C. From myocarditis to cardiomyopathy: mechanisms of inflammation and cell death: learning from the past for the future. Circulation 1999 March 2;99(8):1091-100.

(20)   Noutsias M, Pauschinger M, Kuhl U, Schultheiss HP. [Myocarditis and dilated cardiomyopathy. New methods in diagnosis and therapy]. MMW Fortschr Med 2002 April 4;144(14):36-40.

(21)   Spotnitz MD, Lesch M. Idiopathic dilated cardiomyopathy as a late complication of healed viral (Coxsackie B virus) myocarditis: historical analysis, review of the literature, and a postulated unifying hypothesis. Prog Cardiovasc Dis 2006 July;49(1):42-57.

(22)   Caforio AL, Iliceto S. Genetically determined myocarditis: clinical presentation and immunological characteristics. Curr Opin Cardiol 2008 May;23(3):219-26.

(23)   Shehata ML, Turkbey EB, Vogel-Claussen J, Bluemke DA. Role of cardiac magnetic resonance imaging in assessment of nonischemic cardiomyopathies. Top Magn Reson Imaging 2008 February;19(1):43-57.

(24)   bdel-Aty H, Boye P, Zagrosek A et al. Diagnostic performance of cardiovascular magnetic resonance in patients with suspected acute myocarditis: comparison of different approaches. J Am Coll Cardiol 2005 June 7;45(11):1815-22.

(25) Mahrholdt H, Goedecke C, Wagner A et al. Cardiovascular magnetic resonance assessment of human myocarditis: a comparison to histology and molecular pathology. Circulation 2004 March 16;109(10):1250-8.

(26) Yelgec NS, Dymarkowski S, Ganame J, Bogaert J. Value of MRI in patients with a clinical suspicion of acute myocarditis. Eur Radiol 2007 September;17(9):2211-7.

(27) Bohl S, Wassmuth R, bdel-Aty H et al. Delayed enhancement cardiac magnetic resonance imaging reveals typical patterns of myocardial injury in patients with various forms of non-ischemic heart disease. Int J Cardiovasc Imaging 2008 August;24(6):597-607.

(28) Deb K, Djavidani B, Buchner S et al. Time course of eosinophilic myocarditis visualized by CMR. J Cardiovasc Magn Reson 2008;10(1):21.

(29) Kellman P, Aletras AH, Mancini C, McVeigh ER, Arai AE. T2-prepared SSFP improves diagnostic confidence in edema imaging in acute myocardial infarction compared to turbo spin echo. Magn Reson Med 2007 May;57(5):891-7.

(30) Kuhl U, Pauschinger M, Schwimmbeck PL et al. Interferon-beta treatment eliminates cardiotropic viruses and improves left ventricular function in patients with myocardial persistence of viral genomes and left ventricular dysfunction. Circulation 2003 June 10;107(22):2793-8.

(31) McNamara DM, Rosenblum WD, Janosko KM et al. Intravenous immune globulin in the therapy of myocarditis and acute cardiomyopathy. Circulation 1997 June 3;95(11):2476-8.

(32) Karatolios K, Pankuweit S, Maisch B. Diagnosis and treatment of myocarditis: the role of endomyocardial biopsy. Curr Treat Options Cardiovasc Med 2007 December;9(6):473-81.

(33) McNamara DM, Holubkov R, Starling RC et al. Controlled trial of intravenous immune globulin in recent-onset dilated cardiomyopathy. Circulation 2001 May 8;103(18):2254-9.

(34) Mason JW, O'Connell JB, Herskowitz A et al. A clinical trial of immunosuppressive therapy for myocarditis. The Myocarditis Treatment Trial Investigators. N Engl J Med 1995 August 3;333(5):269-75.

(35) Allanore Y, Vignaux O, Arnaud L et al. Effects of corticosteroids and immunosuppressors on idiopathic inflammatory myopathy related myocarditis evaluated by magnetic resonance imaging. Ann Rheum Dis 2006 February;65(2):249-52.

(36) Fenster BE, Chan FP, Valentine HA et al. Images in cardiovascular medicine. Cardiac magnetic resonance imaging for myocarditis: effective use in medical decision making. Circulation 2006 June 6;113(22):e842-e843.

(37) Dill T, Ekinci O, Hansel J, Kluge A, Breidenbach C, Hamm CW. Delayed contrast-enhanced magnetic resonance imaging for the detection of autoimmune myocarditis and long-term follow-up. J Cardiovasc Magn Reson 2005;7(2):521-3.
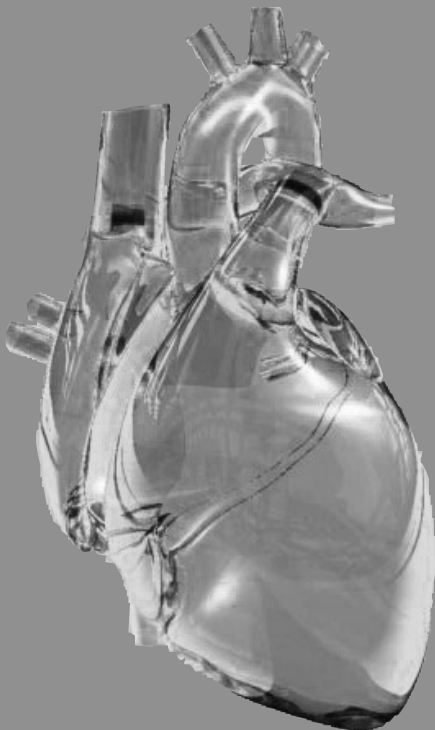
Chapter 8

Combined Cardiac Magnetic Resonance Imaging of cardiac dimensions, left ventricular function, and myocardial tissue characteristics in female patients with chronic fatigue syndrome

Olimulder MA, Galjee MA, Wagenaar LJ, van Es J, van der Palen J, Visser FC, Vermeulen RC, von Birgelen C.

Submitted

Abstract

Purpose: In chronic fatigue syndrome (CFS), only a few imaging and histopathological studies previously assessed either cardiac dimensions/function or myocardial tissue, suggesting smaller left ventricular (LV) dimensions, LV wall motion abnormalities (WMA), and occasionally viral persistence that may lead to cardiomyopathy. The present CMR study is the first to use a combined approach to assess cardiac involvement in CFS patients.

Methods: In a consecutive series of 12 female CFS patients, CMR measurements were compared with 36 age-matched, female controls. With cine images, LV volumes, ejection fraction (EF), mass, and WMA were assessed. T2-weighted images were analyzed for increased signal intensity, reflecting edema (i.e. inflammation). Presence of CE, reflecting fibrosis (i.e. myocardial damage), was also analyzed.

Results: When comparing CFS patients and controls, LVEF (57.9±4.3% vs. 63.7±3.7%;p<0.01), end-diastolic diameter (44±3.7mm vs. 49±3.7mm;p<0.01), as well as body surface area (BSA)-corrected LV end-diastolic volume (77.5±6.2ml/m2 vs. 86.0±9.3ml/m2;p<0.01), LV stroke volume (44.9±4.5ml/m2 vs. 54.9±6.3ml/m2;p<0.001), and LV mass (39.8±6.5g/m2 vs. 49.6±7.1g/m2;p=0.02) were significantly lower in CFS patients. WMA was observed in four CFS patients and CE (fibrosis) in three; none of the controls showed WMA or CE. None of the patients or controls showed increased signal intensity on the T2-weighted images.

Conclusion: In patients with CFS, CMR demonstrated relatively lower dimensions and a mildly reduced function of the left ventricle. The presence of myocardial fibrosis in some CFS patients suggests that further assessment of cardiac involvement is warranted as part of a further scientific exploration of CFS disease. This may imply serial non-invasive CMR examinations.

Introduction

Chronic fatigue syndrome (CFS) is relatively common with an estimated worldwide prevalence of 0.4-1%.[1] Diagnosis of CFS relies on the presence of overwhelming fatigue in combination with a cluster of clinical symptoms.[1-3] Various potential etiologies, including infectious, immunological, neuroendocrine and psychiatric, have been discussed. Ongoing research suggests that latent (chronic active) myocardial infection with Epstein-Barr virus or Human Cytomegalovirus may trigger CFS.[4;5] In this setting, myocardial fibrosis can be present.[6] In patients with CFS, cardiac involvement was reported such as reduced left ventricular dimensions, decreased left ventricular ejection fraction (LVEF), LV wall motion abnormalities (WMA), and even cardiomyopathy with virus persistence in the myocardium.[7] Biopsy samples taken from the myocardium of CFS patients previously demonstrated the presence of cardiomyopathic changes including hypertrophy, disarray, and degeneration of myofibers.[8-10]

Cardiac magnetic resonance imaging (CMR) may be useful for non-invasive assessment of cardiac involvement in patients with CFS. This technique permits the assessment of cardiac morphology and function, and even tissue characterization.[11] Contrast enhanced (CE)-CMR allows the identification of myocardial fibrosis. T2-weighted CMR imaging, on the other hand, allows the visualization of myocardial edema and may be useful for staging myocarditis.[12] To the best of our knowledge, the present CMR study in patients with confirmed CFS is *the first to use a combined CMR approach of cine, contrast enhanced (CE), and T2-weighted imaging* to assess cardiac dimensions and function, and tissue characteristics such as edema or myocardial fibrosis – the consequences of myocardial inflammation.

Methods

Study population. We studied a total of 48 females with a combined CMR approach. A consecutive series of 12 patients with CFS were recruited from a specialized CFS center, to be examined with CMR. The diagnosis of CFS was based on the revised case definition by Fukuda et al.(1) after ruling out other potential causal diseases. Measurements in the 12 CFS patients were then compared with 36 age-matched, healthy female volunteers (compare group), who gave their informed consent prior to CMR examination. The study complied with the Declaration of Helsinki for investigation in human beings, and was performed after approval and supervision of our institutional ethics committee.

CMR data acquisition. CMR examination was performed on a 1.5-T whole body scanner (Achieva scan, Philips Medical System, Best, the Netherlands) using commercially available cardiac CMR software. For signal-reception, a five-element cardiac synergy coil was used. Electrocardiogram

triggering was done with a vector-electrocardiogram-set-up. Subjects were examined in the supine position. Morphologic images in the standard views were acquired by using fast field echo cine images (slice thickness 8.0mm; repetition time 3.4ms; echo time 1.7ms; flip angle 60°; matrix 256×256).

Subsequently, a breath-hold, black-blood, T2-weighted double-inversion recovery sequence with a fat-saturation pulse was performed in 8-10 short-axis slices, with the following parameters: repetition time 1800-2400ms; echo time 80ms; matrix 256x256; field of view 32-40cm; slice thickness 12mm; number of excitations 1. Myocardial scar was assessed on CE multislice standard views, obtained approximately 10 minutes after intravenous bolus injection of 0.2mmol gadolinium per kilogram body weight (Shering AG, Berlin, Germany). A three-dimensional Turbo Field Echo-inversion recovery T1-weighted sequence was used with the following parameters: repetition time 4.0ms; echo time 1.3ms; flip angle 15°; inversion time individually optimized to null myocardial signal (usually between 180-250ms); matrix 157; slice thickness 10-12mm).

CMR data analysis and definitions. CMR data were analyzed on a workstation using dedicated software for cardiac analysis (Philips MR workspace, Release 2.5.3.0 2007-12-03; Philips, the Netherlands). Left ventricular end-diastolic (EDV; ml) and end-systolic volumes (ESV; ml), stroke volume (SV; ml), left ventricular ejection fraction (LVEF; %) cardiac output (CO; l/min), and end-diastolic wall mass (EDWM; g) were calculated from contiguous short-axis loops by segmentation of endocardial and epicardial borders on each frame. Papillary muscles were regarded as part of the ventricular cavity.

The left ventricular wall regions were divided into 17 segments according to a standardized myocardial segmentation model.[13] Normal wall motion was assigned a score of 0, mild hypokinesia 1, severe hypokinesia 2, akinesia 3, and dyskinesia as 4. The wall motion score index (WMSI) was calculated by dividing the sum of scores in each segment by the total number of observed segments. T2-weighted images were considered abnormal if within the myocardium increased signal intensity was (visually) observed.

The CE images were independently evaluated by three experienced observers, who were blinded to patient/control characteristics and to the evaluations of each other. The CE was defined as zone of hyper-enhancement on the late contrast-enhanced images (in contrast with the dark-gray signal of the normal myocardium). The studies were considered as abnormal when at least two independent observers described the same abnormalities with agreement in both presence of CE and CE location (same segment), reproducible in more than one contiguous slice and in more than one projection.

Statistical analysis. Continuous variables had a normal distribution and were expressed as mean ± standard error. Categorical data were expressed as frequencies and percentages. To compare our CMR findings in CFS patients, we used age and gender-matched controls. Student's t-test and Mann-Whitney U test were used to compare continuous variables, and chi-square test and Fisher exact test were used to compare categorical variables. A P value <0.05 was considered statistically significant.

Results

Patient characteristics. Twelve female CFS patients and 36 age and gender-matched controls wer analyzed in this study. The patients and controls were relatively young (36±13 vs. 29±8 years).

All but one CFS patient had a history of infectious mononucleosis disease with IgG-antibodies to Epstein-Barr virus or Human Cytomegalovirus capsid antigen; all of these eleven patients had antibodies to Epstein-Barr virus nuclear antigen. Demographics and baseline characteristics did not differ between both groups. (see also Table 1.)

Table 1. Baseline demographics of CFS patients and age-matched control group of normal, female subjects.

Variables	CFS patients	Control group	P value
Age (y)	36±3	29±8	0.11
Female patients n (%)	12 (100%)	36 (100%)	NA
Body height (cm)	168±6.6	171±6.4	0.28
Body weight (kg)	60.3±9.6	64.7±8.8	0.16
BMI	21.3±2.2	22.2±2.5	0.24
BSA	1.7±0.2	1.7±0.3	0.78
HR (beats/min)	80±16	70±13	0.09
SBP (mm/hg)	133±1	124±17	0.18
DBP (mm/hg)	77±8	75±12	0.63

Data are expressed as mean ± standard deviation or frequencies and percentages. BMI = body mass index, BSA = body surface area, HR = heart rate, SBP = systolic blood pressure, DBP = diastolic blood pressure, NA = not applicable

CMR results. The complete CMR examination protocol was followed in all CFS patients and controls; image sequences of a high quality could be obtained in all cases. CMR data of our CFS population are presented in Table 2. In CFS patients, LVEF (57.9±4.3%; p<0.01), end-diastolic diameter (44±3.7), as well as body surface area (BSA)-corrected end-diastolic LV volume (77.5±6.2ml/m^2; p<0.01), LV stroke volume (44.9±4.5ml/m^2; p<0.001), and LV wall mass (39.8±6.5g/m^2; p=0.02) were significantly lower than age and gender-matched controls. Mild wall motion abnormalities were observed in four CFS patients in the basal and/or mid inferoseptal wall, leading to a WMSI of 0.02±0.04; none of the controls showed WMAs. Myocardial damage

(i.e. fibrosis), as indicated by the presence of CE, was observed in three patients who showed such lesions in the basal inferoseptal, septal, and anteroseptal midwall segments. No CE was seen in healthy controls. Examples are presented in Figure 1-4. Only one patient showed both CE and WMA. Regional or global edema, as indicated by an increased signal intensity on T2-weighted images, was not observed in any patient.

Table 2. CMR findings in CFS patients and comparison with an age-matched control group of normal, female subjects.

Variables	CFS patients	Control group	Mean difference + 95% CI	P value
LVEDD (mm)	44 ±3.7	49±3.7	5 (2.68-7.66)	<0.05
EDV (ml)	129.8 ±16.0	148.9±19.0	19.1 (6.75-31.47)	<0.05
EDV/BSA (ml/ m²)	77.5 ±6.2	86.0±9.3	8.4 (2.58-14.27)	<0.05
LVESD (mm)	29.7 ±4.1	30.5±3.2	0.8 (-1.48-3.18)	0.47
ESV (ml)	54.7 ±10.1	54.0±9.2	0.7 (-6.99-5.71)	0.84
ESV/BSA (ml/ m²)	32.6 ±4.0	30.9±4.8	1.7±1.6 (-4.92-1.48)	0.29
IVS (mm)	7.9 ±0.9	8.1±1.1	0.3 (-0.44-0.97)	0.46
EDWM (g)	60.6 ±10.6	86.6±11.7	26.0 (18.30-33.70)	<0.05
EDWM/BSA (g/ m²)	39.8 ±6.5	49.6±7.1	9.9 (5.16-14.59)	<0.05
SV (ml)	75.0 ±8.9	96.2±11.7	21.2 (13.68-28.73)	<0.05
SV/BSA (ml/ m²)	44.9 ±4.5	54.9±6.3	10.0 (6.07-14.03)	<0.05
CO (l/min)	4.9 ±1.3	6.6±1.2	1.7 (0.77-2.56)	<0.05
LVEF (%)	57.9 ±4.3	63.7±3.7	5.8 (3.19-8.41)	<0.05
WMSI	0.02 ±0.04	0.00±0.00	0.02 (-0.04- -0.01	0.054
T2 weighted oedema (presence, n)	0	NA	NA	
CE (presence, n)	3	0		

Data are expressed as mean ± standard deviation or frequencies and percentages, CI= confidence interval, LVEDD = left ventricle end-diastolic diameter, EDV end-diastolic volume, BSA = body surface area, LVESD = left ventricle end systolic diameter, ESV = end-systolic volume, IVS, interventricular septum, EDWM = end-diastolic wall mass, SV = stroke volume, SVI = stroke volume index, CO = cardiac output, LVEF = left ventricle ejection fraction, WMSI = wall motion score index, CE = contrast enhancement, NA = not applicable
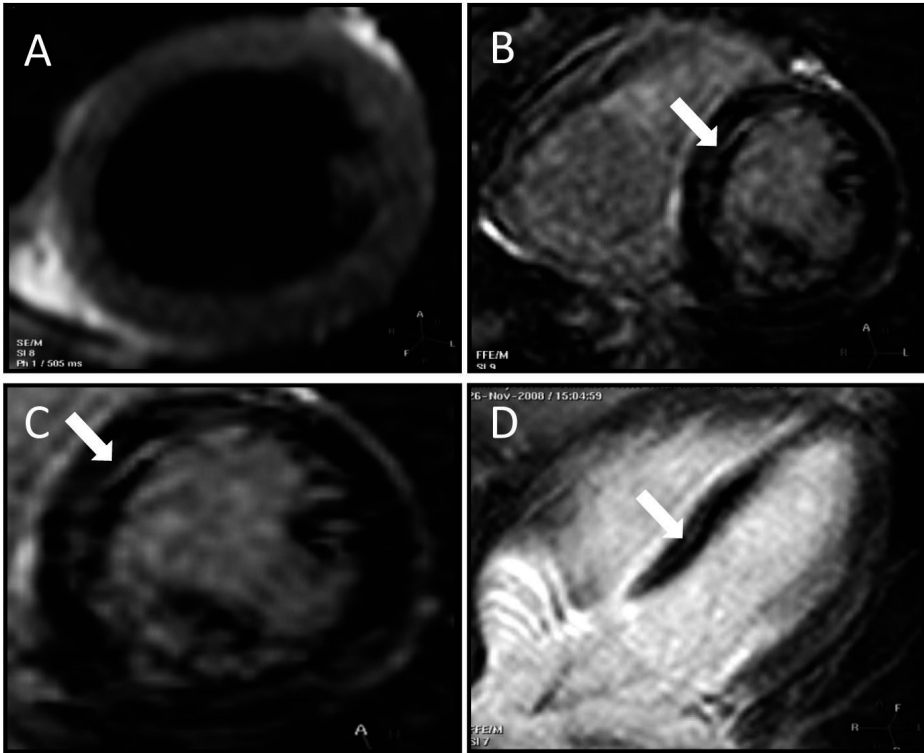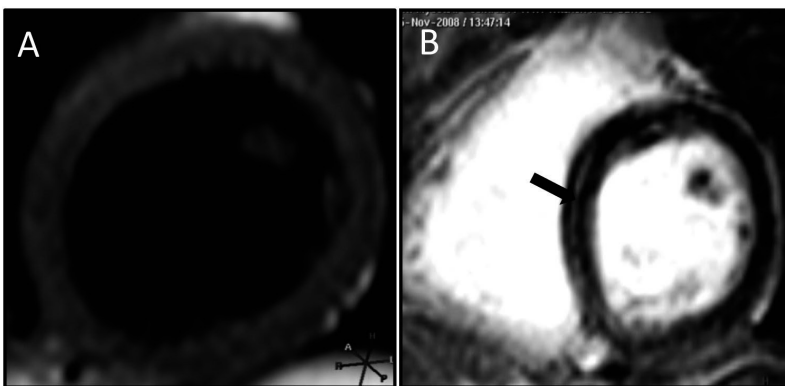
Figure 1. CMR findings in CFS patient 1.
Patient 1. **A:** T2-weighted CMR imaging short-axis view; no presence of increased SI was observed. **B,C,D**: CE-CMR imaging short-axis view and four chamber view; arrow demonstrates midwall CE in the basal inferoseptal, septal, and anteroseptal segments.
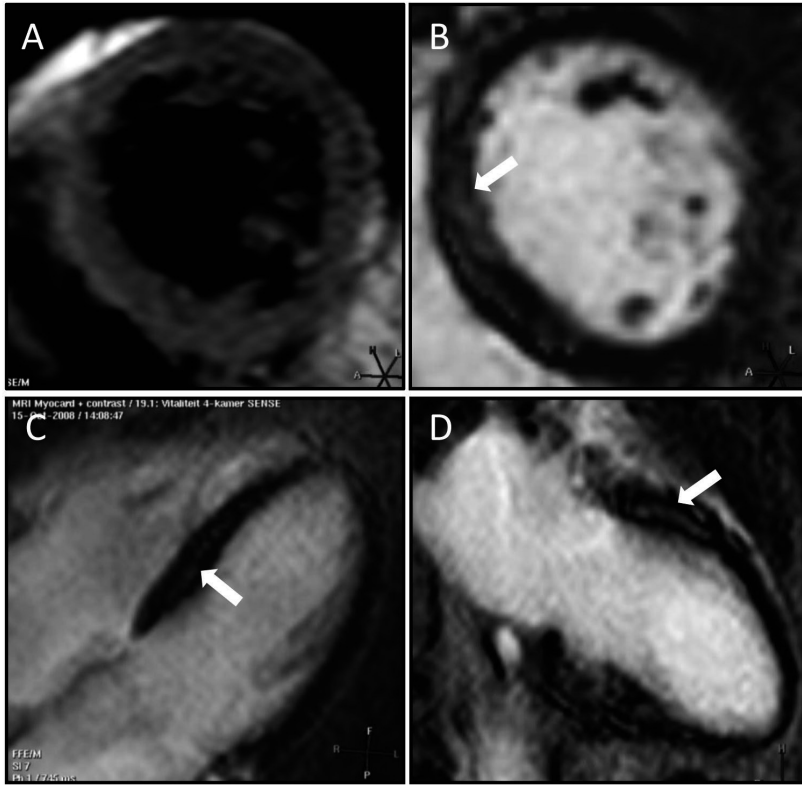
Figure 2. CMR findings in CFS patient 2.
Patient 2. **A**: T2-weighted CMR imaging short-axis view; no presence of increased signal intensity was observed. **B,C,D**: CE-CMR imaging short-axis view, four-chamber view and two-chamber view; arrow demonstrates midwall-CE in the basal inferoseptal, septal and anteroseptal segments.

Figure 3. CMR findings in CFS Patient 3.
Patient 3. **A**: T2-weighted CMR imaging short-axis view; no presence of increased signal intensity was observed. **B**: CE-CMR imaging short-axis view; arrow demonstrates midwall-CE in the basal inferoseptal and septal segments.
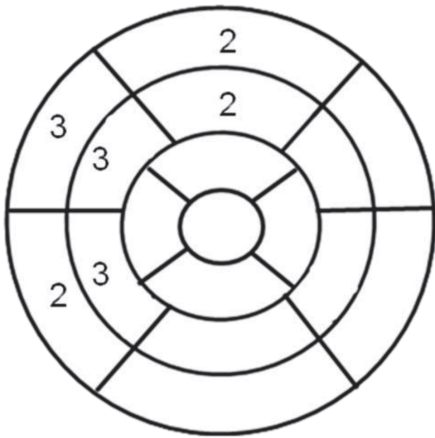
Figure 4. Bulls-eye scheme demonstrating predilection pattern of CE in three patients positive for CE. Typical patterns in CFS patients (n=3/12) with CE (i.e. fibrosis). The "bulls-eye" scheme demonstrates inferoseptal, septal, and anteroseptal predominance of midwall CE lesions.

Discussion

Data of Cardiac Magnetic Resonance imaging. The present CMR study used a *combined* CMR approach of cine, contrast enhanced (CE), and T2-weighted imaging to assess cardiac dimensions, function, and myocardial tissue characteristics in patients with confirmed CFS and healthy controls. Our data demonstrate a lower size, mass, and function of the left ventricle compared to the age and gender-matched controls. Theoretically, this difference could partially explain some mild fatigue in these patients, but it may be more likely that the reduction in LV dimensions and function is the result of a reduced physical activity. These findings are in accordance with a previous echocardiographic study, which revealed in CFS patients a smaller LV chamber with a lower cardiac output during pharmacological stress testing.[14]

Recently, Hollingsworth et al. investigated in 12 CFS patients and 10 healthy controls geometrical and functional LV parameters with CMR, including strain analysis.[2] Although not all analysis gave evidence of myocardial dysfunction in CFS patients, residual torsion at 150% of the end-systolic time was greater in CFS patients than controls, suggesting a delay in the release of torsion. In CFS patients, both residual torsion at 150% of the end-systolic time and torsion to endocardial strain ratio correlated negatively with the end-diastolic volume index. These findings may contribute to the understanding of cardiac functional impairments in CFS patients.[7]

In the present study, we also performed CE imaging in both CFS patients and a control group. We found no increase in signal intensity (i.e. edema) on the T2-weighted CMR images, which demonstrates that our patients did not suffer then from an active state of viral myocardial infection at the time of CMR. Midwall CE, a finding that has frequently been observed in patients with

histopathological evidence of chronic active (or borderline) myocarditis,[15] was found in 3 out of 12 CFS patients. As demonstrated by Mahrholdt et al. in patients with acute myocarditis, CE may not be detectable in approximately 25% of patients at an average follow-up of 4.5 months.[16] Therefore, one may hypothesize that the initial myocardial involvement in our CFS patient population might have been somewhat larger than observed in our CMR examination during chronic state. The presence of a non-permissive, persistent viral infection, in which only a very low level of complete infectious virus is produced, could be a potential explanation of *isolated* midwall CE (*midwall CE in the absence of an edema*)[17] as observed in three of our CFS patients.

Pattern and pathophysiology of myocardial damage. Previous myocarditis CMR studies demonstrated a relation between the type of virus and the pattern of myocardial damage.[3] Accordingly, the distribution of CE may help to distinguish between different viral infections of the myocardium. In our CFS patients, CE was exclusively observed in infero- and anteroseptum, which fits well with myocardial infections by Epstein-Barr-virus or Human Cytomegalovirus; serum antibodies for at least one of these viruses were identified in 11 of our CFS patients. Notably, inferoseptal wall motion abnormalities were observed in one patient with and three patients without CE. In patients with myocarditis, the value and interpretation of CE can be difficult because of the heterogeneous scar distribution and the generally lower signal intensities. In addition, due to limited voxel resolution, smaller myocardial scars may not be detected. Another explanation for this discrepancy could be the absence of CE in the chronic state. To the best of our knowledge, this study is the first to suggest a septal predilection pattern of CE and/ or wall motion abnormalities in CFS patients. In CFS patients, myocardial fibrosis may lead to ventricular dysfunction, as in patients with Chagas myocarditis, for instance, in whom a relation between the amount of CE and late ventricular dysfunction has been described.[18]

Clinical implication and consequences. Few data are available on prevalence and extent of cardiac involvement in CFS patients. With our combined CMR approach, we demonstrated in one examination functional and structural abnormalities of the myocardium, as previously assessed separately with different techniques. Specific treatment of myocarditis remains a challenge.[6;19] A small, randomized, placebo-controlled trial on the use of antiviral therapy for patients with Epstein-Barr virus subset of CFS found a clinical improvement after 6 months.[20] Recently, it has been suggested that EBV can provoke ventricular tachycardia by both acute and chronic myocardial inflammation, emphasizing the clinical importance of this viral infection.[21] To test the hypothesis that Epstein-Barr and/or Human Cytomegalovirus may lead to ventricular dysfunction, myocardial involvement, and CFS, further studies are warranted that should include early and repeat examinations with a combined CMR approach plus targeted myocardial tissue biopsies. Such serial studies may answer the question of whether some CFS patients develop a dilated cardiomyopathy with the inherent risk of an inferior clinical course.[6]

Limitations and technical considerations

We did not perform serial serological tests or myocardial biopsies. It would have been ideal to correlate our CMR findings with targeted endomyocardial biopsies. However, this would have involved an invasive procedure without a direct therapeutic implication. In patients with myocarditis, the value and interpretation of CE can be difficult because of the heterogeneous scar distribution and the generally lower signal intensities.[4;22-24] Although our data are unique, they cannot be used to explain whether the mechanism of reduced cardiac function is the cause of reduced exercise capacity or the result of lower physical activity. Further assessment of the relation between exercise capacity and MRI parameters may be of interest and a subject of future studies.

Conclusion

In patients with Chronic Fatigue Syndrome, CMR demonstrated relatively lower dimensions and a mildly reduced function of the left ventricle. The presence of myocardial fibrosis in some CFS patients suggests that further assessment of cardiac involvement may be warranted as part of a further scientific exploration of the CFS disease. This may imply serial non-invasive examinations with CMR.

References

(1) Devanur LD, Kerr JR. Chronic fatigue syndrome. J Clin Virol 2006 November;37(3):139-50.

(2) Baker R, Shaw EJ. Diagnosis and management of chronic fatigue syndrome or myalgic encephalomyelitis (or encephalopathy): summary of NICE guidance. BMJ 2007 September 1;335(7617):446-8.

(3) Fukuda K, Straus SE, Hickie I, Sharpe MC, Dobbins JG, Komaroff A. The chronic fatigue syndrome: a comprehensive approach to its definition and study. International Chronic Fatigue Syndrome Study Group. Ann Intern Med 1994 December 15;121(12):953-9.

(4) Bohl S, Wassmuth R, bdel-Aty H, Rudolph A, Messroghli D, Dietz R, Schulz-Menger J. Delayed enhancement cardiac magnetic resonance imaging reveals typical patterns of myocardial injury in patients with various forms of non-ischemic heart disease. Int J Cardiovasc Imaging 2008 August;24(6):597-607.

(5) Miwa K, Fujita M. Small heart syndrome in patients with chronic fatigue syndrome. Clin Cardiol 2008 July;31(7):328-33.

(6) Olimulder MA, van EJ, Galjee MA. The importance of cardiac MRI as a diagnostic tool in viral myocarditis-induced cardiomyopathy. Neth Heart J 2009 December;17(12):481-6.

(7) Hollingsworth KG, Hodgson T, Macgowan GA, Blamire AM, Newton JL. Impaired cardiac function in chronic fatigue syndrome measured using magnetic resonance cardiac tagging. J Intern Med 2011 July 27.

(8) Bowles NE, Bayston TA, Zhang HY, Doyle D, Lane RJ, Cunningham L, Archard LC. Persistence of enterovirus RNA in muscle biopsy samples suggests that some cases of chronic fatigue syndrome result from a previous, inflammatory viral myopathy. J Med 1993;24(2-3):145-60.

(9) Grist NR. Myalgic encephalomyelitis: postviral fatigue and the heart. BMJ 1989 November 11;299(6709):1219.

(10) Ishikawa T, Zhu BL, Li DR, Zhao D, Maeda H. Epstein-Barr virus myocarditis as a cause of sudden death: two autopsy cases. Int J Legal Med 2005 July;119(4):231-5.

(11) Friedrich MG. Tissue characterization of acute myocardial infarction and myocarditis by cardiac magnetic resonance. JACC Cardiovasc Imaging 2008 September;1(5):652-62.

(12) Abdel-Aty H, Simonetti O, Friedrich MG. T2-weighted cardiovascular magnetic resonance imaging. J Magn Reson Imaging 2007 September;26(3):452-9.

(13) Cerqueira MD, Weissman NJ, Dilsizian V, Jacobs AK, Kaul S, Laskey WK, Pennell DJ, Rumberger JA, Ryan T, Verani MS. Standardized myocardial segmentation and nomenclature for tomographic imaging of the heart: a statement for healthcare professionals from the Cardiac Imaging Committee of the Council on Clinical Cardiology of the American Heart Association. Circulation 2002 January 29;105(4):539-42.

(14) Miwa K, Fujita M. Cardiac function fluctuates during exacerbation and remission in young adults with chronic fatigue syndrome and "small heart". J Cardiol 2009 August;54(1):29-35.

(15) De Cobelli F, Pieroni M, Esposito A, Chimenti C, Belloni E, Mellone R, Canu T, Perseghin G, Gaudio C, Maseri A, Frustaci A, Del MA. Delayed gadolinium-enhanced cardiac magnetic resonance in patients with chronic myocarditis presenting with heart failure or recurrent arrhythmias. J Am Coll Cardiol 2006 April 18;47(8):1649-54.

(16) Mahrholdt H, Wagner A, Deluigi CC, Kispert E, Hager S, Meinhardt G, Vogelsberg H, Fritz P, Dippon J, Bock CT, Klingel K, Kandolf R, Sechtem U. Presentation, patterns of myocardial damage, and clinical course of viral myocarditis. Circulation 2006 October 10;114(15):1581-90.

(17) Lerner AM, Zervos M, Dworkin HJ, Chang CH, O'Neill W. Hypothesis: A unified theory of the cause of chronic fatigue syndrome. Infectious diseases in Clinical Practice 1997 May;6(4):239-43.

(18) Rochitte CE, Oliveira PF, Andrade JM, Ianni BM, Parga JR, Avila LF, Kalil-Filho R, Mady C, Meneghetti JC, Lima JA, Ramires JA. Myocardial delayed enhancement by magnetic resonance imaging in patients with Chagas' disease: a marker of disease severity. J Am Coll Cardiol 2005 October 18;46(8):1553-8.

(19) Cocker MS, bdel-Aty H, Strohm O, Friedrich MG. Age and Gender Effects on the Extent of Myocardial Involvement in Acute Myocarditis - A Cardiovascular Magnetic Resonance (CMR) Study. Heart 2009 August 25.

(20) Lerner AM, Beqaj SH, Deeter RG, Dworkin HJ, Zervos M, Chang CH, Fitzgerald JT, Goldstein J, O'Neill W. A six-month trial of valacyclovir in the Epstein-Barr virus subset of chronic fatigue syndrome: improvement in left ventricular function. Drugs Today (Barc) 2002 August;38(8):549-61.

(21)   Mavrogeni S, Spargias K, Bratis C, Kolovou G, Papadopoulou E, Pavlides G. EBV Infection as a Cause of VT: Evaluation by CMR. JACC Cardiovasc Imaging 2011 May;4(5):561-2.

(22)   Mahrholdt H, Goedecke C, Wagner A, Meinhardt G, Athanasiadis A, Vogelsberg H, Fritz P, Klingel K, Kandolf R, Sechtem U. Cardiovascular magnetic resonance assessment of human myocarditis: a comparison to histology and molecular pathology. Circulation 2004 March 16;109(10):1250-8.

(23)   Wu KC, Weiss RG, Thiemann DR, Kitagawa K, Schmidt A, Dalal D, Lai S, Bluemke DA, Gerstenblith G, Marban E, Tomaselli GF, Lima JA. Late gadolinium enhancement by cardiovascular magnetic resonance heralds an adverse prognosis in nonischemic cardiomyopathy. J Am Coll Cardiol 2008 June 24;51(25):2414-21.

(24)   Yokokawa M, Tada H, Koyama K, Ino T, Hiramatsu S, Kaseno K, Naito S, Oshima S, Taniguchi K. The characteristics and distribution of the scar tissue predict ventricular tachycardia in patients with advanced heart failure. Pacing Clin Electrophysiol 2009 Mar 32(3):314-22

Chapter 9

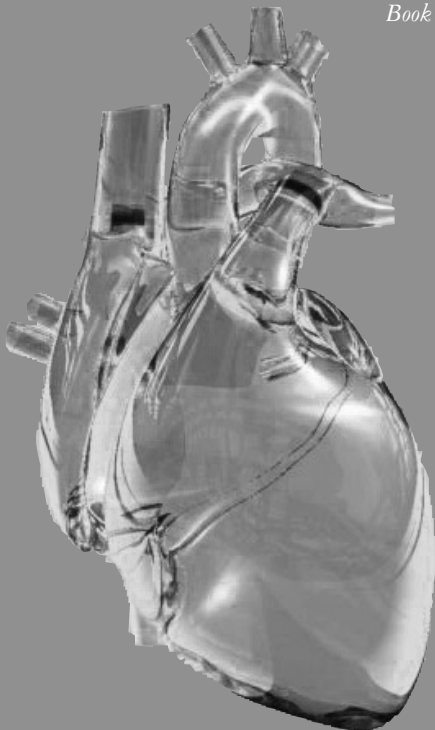## Further applications and future perspectives of CMR with contrast enhancement

Further applications and future perspectives of CMR with contrast enhancement

1.   Introduction

Nowadays, CMR permits in a single examination the assessment of LV geometry, LV function, and the characteristics of infarcted myocardium. Particularly, the development of the LGE technique expands the spectrum of clinical indications for CMR assessment in patients with ischemic and non-ischemic heart diseases. The indications comprise a detailed evaluation of cardiac diseases, guidance of optimal therapy, and prediction of clinical outcome. Compared to other non-invasive imaging modalities, a combined CMR approach (i.e., cine, T2-weighted and LGE-imaging) is unique as it permits the broadest evaluation of structural and functional parameters of the heart. While the previous chapters of this thesis discuss several main indications for LGE-CMR, the present chapter illustrates and discusses additional applications of CMR that provide further insights into the morphology and function of the heart. Future development of CMR and its current limitations are addressed in the second part of this chapter.

2.   Further applications of CMR

2.1   *CMR in ischemic heart disease*

In the setting of ischemic heart disease, a more detailed infarct tissue characterization than discussed in the previous chapters can be accomplished with LGE-CMR. The area of LGE tends to be larger in the acute phase of MI (during the first week) and then progressively decreases during healing (in week 1–4); the infarcted myocardium subsequently reaches the state of so-called healed myocardial infarction (> 4 weeks).[1] This is consistent with the established course of LV remodeling following MI, in which myocardial edema subsequently regresses and necrotic myocardium is replaced by scar tissue.[2]

LGE-CMR studies have revealed that the final MI size is strongly influenced by the extent of the edema in the acute phase. By combining T2-weighted imaging to visualize myocardial edema (i.e., *area at risk*) and LGE-CMR to visualize scar (i.e., *final infarct size*), a *myocardial salvage index* can be calculated by subtracting the final infarct size from the area at risk.[3] The myocardial salvage index has shown to be independently associated with less adverse LV remodeling and early ST-segment resolution[4], and may represent an interesting parameter for the assessment of novel reperfusion strategies in patients with myocardial infarction. In addition, in the subacute phase of an MI, the presence of a larger heterogeneous zone of the total infarcted tissue may be associated with an increased risk of developing ventricular tachycardia.[5]

Some patients develop in the acute phase of a MI a microvascular obstruction within the ischemic myocardium.[4] In Gadolinium-enhanced images acquired after 3 to 5 minutes from contrast injection, microvascular obstruction is represented by a dark zone within the infarcted LV region and usually located in the subendocardium, as the contrast medium generally does not reach this area (Figure 1 a,b). The presence of microvascular obstruction is associated with more adverse left ventricular remodeling and with inferior clinical outcome.[6]
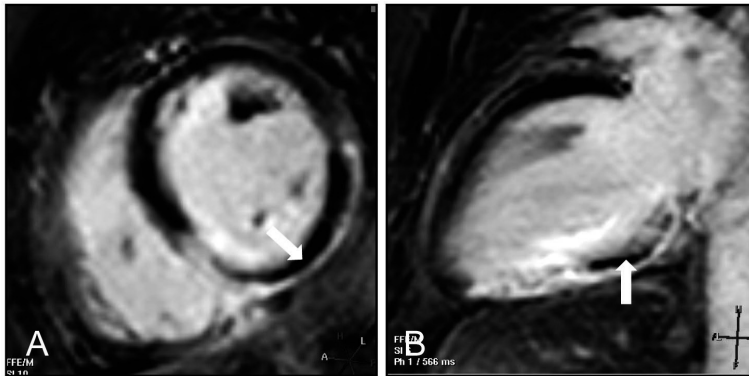
Figure 1. LGE-CMR patterns post-MI. **A,B:** LGE short axis and long axis view showing an inferior infarction with microvascular obstruction (white arrow).

Tagging can be used to estimate regional myocardial function (i.e., myocardial strain, strain rate, twist, torsion, and septal-to-lateral delay) and to optimize selection of candidates for cardiac resynchronization therapy following MI. Different tagging techniques are currently available, such as: spatial modulation of magnetization (SPAMM), delay alternating with nutation for tailored excitation (DANTE), complementary SPAMM, harmonic phase (HARP), displacement encoding with stimulated echoes (DENSE), and strain encoding (SENC).[7;8]

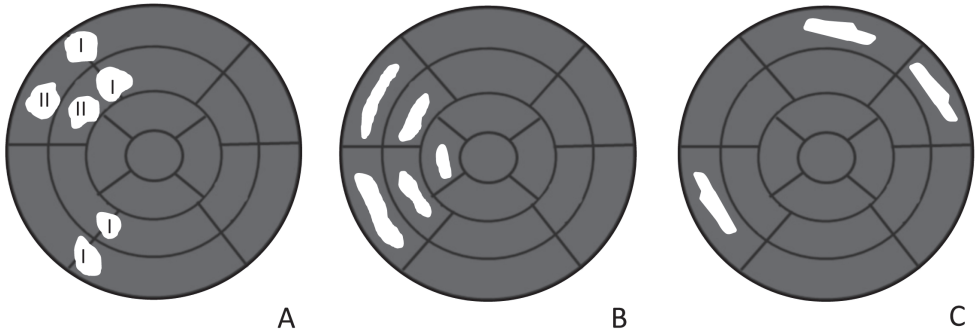## 2.2 CMR in non-ischemic cardiomyopathies

2.2.1   Hypertrophic cardiomyopathy

Hypertrophic cardiomyopathy is a primary myocardial disease that is characterized by an often focal (mostly septal) left ventricular wall thickening with or without left ventricular outflow obstruction; histopathological studies have demonstrated the presence of myocardial fibrosis as well as myofibrillar hypertrophy and disarray.[9]

There are predilection patterns of LGE in patients with hypertrophic cardiomyopathy. More than 80% of patients exhibit patchy fibrosis of the LV at the right ventricular insertion points and in the anteroseptal wall in the region of septal thickening (Figure 2 a,b; Figure 3a).[10;11] However, myocardial fibrosis is also located in non-hypertrophic segments of the LV.[12]
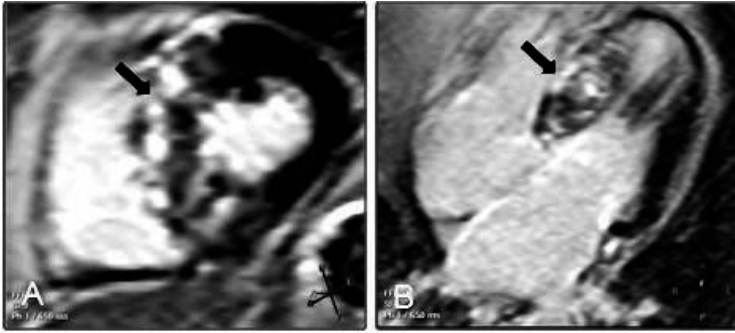
Figure 2. A,B: LGE short axis and long axis view showing hypertrophic cardiomyopathy with patchy LGE septal and in the right ventricular insertion points. (black arrow).


Figure 3. Bulls eye scheme according to the 17 segmental model, demonstrating typical LGE patterns in nonischemic cardiomyopathies. **A:** Hypertrophic cardiomyopathy with predilection LGE (i.e., fibrosis) pattern at the right ventricular insertion points (I) and anteroseptal (II). Myocardial fibrosis is also located in non-hypertrophic segments. **B:** Idiopathic dilated cardiomyopathy with LGE predominantly located in the midwall with septal predominance. **C:** Arrhythmogenic right ventricular cardiomyopathy with midwall LGE found in the basal anterior, anterolateral and inferolateral region. LGE is also found int the right ventricular outflow tract.

Post-contrast T1 mapping, which allows the pixel-based quantification of Gadolinium retention and reveals an absolute value that reflects collagen content, is an emerging CMR technique that may be of particular value for the non-invasive assessment of *diffuse* myocardial fibrosis in patients with hypertrophic cardiomyopathy.[13] As the amount of LGE in hypertrophic cardiomyopathy often corresponds with functional parameters and the incidence of cardiac events, LGE-CMR might be useful for risk stratification and thus selection of recipients of implantable cardioverter defibrillator.[14] In addition, the presence and extent of LGE following percutaneous transluminal septal myocardial ablation for the treatment of significant LV outflow tract obstruction indicates both location and extent of therapeutic myocardial tissue destruction.[15]

2.2.2 Idiopathic dilated cardiomyopathy

Idiopathic dilated cardomyopathy is characterized by dilation and impaired contractility of the LV (or both ventricles) in the absence of abnormal loading conditions (e.g., arterial hypertension; valvular disease) or a distinct cause (e.g., ischemic heart disease; peripartum cardiomyopathy; toxin, chemotherapy or tachycardia-induced cardiomyopathy; certain endocrinopathies).[16] In idiopathic dilated cardiomyopathy, histology is nonspecific and a variety of myocardial tissue alterations, such as myocyte hypertrophy and segmental or diffuse interstitial fibrosis, may coexist. Myocardial fibrosis in idiopathic dilated cardiomyopathy is mostly seen in the LV midwall with a septal predominance and a linear pattern (Figure 4 a,b; Figure 3b); however, fibrosis with a more patchy pattern has also been described occasionally at subendocardial and subepicardial locations.[12]
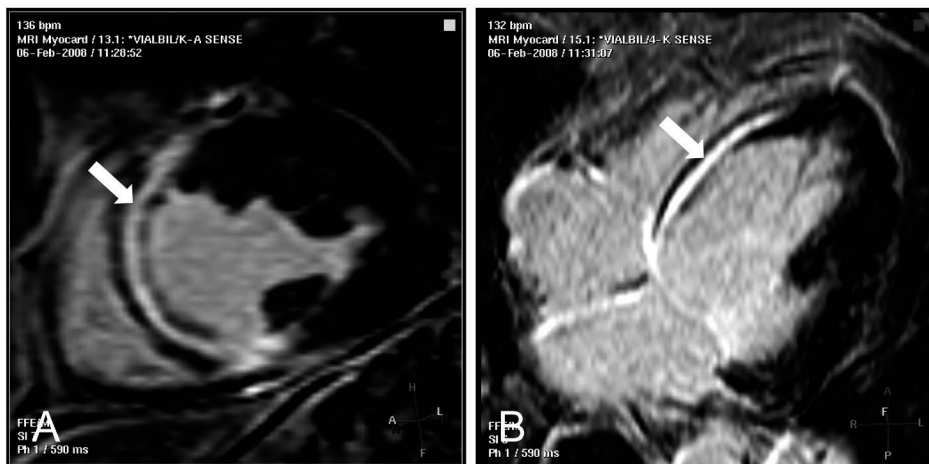
Figure 4 A,B: LGE short axis and long axis view showing dilated cardiomyopathy with LGE having septal midwall predominance (white arrow).

In various CMR studies of patients with idiopathic dilated cardiomyopathy, the prevalence of myocardial fibrosis varied from 13% to 62%.[17;18] This wide variation may partly results from the fact that current LGE-CMR techniques are unlikely to detect the diffuse types of myocardial fibrosis due to a limited voxel resolution.[19] It has been suggested that the degree of LGE (i.e., fibrosis) may correlate with functional LV impairment;[20] preliminary data demonstrate that the presence of LGE is associated with an unfavorable clinical outcome and may be a predictor of sudden death in patients with idiopathic dilated cardiomyopathy.[18;21;22] It has recently been shown that T1 mapping offers the potential to reliably differentiate between diffusely diseased myocardium and healthy myocardium in patients with dilated cardiomyopathy.[23]

2.2.3 Arrhythmogenic right ventricular cardiomyopathy

The arrhythmogenic right ventricular cardiomyopathy is characterized by structural and functional abnormalities, with progressive fibrous and fatty infiltration of the myocardium, involving variable regions of the right and left ventricles.[12;24] Diagnosis of this condition remains a challenge, as abnormalities on echocardiographic and angiographic examinations are often nonspecific. Endomyocardial biopsy has a low sensitivity, as samples are usually taken from the septum, a region that is infrequently involved in this disase.[25] Information from LGE-CMR may help to guide targeted endomyocardial biopsies. In the RV, LGE is frequently observed anterolateral, in the right ventricular outflow tract, and in the apex. In the LV, LGE predilection patterns with midwall LGE are found basal anterolateral and inferolateral (Figure 3c).[26] These patterns of fibrosis correlate with fibro-fatty replacement of myocardium at histolopathological assessment and predict the induction of ventricular tachycardia during electrophysiological assessment.[27] As the presence of arrhythmogenic right ventricular cardiomyopathy cannot be ruled out based on CMR findings alone, standardized guidelines propose the use of morphological, functional, electrocardiographic, histological, and genetic criteria.[24;28]

2.3 CMR in systemic diseases

2.3.1 Sarcoidosis

Cardiac involvement in patients with sarcoidosis is clinically often asymptomatic (95%) while autopsy reveals cardiac manifestations of the disease in up to 60%.[29] During the acute stage, regions of active inflammation and edema are visible on T2-weighted images as areas of increased signal intensity. During the chronic stage, LGE will typically appear as a midwall or epicardial nonischemic pattern (Figure 5b). Occasionally, subendocardial or transmural LGE may be observed, mimicking the scar pattern of patients with previous MI. LGE has been observed in 50% of all patients, diagnosed with sarcoidosis. In a CMR study of 16 patients with sarcoidosis, LGE was markedly diminished after one month of steroid therapy.[30] LGE-CMR may not only be useful to evaluate the response to therapy, but preliminary data suggest that it may also help to determine the prognosis.[29]
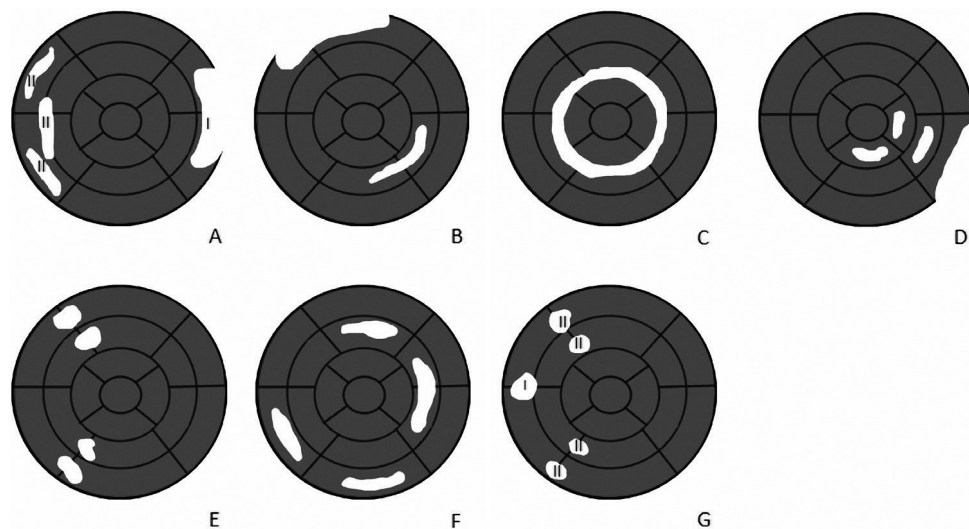
Figure 5. Bulls eye scheme according to the 17 segmental model, demonstrating typical LGE patterns in nonischemic cardiomyopathies. **A:** Myocarditis with CE frequently located in the lateral wall originating from the epicardium (I). CE patterns in myocarditis differ according to viral origin, with parvovirus B19 having CE in the lateral free wall (I), HHV6 having CE frequently in the interventricular midwall (II), and chronic fatigue syndrome myocarditis having CE anteroseptal and inferoseptal (III). **B:** Sarcoidosis with CE midwall or epicardial; however subendocardial or transmural CE may be observed. **C:** Amyloidosis , usually with a global diffuse CE pattern, frequently involving the subendocardium. **D:** Chagas' disease with CE epicardial or midwall, with a predilection pattern inferolateral. **E:** Pulmonary hypertension with CE involving the right ventricular insertion points and the interventricular septum. **F:** Muscular dystrophy with CE observed in the midwall. **G:** Chloroquine induced cardiomyopathy with hypertrophy and accompanying CE in the basal septum (I) and the right ventricular insertion points (II).

2.3.2 Amyloidosis

Both primary and secondary amyloidosis are characterized by extracellular deposition of fibrillar proteins,[16] which may lead to restrictive cardiomyopathy with an initially preserved systolic LV function.[31] In cardiac amyloidosis, LGE is commonly found as a result of the expansion of interstitial space and some extent of endomyocardial fibrosis,[32] leading to a usually global and a diffuse LGE pattern. Although the subendocardium is commonly involved, as is the case in ischemic heart disease, LGE distribution is not related to a myocardial perfusion area of a particular coronary artery (Figure 5c).[33] Moreover, in cardiac amyloidosis LGE is often found in the right ventricle and the atria.

2.3.3 Chagas' disease

The parasitic protozoan Trypanosoma cruzi causes Chagas' disease, which is endemic in Latin America.[33] During chronic disease, the heart is the most frequently affected organ, and patients present with refractory heart failure, disorders of the conduction system, or ventricular tachycardia.[2;34] The involved pathological processes include an inflammatory response, cellular

damage with a broad variation of intensity (minimal alterations up to extensive necrosis), and myocardial fibrosis.[35] Early cardiac involvement may be detected by LGE-CMR before symptom onset.[35] LGE is often located epicardially or in the LV midwall with an inferolateral predilection pattern (Figure 5d); however, other LV regions, such as the apex, may sometimes also be affected.[33]

2.3.4 Pulmonary arterial hypertension

Pulmonary arterial hypertension, both primary and secondary, is characterized by an increased pulmonary vascular resistance that results in pressure overload of the right ventricle.[36] Cine CMR permits accurate assessment of right ventricular mass and volumes, which are often difficult to assess with other imaging modalities.[2] LGE is frequently observed in patients with severe symptomatic pulmonary artery hypertension with predilection patterns involving the two right ventricular septal insertion points and the interventricular septum (Figure 5e). LGE in the interventricular septum was found to be associated with septal bowing on cine CMR, and its extent correlated inversely with right ventricular systolic function.[37]

2.3.5 Muscular dystrophy

Both Becker and Duchenne muscular dystrophies are progressive X chromosome-linked recessive neuromuscular diseases with myocardial involvement in up to 72% of patients with various degrees of impairment of LV function (up to severe dilated cardiomyopathy). Cardiac myocyte dystrophin deficiency leads to myocardial necrosis and replacement of myocardium by connective tissue and fat in both ventricles. On LGE-CMR images, hyperenhancement of the LV midwall has been reported in 73-100% of patients.[38] In addition, hyperenhancement has also been observed subepicardially in the inferolateral LV wall with an age-dependent increase in its extent (Figure 5f)[39] CMR including LGE assessment and tagging enables the detection of subtle (often regional) morphological and functional abnormalities and may be ideally for the evaluation of cardiac involvement, disease progression, and monitoring of the potential effect of therapies. Earlier CMR-based recognition of myocardial involvement may help to earlier initiate medical treatment, which may increase life expectancy.

2.3.6 Chloroquine-induced cardiomyopathy

Chloroquine-induced cardiomyopathy is a rare iatrogenic disease that is associated with long-term intake of chloroquine, which is most frequently prescribed for treatment of rheumatoid arthritis and malaria prophylaxis.[40] This cardiomyopathy is characterized by ineffective lysosomal metabolism because of an increase in pH that leads to accumulation of lysosomal glycosphingolipids and finally myocardial thickening.[41] The time interval between the start of chloroquine therapy and disease manifestation varies greatly, ranging from several months to more than 20 years.[40] CMR may demonstrate the presence of left ventriucular hypertrophy with accompanying areas of LGE in the basal septum and at the insertion point of the right ventricle (Figure 5g). Fabry disease,

an X chromosome-linked lysosomal storage disease caused by a deficient activity of the enzyme α-galactosidase A, can also result in the accumulation of glycosphingolipids in the heart (as well as other organs).[41;42] In the absence of arterial hypertension or valvular disease, Fabry disease cardiomypathy should therefore always be considered as a differential diagnosis of "idiopathic" LV hypertrophy.

2.4 CMR in other diseases

2.4.1 Tsako Tsubo cardiomyopathy

This more recently recognized cardiomyopathy is characterized by an acute, rapidly reversible distinctive regional LV dysfunction in the absence of significant coronary artery disease. Japanese investigators were intrigued by the unusual end-systolic shape of the left ventricle, resembling the original Japanese octupus trap;[43] consequently, the term Tsako Tsubo cardiomyopathy was introduced. Several pathophysiological mechanisms have been proposed, including multivessel coronary spasm, catecholamine-induced myocardial stunning, coronary emboli with spontaneous fibrinolysis, and myocardial inflammation.[44] Recently, variant forms of this disease have been described, including inverted Tako Ttsubo cardiomyopathy and mid-ventricular ballooning cardiomyopathy.[45;46] In the setting of Tako Tsubo cardiomyopathy, CMR including T2-weighted imaging may identify myocardial edema (as well as normalization thereof as LV function improves).[47] Of note, with only few exceptions,[48] no LGE is present in this cardiomyopathy, which is consistent with the preserved viability of the affected LV regions and the transient nature of dyfunction.[44;49] At follow up, LV function is generally normalized in the absence of oedema, pericardial effusion, or LGE.[44;47] The lack of LGE, both initially and at follow-up, permits the distinction of this syndrome from MI, mycoarditis, or infiltrative diseases. Thus, CMR in combination with T2 and LGE imaging may provide valuable additional information for the differential diagnosis and therapeutic decision-making in patients suspected to have Tako Tsubo cardiomyopathy.

2.4.2   *Noncompaction cardiomyopathy*

Noncompaction cardiomyopathy is characterized by a thin, compacted epicardial layer and a thick endocardial layer with prominent trabeculation and deep recesses.[50] It can be present as solitary abnormality or may be associated with different congenital cardiac malformations. Accurate diagnostic criteria are important, as noncompaction cardiomyopathy can be associated with the development of severe LV dysfunction, thrombo-embolism, and ventricular arrhythmia. It has been shown that CMR-based end-systolic measurement of LV dimensions has a particularly strong association with the occurrence of adverse clinical events and the development of systolic dysfunction and congestive heart failure.[51] According to Jacuier et al., the presence of a CMR-assessed trabeculated LV mass of more than 20% of the global LV mass is highly sensitive and specific for the diagnosis of LV noncompaction.[50] In 70% of patients with LV noncompaction,

LGE (i.e., fibrosis) was observed.[52]   Dodd et al. showed that the extent of LGE in patients with LV noncompaction is inversely related with the ejection fraction of the LV.[53] In addition, right ventricular noncompaction, which can be easily assessed with CMR, is reported in up to 60% of patients with LV noncompaction.[52]

2.4.3 Chemotherapy-induced cardiomyopathy

Several chemotherapeutic agents for the treatment of malignancies have been shown to be associated with the development of LV dysfunction. Chemotherapies with a high incidence of congestive heart failure are anthracyclines (3-26%; e.g. doxorubicin), and monoclonal antibodies (2-28%; e.g. trastuzumab).[54] The cumulative dose, the administration schedule, concomitant use of other cardiotoxic therapies, and a history of cardiovascular disease determine the likelihood of inducing a cardiomyopathy. There is limited knowledge about the utility of LGE-CMR in the assessment of chemotherapy-induced cardiomyopathy. Fallah-Rad et al. reported the presence of epicardial LGE in 10 out of 160 breast cancer patients with trastuzumab-induced cardiomyopahty, defined as a left ventricular ejection fraction of less than 40%.[55] Recently, Kirthy et al. studied with LGE-CMR 12 breast cancer patients, who were treated with trastuzumab, and found that despite the presence of left ventricular dysfunction there was no evidence of necrosis or fibrosis.[56] In a study in long-term survivors of a malignant disease with anthracycline exposure during childhood, myocardial fibrosis was not detected after a median follow-up of 7.8 years.[57] LGE-CMR data on other chemotherapy-induced cardiomypathies are scarce.[58-60]

2.4.4 LGE-CMR-guided endomyocardial biopsy

As the location of scar/fibrosis on LGE-CMR may serve as a map to locate optimal target spots for endomyocardial biopsies, the LGE pattern on CMR imaging might help enhance diagnostic accuracy of this intervention. A small study in patients with myocarditis has suggested an increased diagnostic performance of LGE-CMR-guided endomyocardial biopsies.[61;62] However, another study was unable to confirm the value of LGE-CMR for guidance of endomyocardial biopsies.[63] In fact, the often small size of LGE areas and the limited steerability of bioptomes limit the practicability of performing endomyocardial biopsies with LGE-CMR-guidance.[63]

2.4.5 Screening for cardiomyopathy

Patients can develop a cardiomyopathy as part of inherited syndromes. For instance, a huge number of gene mutations have been linked to hypertrophic cardiomyopathy. These gene mutations predominantly encode for contractile proteins, such as cardiac myosin-binding protein C (MYBPC3) and beta-myosin heavy chain (MYH7) (thick filament of the sarcomere), and troponin T and troponin I.[64] Besides sarcomeric mutations, several metabolic disorders have been linked to the phenotype of hypertrophic cardiomyopathy. An example may be the X chromosome-linked lysosomal storage disorder called Fabry disease.[64] Currently, there is still no consensus

about a definitive screening test for hypertrophic cardiomyopathy, based on a genetic assessment. In addition, genetic screening is unable to differentiate between gene mutation carriers who also express the disease phenotype, and asymptomatic gene mutation carriers who merely carry the mutation.[65] As a consequence of the often-heterogeneous expression of gene mutations, the carriers may be completely asymptomatic and healthy individuals or patients with myocardial fibrosis and hypertrophic cardiomyopathy, who may develop–among others–symptoms of congestive heart failure. In contrast, the use of LGE-CMR imaging permits an accurate assessment of myocardial tissue and LV function within a single examination. In particular for autosomal dominant disorders, familial screening with LGE-CMR may be very important as individual findings may have significant therapeutic consequences. For example, in our centre, an 18-year-old female patient was diagnosed with familiar hypertrophic cardiomyopathy (cardiac myosin-binding protein C): LGE-CMR imaging revealed an asymmetrical septal hypertrophy (diameter of the interventricular septum was 38 mm) and the presence of myocardial fibrosis (Figure 6).
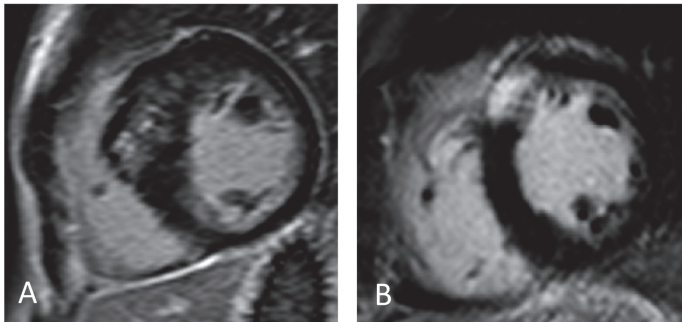
Figure 6. Screening relatives for cardiomyopathy. **A:** 18-year-old female with a genetic disorder of the cardiac myosin-binding protein C; short axis view showing asymmetrical septal hypertrophy with LGE in the anteroseptal region. **B:** 56-year-old male (father) with the same genetic disorder; short axis view showing a very similar LGE pattern in the anteroseptal region of the LV.

Following the guidelines[66] septal thickness >30 mm in combination with medical history of collapse), the young lady was selected for implantation of a cardioverter defibrillator. Her father (familiar screening revealed that he had the same genetic disorder) showed the same pattern of asymmetrical septal hypertrophy (septal thickness of 24 mm) and presence of fibrosis with LGE-CMR, which, according to the guidelines, represented no indication for implantable cardioverter defibrillator therapy. As previously discussed, the amount of LGE in hypertrophic cardiomyopathies often corresponds with functional parameters and the frequency of cardiac events; therefore, LGE-CMR might be useful for risk stratification and the selection of recipients of an implantable cardioverter defibrillator.

3. Future perspectives

Novel therapeutic strategies for the treatment of patients with cardiomyopathies are currently being developed, including the transplantation of primitive cell types (e.g., stem cells or myoblasts) into the damaged myocardium in an attempt to promote trans-differentiation into functional myocardial cells. LGE-CMR imaging can be used to monitor such studies and to evaluate the results of novel therapeutic strategies such as direct injection of primitive cell types into infarcted LV segments.[67;68] In animal models, mesenchymal stem cells have been labeled with iron-based contrast agents to examine the process of 'homing' of such cells in the myocardium.[69-71]

Recently, 3.0-T CMR imaging with a 3D inversion recovery gradient-echo sequence was compared with standard 2D imaging. The 3D technique showed a superior spatial image resolution, a shorter image acquisition time, a preserved contrast-to-noise ratio, and intra- and interobserver variabilities that were similar to the 2D approach; all in all, the 3D technique could improve the clinical utility of LGE-CMR in the future.[72] Nevertheless, motion artefacts can be seen at higher heart rates. Due to the increased T_1 relaxation time inherent to the higher field strength, the optimal inversion delay time to null the signal of normal myocardium needs to be longer at 3 T for the same dose of contrast agent.[73]

LGE-CMR can also be used to assess scar distribution in the left atrium. In this respect, correlations between atrial scar and low-voltage regions delineated by electroanatomic voltage mapping have already been shown.[74;75] Early studies have suggested that LGE-CMR of the left atrium may predict the short-term procedural outcome of ablation and can assist in performing ablation procedures.[74;76] However, according to the initial experience of Spragg et al., the resolution of scar mapping may be insufficient to reliably predict ablation gaps and pulmonary vein reconnection sites in patients undergoing repeat pulmonary vein isolation for recurrent atrial fibrillation.[75]

The ability of CMR to identify *diffuse* myocardial fibrosis with (post-contrast) T1 mapping provides a novel approach to the detection of diffuse cellular changes, such as those recognized to occur with aging, hypertension, atrial fibrillation, diabetes, and (infiltrative) myocardial diseases. It may also become a powerful "imaging biomarker" for the effects of current and novel antifibrotic therapies.[77;78] With current clinically applied CMR technologies, spatial resolution imposes constraints especially on what type of tissue is concealed within the peri-infarct zone, characterized by intermediate signal intensities. High-resolution LGE-CMR imaging with 1000-fold higher resolution than clinical scans may bear the potential to obtain further insights in experimental settings.[79]

4. Limitations of CMR and LGE

Besides some key points, discussed above, clinical use of CMR is frequently challenged by the often limited CMR scanner availability and the relatively long duration of scan time and post-processing as well as economic constraints. In fact, a wide variety of CMR sequences can be accomplished, but this is time-consuming. Therefore it is desirable that the image scan protocol is tailored to fit the clinical question of an individual patient.

Metallic implants, implantable pacemakers, and implantable cardiac defibrillators are considered a contraindication for CMR. However, recent studies show that CMR can be performed safe and feasible in patietns with implantable devices.[80-82] CMR may be performed safely when limiting specific absorption rate, performing patient monitoring, and appropriately device reprogramming.[82] Artefacts caused by the implanted systems limit the diagnostic value of CMR in patients with left sided devices (especially imaging of anterior myocardial infarcts), whereas image quality and diagnostic value of CMR in patients with right sided devices are not affected by device-related artifacts.[82] Relative contra-indications are severe claustrophobia, clinical instability, and the first trimester of pregnancy.[83] In addition, clinical use of LGE-CMR is currently limited to patients without advanced renal dysfunction.[84]

Observers should be aware of potential pitfalls and artifacts that may generate hyperintense areas that mimic myocardial scar such as partial volume effects, epicardial and pericardial fat, and hyperintense blood between myocardium and papillary muscles.[85] In this respect, it is important to confirm the presence of a hyperintense area in more than one contiguous slice, in more than one projection, and by assessing the corresponding cine images. Moreover, hyperintese areas should be confirmed by at least two independent observers.[86]

5. Conclusion

CMR is increasingly used in patients with (or with suspicion of) a variety of cardiac anomalies and diseases, both as part of an experimental approach as well as in routine clinical practice to establish the diagnosis, define the etiology, monitor therapeutic strategies, and/or obtain prognostic information.

References

(1) Thygesen K, Alpert JS, White HD. Universal definition of myocardial infarction. Eur Heart J 2007;28:2525-2538.

(2) Marcu CB, Nijveldt R, Beek AM, van Rossum AC. Delayed contrast enhancement magnetic resonance imaging for the assessment of cardiac disease. Heart Lung Circ 2007;16:70-78.

(3) Aletras AH, Tilak GS, Natanzon A et al. Retrospective determination of the area at risk for reperfused acute myocardial infarction with T2-weighted cardiac magnetic resonance imaging: histopathological and displacement encoding with stimulated echoes (DENSE) functional validations. Circulation 2006;113:1865-1870.

(4) Masci PG, Ganame J, Strata E et al. Myocardial salvage by CMR correlates with LV remodeling and early ST-segment resolution in acute myocardial infarction. JACC Cardiovasc Imaging 2010;3:45-51.

(5) Robbers LF, Delewi R, Nijveldt R et al. Myocardial infarct heterogeneity assessment by late gadolinium enhancement cardiovascular magnetic resonance imaging shows predictive value for ventricular arrhythmia development after acute myocardial infarction. Eur Heart J Cardiovasc Imaging 2013.

(6) Nijveldt R, Beek AM, Hirsch A et al. Functional recovery after acute myocardial infarction: comparison between angiography, electrocardiography, and cardiovascular magnetic resonance measures of microvascular injury. J Am Coll Cardiol 2008;52:181-189.

(7) Biglands JD, Radjenovic A, Ridgway JP. Cardiovascular magnetic resonance physics for clinicians: Part II. J Cardiovasc Magn Reson 2012;14:66.

(8) Ibrahim e. Myocardial tagging by cardiovascular magnetic resonance: evolution of techniques--pulse sequences, analysis algorithms, and applications. J Cardiovasc Magn Reson 2011;13:36.

(9) Lamke GT, Allen RD, Edwards WD, Tazelaar HD, Danielson GK. Surgical pathology of subaortic septal myectomy associated with hypertrophic cardiomyopathy. A study of 204 cases (1996-2000). Cardiovasc Pathol 2003;12:149-158.

(10) Choudhury L, Mahrholdt H, Wagner A et al. Myocardial scarring in asymptomatic or mildly symptomatic patients with hypertrophic cardiomyopathy. J Am Coll Cardiol 2002;40:2156-2164.

(11) Moon JC, McKenna WJ, McCrohon JA, Elliott PM, Smith GC, Pennell DJ. Toward clinical risk assessment in hypertrophic cardiomyopathy with gadolinium cardiovascular magnetic resonance. J Am Coll Cardiol 2003;41:1561-1567.

(12) Bohl S, Wassmuth R, bdel-Aty H et al. Delayed enhancement cardiac magnetic resonance imaging reveals typical patterns of myocardial injury in patients with various forms of non-ischemic heart disease. Int J Cardiovasc Imaging 2008;24:597-607.

(13) Ellims AH, Iles LM, Ling LH, Hare JL, Kaye DM, Taylor AJ. Diffuse myocardial fibrosis in hypertrophic cardiomyopathy can be identified by cardiovascular magnetic resonance, and is associated with left ventricular diastolic dysfunction. J Cardiovasc Magn Reson 2012;14:76.

(14) Rubinshtein R, Glockner JF, Ommen SR et al. Characteristics and clinical significance of late gadolinium enhancement by contrast-enhanced magnetic resonance imaging in patients with hypertrophic cardiomyopathy. Circ Heart Fail 2010;3:51-58.

(15) Sievers B, Moon JC, Pennell DJ. Images in cardiovascular Medicine. Magnetic resonance contrast enhancement of iatrogenic septal myocardial infarction in hypertrophic cardiomyopathy. Circulation 2002;105:1018.

(16) Mueller GC, Attili A. Cardiomyopathy: magnetic resonance imaging evaluation. Semin Roentgenol 2008;43:204-222.

(17) Isbell DC, Kramer CM. The evolving role of cardiovascular magnetic resonance imaging in nonischemic cardiomyopathy. Semin Ultrasound CT MR 2006;27:20-31.

(18) Yokokawa M, Tada H, Koyama K et al. The characteristics and distribution of the scar tissue predict ventricular tachycardia in patients with advanced heart failure. Pacing Clin Electrophysiol 2009;32:314-322.

(19) Vohringer M, Mahrholdt H, Yilmaz A, Sechtem U. Significance of late gadolinium enhancement in cardiovascular magnetic resonance imaging (CMR). Herz 2007;32:129-137.

(20) Koito H, Suzuki J, Ohkubo N, Ishiguro Y, Iwasaka T, Inada M. [Gadolinium-diethylenetriamine pentaacetic acid enhanced magnetic resonance imaging of dilated cardiomyopathy: clinical significance of abnormally high signal intensity of left ventricular myocardium]. J Cardiol 1996;28:41-49.

(21) Assomull RG, Prasad SK, Lyne J et al. Cardiovascular magnetic resonance, fibrosis, and prognosis in dilated cardiomyopathy. J Am Coll Cardiol 2006;48:1977-1985.

(22) Yokokawa M, Tada H, Koyama K, Naito S, Oshima S, Taniguchi K. Nontransmural scar detected by magnetic resonance imaging and origin of ventricular tachycardia in structural heart disease. Pacing Clin Electrophysiol 2009;32 Suppl 1:S52-S56.

(23) Puntmann VO, Voigt T, Chen Z et al. Native T1 mapping in differentiation of normal myocardium from diffuse disease in hypertrophic and dilated cardiomyopathy. JACC Cardiovasc Imaging 2013;6:475-484.

(24) Marcus FI, McKenna WJ, Sherrill D et al. Diagnosis of arrhythmogenic right ventricular cardiomyopathy/dysplasia: proposed modification of the task force criteria. Circulation 2010;121:1533-1541.

(25) Basso C, Ronco F, Marcus F et al. Quantitative assessment of endomyocardial biopsy in arrhythmogenic right ventricular cardiomyopathy/dysplasia: an in vitro validation of diagnostic criteria. Eur Heart J 2008;29:2760-2771.

(26) Marra MP, Leoni L, Bauce B et al. Imaging study of ventricular scar in arrhythmogenic right ventricular cardiomyopathy: comparison of 3D standard electroanatomical voltage mapping and contrast-enhanced cardiac magnetic resonance. Circ Arrhythm Electrophysiol 2012;5:91-100.

(27) Tandri H, Saranathan M, Rodriguez ER et al. Noninvasive detection of myocardial fibrosis in arrhythmogenic right ventricular cardiomyopathy using delayed-enhancement magnetic resonance imaging. J Am Coll Cardiol 2005;45:98-103.

(28) McKenna WJ, Thiene G, Nava A et al. Diagnosis of arrhythmogenic right ventricular dysplasia/cardiomyopathy. Task Force of the Working Group Myocardial and Pericardial Disease of the European Society of Cardiology and of the Scientific Council on Cardiomyopathies of the International Society and Federation of Cardiology. Br Heart J 1994;71:215-218.

(29) Patel MR, Cawley PJ, Heitner JF et al. Detection of myocardial damage in patients with sarcoidosis. Circulation 2009;120:1969-1977.

(30) Shimada T, Shimada K, Sakane T et al. Diagnosis of cardiac sarcoidosis and evaluation of the effects of steroid therapy by gadolinium-DTPA-enhanced magnetic resonance imaging. Am J Med 2001;110:520-527.

(31) Wynne J, Braunwald E. Restrictive and infiltrative cardiomyopathies. In: Zipes DP, Libby P, Bonow RO, Braunwald E, eds. Braunwald's heart disease: a textbook of cardiovascular medicine. Elsevier Saunders; 2005;1682-1692.

(32) Maceira AM, Prasad SK, Hawkins PN, Roughton M, Pennell DJ. Cardiovascular magnetic resonance and prognosis in cardiac amyloidosis. J Cardiovasc Magn Reson 2008;10:54.

(33) Jackson E, Bellenger N, Seddon M, Harden S, Peebles C. Ischaemic and non-ischaemic cardiomyopathies--cardiac MRI appearances with delayed enhancement. Clin Radiol 2007;62:395-403.

(34) Rochitte CE, Oliveira PF, Andrade JM et al. Myocardial delayed enhancement by magnetic resonance imaging in patients with Chagas' disease: a marker of disease severity. J Am Coll Cardiol 2005;46:1553-1558.

(35) Rochitte CE, Nacif MS, de Oliveira Junior AC et al. Cardiac magnetic resonance in Chagas' disease. Artif Organs 2007;31:259-267.

(36) Kovacs G, Reiter G, Reiter U, Rienmuller R, Peacock A, Olschewski H. The emerging role of magnetic resonance imaging in the diagnosis and management of pulmonary hypertension. Respiration 2008;76:458-470.

(37) Blyth KG, Groenning BA, Martin TN et al. Contrast enhanced-cardiovascular magnetic resonance imaging in patients with pulmonary hypertension. Eur Heart J 2005;26:1993-1999.

(38) Yilmaz A, Gdynia HJ, Baccouche H et al. Cardiac involvement in patients with Becker muscular dystrophy: new diagnostic and pathophysiological insights by a CMR approach. J Cardiovasc Magn Reson 2008;10:50.

(39) Yilmaz A, Sechtem U. Cardiac involvement in muscular dystrophy: advances in diagnosis and therapy. Heart 2012;98:420-429.

(40) Reffelmann T, Naami A, Spuentrup E, Kuhl HP. Images in cardiovascular medicine. Contrast-enhanced magnetic resonance imaging of a patient with chloroquine-induced cardiomyopathy confirmed by endomyocardial biopsy. Circulation 2006;114:e357-e358.

(41) Pieroni M, Bellocci F, Crea F. Letter by Pieroni et al regarding article, "Contrast-enhanced magnetic resonance imaging of a patient with chloroquine-induced cardiomyopathy confirmed by endomyocardial biopsy". Circulation 2007;115:e67.

(42) Gange CA, Link MS, Maron MS. Utility of cardiovascular magnetic resonance in the diagnosis of Anderson-Fabry disease. Circulation 2009;120:e96-e97.

(43) Sharkey SW, Lesser JR, Maron MS, Maron BJ. Why not just call it tako-tsubo cardiomyopathy: a discussion of nomenclature. J Am Coll Cardiol 2011;57:1496-1497.

(44) Eitel I, Lucke C, Grothoff M et al. Inflammation in takotsubo cardiomyopathy: insights from cardiovascular magnetic resonance imaging. Eur Radiol 2010;20:422-431.

(45) Marti V, Carreras F, Pujadas S, De Rozas JM. Transient left ventricular basal ballooning-"inverted" Tako-tsubo. Clin Cardiol 2009;32:E20-E21.

(46) Yasu T, Tone K, Kubo N, Saito M. Transient mid-ventricular ballooning cardiomyopathy: a new entity of Takotsubo cardiomyopathy. Int J Cardiol 2006;110:100-101.

(47) Stensaeth KH, Fossum E, Hoffmann P, Mangschau A, Skretteberg PT, Klow NE. Takotsubo cardiomyopathy in acute coronary syndrome; clinical features and contribution of cardiac magnetic resonance during the acute and convalescent phase. Scand Cardiovasc J 2011;45:77-85.

(48) Koeth O, Mark B, Kilkowski A et al. Clinical, angiographic and cardiovascular magnetic resonance findings in consecutive patients with Takotsubo cardiomyopathy. Clin Res Cardiol 2008;97:623-627.

(49) Deetjen AG, Conradi G, Mollmann S, Rad A, Hamm CW, Dill T. Value of gadolinium-enhanced magnetic resonance imaging in patients with Tako-Tsubo-like left ventricular dysfunction. J Cardiovasc Magn Reson 2006;8:367-372.

(50) Jacquier A, Thuny F, Jop B et al. Measurement of trabeculated left ventricular mass using cardiac magnetic resonance imaging in the diagnosis of left ventricular non-compaction. Eur Heart J 2010;31:1098-1104.

(51) Stacey RB, Andersen MM, St CM, Hundley WG, Thohan V. Comparison of Systolic and Diastolic Criteria for Isolated LV Noncompaction in CMR. JACC Cardiovasc Imaging 2013.

(52) Dursun M, Agayev A, Nisli K et al. MR imaging features of ventricular noncompaction: emphasis on distribution and pattern of fibrosis. Eur J Radiol 2010;74:147-151.

(53) Dodd JD, Holmvang G, Hoffmann U et al. Quantification of left ventricular noncompaction and trabecular delayed hyperenhancement with cardiac MRI: correlation with clinical severity. AJR Am J Roentgenol 2007;189:974-980.

(54) Yeh ET, Bickford CL. Cardiovascular complications of cancer therapy: incidence, pathogenesis, diagnosis, and management. J Am Coll Cardiol 2009;53:2231-2247.

(55) Fallah-Rad N, Lytwyn M, Fang T, Kirkpatrick I, Jassal DS. Delayed contrast enhancement cardiac magnetic resonance imaging in trastuzumab induced cardiomyopathy. J Cardiovasc Magn Reson 2008;10:5.

(56) Kirthy V, Schultz C, Davies S. cardiac imaging of trastuzumab-induced cardiomyopathy. [European Journal of Heart Failure Supplements]. 2011. Ref Type: Generic

(57) Ylanen K, Poutanen T, Savikurki-Heikkila P, Rinta-Kiikka I, Eerola A, Vettenranta K. Cardiac magnetic resonance imaging in the evaluation of the late effects of anthracyclines among long-term survivors of childhood cancer. J Am Coll Cardiol 2013;61:1539-1547.

(58) Lightfoot JC, D'Agostino RB, Jr., Hamilton CA et al. Novel approach to early detection of doxorubicin cardiotoxicity by gadolinium-enhanced cardiovascular magnetic resonance imaging in an experimental model. Circ Cardiovasc Imaging 2010;3:550-558.

(59) Wassmuth R, Lentzsch S, Erdbruegger U et al. Subclinical cardiotoxic effects of anthracyclines as assessed by magnetic resonance imaging-a pilot study. Am Heart J 2001;141:1007-1013.

(60) Wu CF, Chuang WP, Li AH, Hsiao CH. Cardiac magnetic resonance imaging in sunitinib malate-related cardiomyopathy: no late gadolinium enhancement. J Chin Med Assoc 2009;72:323-327.

(61) Mahrholdt H, Goedecke C, Wagner A et al. Cardiovascular magnetic resonance assessment of human myocarditis: a comparison to histology and molecular pathology. Circulation 2004;109:1250-1258.

(62) Mahrholdt H, Wagner A, Deluigi CC et al. Presentation, patterns of myocardial damage, and clinical course of viral myocarditis. Circulation 2006;114:1581-1590.

(63) Yilmaz A, Kindermann I, Kindermann M et al. Comparative evaluation of left and right ventricular endomyocardial biopsy: differences in complication rate and diagnostic performance. Circulation 2010;122:900-909.

(64) Brouwer WP, van Dijk SJ, Stienen GJ, van Rossum AC, van d, V, Germans T. The development of familial hypertrophic cardiomyopathy: from mutation to bedside. Eur J Clin Invest 2011;41:568-578.

(65) Devlin AM, Ostman-Smith I. Diagnosis of hypertrophic cardiomyopathy and screening for the phenotype suggestive of gene carriage in familial disease: a simple echocardiographic procedure. J Med Screen 2000;7:82-90.

(66) Maron BJ, McKenna WJ, Danielson GK et al. American College of Cardiology/European Society of Cardiology clinical expert consensus document on hypertrophic cardiomyopathy. A report of the American College of Cardiology Foundation Task Force on Clinical Expert Consensus Documents and the European Society of Cardiology Committee for Practice Guidelines. J Am Coll Cardiol 2003;42:1687-1713.

(67) Orlic D, Hill JM, Arai AE. Stem cells for myocardial regeneration. Circ Res 2002;91:1092-1102.

(68) Williams AR, Trachtenberg B, Velazquez DL et al. Intramyocardial stem cell injection in patients with ischemic cardiomyopathy: functional recovery and reverse remodeling. Circ Res 2011;108:792-796.

(69) Garot J, Unterseeh T, Teiger E et al. Magnetic resonance imaging of targeted catheter-based implantation of myogenic precursor cells into infarcted left ventricular myocardium. J Am Coll Cardiol 2003;41:1841-1846.

(70) Hill JM, Dick AJ, Raman VK et al. Serial cardiac magnetic resonance imaging of injected mesenchymal stem cells. Circulation 2003;108:1009-1014.

(71) Kraitchman DL, Heldman AW, Atalar E et al. In vivo magnetic resonance imaging of mesenchymal stem cells in myocardial infarction. Circulation 2003;107:2290-2293.

(72) Bauner KU, Muehling O, Theisen D et al. Assessment of Myocardial Viability with 3D MRI at 3 T. AJR Am J Roentgenol 2009;192:1645-1650.

(73) Cheng AS, Robson MD, Neubauer S, Selvanayagam JB. Irreversible myocardial injury: assessment with cardiovascular delayed-enhancement MR imaging and comparison of 1.5 and 3.0 T--initial experience. Radiology 2007;242:735-742.

(74) Oakes RS, Badger TJ, Kholmovski EG et al. Detection and quantification of left atrial structural remodeling with delayed-enhancement magnetic resonance imaging in patients with atrial fibrillation. Circulation 2009;119:1758-1767.

(75) Spragg DD, Khurram I, Zimmerman SL et al. Initial experience with magnetic resonance imaging of atrial scar and co-registration with electroanatomic voltage mapping during atrial fibrillation: success and limitations. Heart Rhythm 2012;9:2003-2009.

(76) McGann CJ, Kholmovski EG, Oakes RS et al. New magnetic resonance imaging-based method for defining the extent of left atrial wall injury after the ablation of atrial fibrillation. J Am Coll Cardiol 2008;52:1263-1271.

(77) Ling LH, Kistler PM, Ellims AH et al. Diffuse ventricular fibrosis in atrial fibrillation: noninvasive evaluation and relationships with aging and systolic dysfunction. J Am Coll Cardiol 2012;60:2402-2408.

(78) Neilan TG, Coelho-Filho OR, Shah RV et al. Myocardial extracellular volume fraction from t1 measurements in healthy volunteers and mice: relationship to aging and cardiac dimensions. JACC Cardiovasc Imaging 2013;6:672-683.

(79) Schelbert EB, Hsu LY, Anderson SA et al. Late gadolinium-enhancement cardiac magnetic resonance identifies postinfarction myocardial fibrosis and the border zone at the near cellular level in ex vivo rat heart. Circ Cardiovasc Imaging 2010;3:743-752.

(80) Junttila MJ, Fishman JE, Lopera GA et al. Safety of serial MRI in patients with implantable cardioverter defibrillators. Heart 2011;97:1852-1856.

(81) Martin ET, Coman JA, Shellock FG, Pulling CC, Fair R, Jenkins K. Magnetic resonance imaging and cardiac pacemaker safety at 1.5-Tesla. J Am Coll Cardiol 2004;43:1315-1324.

(82) Naehle CP, Kreuz J, Strach K et al. Safety, feasibility, and diagnostic value of cardiac magnetic resonance imaging in patients with cardiac pacemakers and implantable cardioverters/defibrillators at 1.5 T. Am Heart J 2011;161:1096-1105.

(83) Parsai C, O'Hanlon R, Prasad SK, Mohiaddin RH. Diagnostic and prognostic value of cardiovascular magnetic resonance in non-ischaemic cardiomyopathies. J Cardiovasc Magn Reson 2012;14:54.

(84) Paterson I, Mielniczuk LM, O'Meara E, So A, White JA. Imaging heart failure: current and future applications. Can J Cardiol 2013;29:317-328.

(85) Turkbey EB, Nacif MS, Noureldin RA et al. Differentiation of myocardial scar from potential pitfalls and artefacts in delayed enhancement MRI. Br J Radiol 2012;85:e1145-e1154.

(86) Olimulder MA, Galjee MA, Wagenaar LJ, van Es J, van der Palen J, Visser FC, Vermeulen RC, von Birgelen C. Combined Cardiac Magnetic Resonance imaging of cardiac dimensions, left ventricular function, and myocardial tissue characteristics in female patients with chronic fatigue syndrome. Submitted

Chapter 10

Summary and Conclusions
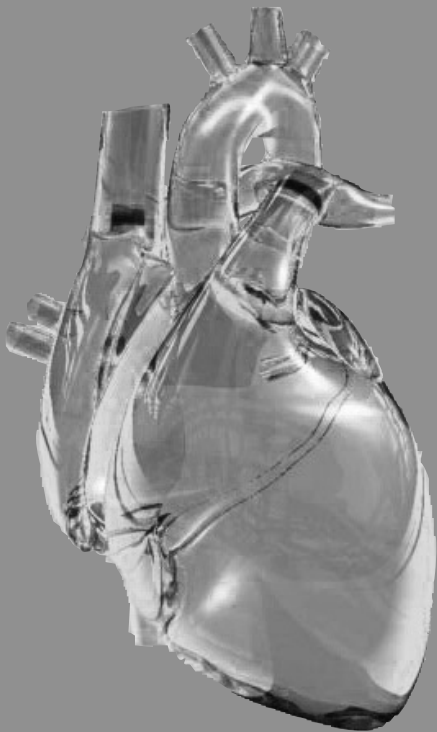
Summary

Non-invasive cardiovascular magnetic resonance imaging (CMR) has been enriched by the introduction of the contrast enhancement technique, an imaging modality that is increasingly used in a broad spectrum of clinical applications and permits the assessment of left ventricular (LV) dimensions and function as well as tissue characterization in a single examination.

Chapter 1

In the introductory chapter of this thesis, after outlining a short history of developments of CMR techniques, a brief technical background of the utilization of cine and late-gadolinium enhancement (LGE)-CMR imaging is given. With the application of post-processing techniques, various infarct tissue characteristics can be quantified, which might be of prognostic value. After a brief overview on some methods of image analysis and definitions, the value of LGE-CMR in patients with ischemic heart disease is discussed and illustrated, serving as an introduction to Chapters 2 to 6 of this thesis. In addition, the clinical application of LGE-CMR in the setting of myocarditis is reviewed in order to introduce the subject of Chapters 7 and 8.

Chapter 2

In this chapter, the long-term effect of successful early revascularization by means of primary percutaneous coronary intervention (primary PCI) on LV dimensions, LV function, and infarct tissue characteristics is investigated. A consecutive series of 69 patients with previous MI, referred for cardiac evaluation for various clinical reasons, were investigated with LGE-CMR >1 month after the MI. Patients with successful early revascularization by means of primary PCI (n=33) had less wall motion abnormalities, a better LV ejection fraction, and a smaller end-systolic LV volume than patients without successful early revascularization (n=36). However, no significant difference was found in core, heterogeneous, and total infarct size. The transmural extent of scar, however, tended to be lower following successful early revascularization. Hence, LV dilatation and wall motion abnormalities were less pronounced after successful early revascularization. The potential effect of successful primary PCI on scar size – in particular transmurality of scar – was more subtle in this study and did not reach statistical significance.

Chapter 3

To get further insight into the impact of a successful early revascularization on the relationship between infarcted tissue characteristics and LV remodeling, we examined 93 patients with LGE-CMR >1 month after an MI. Of these patients, a total of 46 patients had undergone (< 12 hours after symptom onset) a successful revascularization by means of percutaneous coronary intervention or (in the era of thrombolytic treatment) intravenous thrombolysis. Only in patients with successful early revascularization, a correlation between infarct tissue characteristics and

LV remodeling was observed; a larger area of infarcted tissue was related to LV remodeling with peri-infarct size being the best determinant of remodeling. These findings suggest taking infarct tissue characteristics and the success of early revascularization procedures into account when studying LV remodeling.

Chapter 4

Only limited data are available on the potential value of estimated cardiovascular event risk for the prediction of LV remodeling and size of infarcted tissue. For that reason, we assessed in a consecutive series of 25 patients with a successfully treated first ST-elevation MI and single-vessel disease the potential relationship between the Framingham Risk Score and parameters of both LV remodeling and infarct tissue characteristics, as determined 6 months after the MI by LGE-CMR. The Framingham Risk Score showed significant relations with multiple parameters of LV remodeling but no relation with infarct tissue characteristics. In fact, this small study underlines the supremacy of multifactorial risk scores as tools for prediction of unfavorable cardiovascular outcome and supports the hypothesis that there might be a future role for a novel and specific risk score in predicting LV remodeling.

Chapter 5

Scar formation of infarcted myocardial tissue is often the anatomical substrate for ventricular arrhythmias in patients with previous MI. Knowledge on infarct tissue characteristics might help improve risk stratification for implantable cardioverter-defibrillator (ICD) implantation. We used LGE-CMR in 95 ICD recipients to assess potential differences in infarct tissue characteristics between patients with prior life-threatening ventricular arrhythmia (secondary prevention) versus patients with prophylactic ICD implantation (primary prevention). During follow-up, the frequency of applied shocks or other ICD therapies for ventricular arrhythmias was significantly higher in the secondary prevention group (31% vs. 5%; p<0.01), but there was no difference in infarct tissue characteristics between the primary and the secondary prevention groups.

Chapter 6

Microvolt T-wave alternans (MTWA) indicates an increased risk of sudden cardiac death (SCD). We therefore investigated in 68 patients with ischemic cardiomyopathy (ICM) or dilated cardiomyopathy (DCM) the relationship between MTWA and scar/fibrosis as determined by LGE-CMR. In the ICM and DCM patient groups, we observed no relationship between the occurrence of MTWA and the presence, extent, and transmurality of myocardial scar. The question whether MTWA, LGE-CMR, or a combination of both might improve risk stratification in candidates for ICD implantation can only be answered based on data from a larger study population with long-term follow-up data.

Chapter 7

This chapter reviews the role of CMR for the evaluation of myocarditis and myocarditis-induced inflammatory cardiomyopathies. Increasing knowledge on the progression from acute myocarditis to chronic myocarditis or DCM suggests that the early and accurate identification of patients with acute myocarditis might be useful. This can be non-invasively achieved with a combined CMR approach consisting of cine CMR, LGE-CMR, and T2 acquisitions. The LGE distribution pattern is particularly important within the differential diagnostic workup, as it can rule out ischemic causes or may strongly suggest the presence of myocardial inflammation. CMR-evidence of persistent myocardial inflammation may have prognostic implications and could be used to triage patients for appropriate treatment. In addition, CMR-derived information on changes in LV function and myocardial inflammation may be useful to monitor the disease process and/or assess the effect of treatment.

Chapter 8

Ongoing research suggests that latent (chronic active) myocardial infection with Epstein-Barr virus or Human Cytomegalovirus may trigger development of the chronic fatigue syndrome (CFS). Therefore, we used a combined CMR approach to assess cardiac involvement in 12 female CFS patients. The findings of these patients were compared to that of 36 age-matched, healthy women who served as a control group. The CFS patients demonstrated relatively smaller LV dimensions and a mild reduction in global LV function. The presence of myocardial fibrosis in some CFS patients suggests that in the scientific exploration of CFS the assessment of cardiac involvement with CMR may be warranted.

Chapter 9

Advances in CMR techniques allow to explore scientific questions and clinical indications that go beyond the utilization of CMR, as described in the previous chapters. We discuss and illustrate the potential benefit of such CMR approaches for the assessment of patients with ischemic and non-ischemic heart diseases. Moreover, future perspectives and limitations of novel CMR methods are reviewed, including 3.0 T CMR imaging and the ability to identify diffuse myocardial fibrosis with post-contrast T1 mapping.

Conclusions

Contrast-enhanced CMR allows myocardial tissue characterization in a cardiac MR examination in addition to the assessment of LV dimensions and function. LGE-CMR-based assessment of infarct tissue characteristics bears the potential of improving risk stratification, for instance in patients with previous MI. In MI patients with successful early revascularization, who generally show less adverse LV remodeling and probably also less transmurality of scar, the size of infarcted tissue showed a relationship with (adverse) LV remodeling. Nevertheless, the combination of multiple clinical factors as used in the multifactorial Framingham Risk Score also showed a significant relationship with LV remodeling (but not with infarct tissue characteristics). These findings suggest that when studying LV remodeling it may be wise to take infarct tissue characteristics and the success of early revascularization procedures into account.

Risk stratification for ICD implantation could theoretically be improved by knowledge on infarct tissue characteristics. But in our study population, there was no difference in infarct tissue characteristics between ICD recipients for primary versus secondary prevention (while the frequency of applied ICD therapies for ventricular arrhythmias was significantly higher in the secondary prevention group). In addition, we found no relationship between the occurrence of microvolt T-wave alternans and the presence, extent, and transmurality of myocardial scar. While the question whether LGE-CMR may or may not improve risk stratification in ICD candidates can only be answered definitely by large studies with long-term follow-up, our findings give no cause to being overly optimistic.

In patients suspected of suffering from a myocarditis, cardiac assessment with a combined CMR approach (of cine CMR, LGE-CMR, and T2 acquisitions) may be useful. CMR-evidence of persistent myocardial inflammation may even have prognostic implications and might help to triage patients for appropriate treatment. CMR-derived information on changes in LV function and myocardial inflammation may be useful to monitor the disease process and the effect of treatment. In addition, the presence of myocardial fibrosis in some patients with chronic fatigue syndrome, which is thought to be triggered by certain latent viral infections, suggests that CMR assessment of cardiac involvement may be warranted in the scientific exploration of the chronic fatigue syndrome.

Chapter 11

Samenvatting en Conclusies
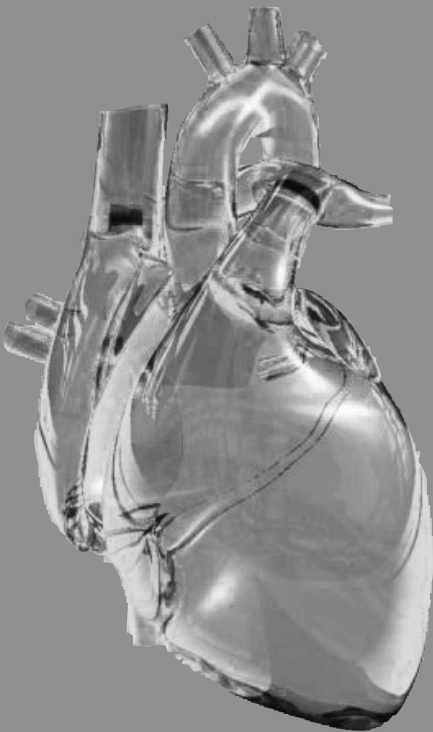
Samenvatting

De introductie van de contrast enhancement techniek is een verrijking voor de niet-invasieve cardiovasculaire magnetische resonantie (CMR). Deze beeldvormingsmodaliteit wordt in toenemende mate in een breed spectrum aan klinische toepassingen gebruikt en maakt het mogelijk om in één onderzoek linker ventrikel (LV) dimensies en functies, maar ook weefselkarakterisatie te beoordelen.

Hoofdstuk 1

In de inleiding van dit proefschrift wordt vanuit historisch perspectief de ontwikkeling van de CMR techniek behandeld, tevens wordt beknopt de technische achtergrond van cine en late gadolinium enhancement (LGE)-CMR beeldvorming weergegeven.

Met de toepassing van post-processing technieken kunnen diverse infarct weefsel karakteristieken worden gekwantificeerd, dit kan van prognostische waarde zijn. Na een kort overzicht van enkele belangrijke analyse methoden en definities wordt de waarde van LGE-CMR in patiënten met ischemische hartziekten besproken en geïllustreerd, dit als een inleiding op Hoofdstuk 2 t/m 6 van dit proefschrift. Ook worden klinische applicaties van LGE-CMR in myocarditis besproken, dit als inleiding op Hoofdstuk 7 en 8.

Hoofdstuk 2

In dit hoofdstuk worden de lange-termijn effecten van succesvolle vroege revascularisatie door middel van primaire percutane coronaire interventie (primaire PCI) op LV dimensies, LV functie en infarct weefsel karakteristieken onderzocht. Een opeenvolgende serie van 69 patiënten met een MI in de voorgeschiedeins, verwezen voor cardiale evaluatie om verschillende klinische redenen, werden onderzocht met LGE-MCR > 1 maand na het MI.

Patiënten met succesvolle vroege revascularisatie door middel van primaire PCI (n=33) hadden minder wandbewegingsstoornissen, een betere LV ejectie fractie, en een kleiner eind-systolisch LV volume dan patiënten zonder succesvolle vroege revascularisatie (n=36). Echter, er waren geen significante verschillen in kern, heterogene, en totale infarct grootte.

De transmuraliteit van het litteken had de tendens lager te zijn na succesvolle vroege revascularisatie. Derhalve, LV dilatatie en wandbewegingsstoornissen waren minder uitgesproken na succesvolle vroege revascularisatie. Het potentiële effect van succesvolle primaire PCI op litteken grootte – voornamelijk transmuraliteit van het litteken – was aanwezig in deze studie maar was niet statistisch significant aantoonbaar.

Hoofdstuk 3

Om meer inzicht te verkrijgen in de invloed van succesvolle vroege revascularisatie op de relatie tussen infarct weefel karakteristieken en LV remodeling, onderzochten we 93 patiënten met LGE-CMR > 1 maand na het MI. Van deze patiënten hadden 46 patiënten succesvolle revascularisatie (<12 uur na begin van klachten) ondergaan door middel van percutane coronaire interventie of (in het tijdperk van trombolyse) intraveneuze trombolyse. Alleen bij patiënten met succesvolle vroege revascularisatie werd een correlatie gezien tussen infarct weefsel karakteristieken en LV remodeling; een groter gebied met geïnfarceerd weefsel was gerelateerd aan LV remodeling waarbij de peri-infarct grootte de beste voorspeller van remodeling was. Deze bevindingen suggereren dat infarct weefel karakteristieken en het succes van vroege revascularisatie moeten worden meegenomen wanneer het proces van LV remodeling wordt onderzocht.

Hoofdstuk 4

Beschikbare data voor de potentiële waarde van het geschatte cardiovasculaire event risico als voorspeller van LV remodeling en grootte van infarct weefsel is beperkt. Daarom onderzochten we, 6 maanden na het MI, in een opeenvolgende serie van 25 patiënten met een succesvol behandeld eerste ST-segment-geëleveerd MI en één-vatslijden, de potentiële relatie tussen de Framingham Risico Score en parameters van LV remodeling en infarct weefsel karakteristieken bepaald met LGE-CMR. De Framingham Risico Score toonde meerdere significante relaties met parameters van LV remodeling maar er was geen relatie met infarct weefsel karakteristieken. Feitelijk onderstreept dit kleine onderzoek het buitengewone belang van multifactoriële risico scores als tool voor de voorspelling van ongunstige cardiovasculaire uitkomsten en de hypothese dat er mogelijk een toekomstige rol is weggelegd voor een nieuwe en specifieke risico score voor het voorspellen van LV remodeling wordt hiermee ondersteund.

Hoofdstuk 5

Litteken vorming van geïnfarceerd myocard weefsel is vaak het anatomische substraat voor ventriculaire arritmieen in patiënten met een MI in de voorgeschiedenis. Kennis van en inzicht in infarct weefsel karakteristieken zou mogelijk risicostratificatie voor potentiële implanteerbare defibrillatoren (ICD) kandidaten verbeteren. In 95 patiënten die een ICD ontvingen werd LGE-CMR toegepast om potentiële verschillen in infarct weefsel karakteristieken tussen patiënten met doorgemaakte levensbedreigende ventriculaire arritmieën (secundaire preventie) versus patiënten met prophylactische ICD implantatie (primaire preventie) te evalueren. Gedurende follow-up was het aantal toegepaste shocks of andere ICD therapieën voor ventriculaire arritmieën significant hoger in de secundaire preventie groep (31% vs. 5%; p<0.01), maar er werd geen verschil gezien in infarct weefsel karakteristieken tussen de primaire en secundaire preventie groep.

Hoofdstuk 6

Microvolt T-wave alternans (MTWA) wordt geassocieerd met een verhoogd risico op plotse hartdood. Daarom onderzochten we bij 68 patiënten met ischemische cardiomyopathie (ICM) of gedilateerde cardiomyopathie (DCM) de relatie tussen MTWA en litteken/fibrose vastgesteld met LGE-CMR. In de ICM en DCM patiënten groepen werd geen relatie gezien tussen het optreden van MTWA en de aanwezigheid, omvang en transmuraliteit van myocardiaal littekenweefsel. De vraag of MTWA, LGE-CMR, of een combinatie van beide mogelijk risicostratificatie in kandidaten voor ICD implantatie verbeterd, kan alleen beantwoord worden met grotere studie populaties en langere follow-up data.

Hoofdstuk 7

Dit hoofdstuk geeft een overzicht van de rol van CMR in de evaluatie van myocarditis en myocarditis-geïnduceerde inflammatoire cardiomyopathieën. Met de toegenomen kennis over de progressie van acute myocarditis naar chronische myocarditis of DCM suggereert dat vroege en accurate identificatie van patiënten met acutue myocarditis waardevol is. Dit kan niet-invasief worden gedaan met een gecombineerde CMR toepassing bestaande uit cine CMR, LGE-CMR en T2 acquisities. Het LGE distributie patroon is voornamelijk belangrijk als differentiaal diagnostische work-up, daar het een ischemische oorzaak kan uitsluiten maar ook (gecombineerd met T2 beeldvorming) aanwezigheid van myocardiale inflammatie kan identificeren. Persisterende myocardiale inflammatie aangetoond middels CMR kan belangrijke prognostische implicaties hebben en zou daarom kunnen worden gebruikt om patiënten te triëren voor juiste behandelingsstrategieën. Daarnaast kan informatie betreffende veranderingen in LV functie en myocard inflammatie verkregen met CMR, geschikt zijn om het ziekte proces te monitoren en/of het effect van de behandeling in te schatten.

Hoofdstuk 8

In onderzoek naar latente (chronich actieve) myocardiale infectie met Epstein-Barr virus of Humaan Cytomegalovirus wordt gesuggereerd dat dit de ontwikkeling van het chronisch vermoeidheidssyndroom (CVS) kan uitlokken. Daarom werd met behulp van een gecombineerde CMR toepassing cardiale betrokkenheid in 12 CVS patiënten van het vrouwelijk geslacht onderzocht. De bevindingen van deze patiënten werden vergeleken met 36 leeftijds-gematchte, gezonde vrouwen die dienden als controle groep.

CVS patiënten demonstreerden relatief kleinere LV dimensies en een milde reductie in globale LV functie. De aanwezigheid van fibrose in het myocardweefsel bij enkele CVS patiënten suggereert dat in wetenschappelijk onderzoek van CVS de beoordeling van cardiale betrokkenheid middels CMR van belang is.

Hoofdstuk 9

Zoals beschreven in de voorgaande hoofdstukken maken de ontwikkelingen in de CMR techniek het mogelijk om wetenschappelijke vraagstukken en klinische indicaties naast de gebruikelijke toepassing van CMR te onderzoeken. Dit hoofdstuk geeft een overzicht, bediscussieerd en illustreert het potentiële nut van dergelijke CMR toepassingen voor de beoordeling van patiënten met ischemische en niet-ischemische hartziekten.

Daarnaast wordt een overzicht gegeven over toekomstperspectieven en beperkingen van nieuwere CMR methoden, waaronder 3.0 CMR beeldvorming en de mogelijkheid om diffuse myocardiale fibrose te identificeren met post-contrast T1 mapping.

Conclusies

Contrast-enhancement CMR maakt het mogelijk om in één onderzoek LV dimensies en functies, maar ook weefsel karakteristieken te beoordelen. Beoordeling van infarct weefel karakteristieken met LGE-CMR heeft de potentie om bijvoorbeeld risicostratificatie te optimaliseren bij patiënten met een MI in de voorgeschiedenis.

In MI patiënten met succesvolle vroege revascularisatie, die over het algemeen minder LV remodeling en vermoedelijk ook minder transmuraliteit van het litteken vertoonden, was er een relatie tussen het geïnfarceerde weefsel en LV remodeling. Desalniettemin, toonde de combinatie van multipele klinische factoren zoals gebruikt in de multifactoriële Framingham Risico Score ook een significante relatie met LV remodeling (maar niet met infarct weefsel karakteristieken).

Deze bevindingen suggereren dat, indien onderzoek wordt gedaan naar het proces van LV remodeling, het verstandig is om ook infarct weefsel karakteristieken en het succes van vroege revascularisatie in acht te nemen, In theorie kan risicostratificatie voor ICD implantatie worden verbeterd door kennis van infarct weefsel karakteristieken. Echter, in onze studie populatie konden we geen verschil in infarct weefsel karakteristieken aantonen tussen patiënten die een ICD ontvingen voor primaire versus secundaire preventie (hoewel de frequentie van toegepaste ICD therapie voor ventriculaire arritmieën significant hoger was in de secundaire preventie groep).

Ook vonden we geen relatie tussen het optreden van microvolt T-wave alternans en de aanwezigheid, omvang en transmuraliteit van myocard litteken. Hoewel de vraag of LGE-CMR wel of niet risicostratificatie in ICD kandidaten kan verbeteren alleen kan worden beantwoord door grotere studiepopulaties met langere follow-up duur, zijn onze bevinding geen aanleiding om overwegend optimistisch te zijn.

In patiënten verdacht voor myocarditis kan cardiale beoordeling met een gecombineerde CMR toepassing (gebruik makende van cine CMR, LGE-CMR en T2 acquisities) zinvol zijn. Persisterende myocardiale inflammatie aangetoond met CMR kan zelfs van prognostische waarde zijn en kan helpen om voor patiënten de juiste behandelingsstrategieën te kiezen.

Veranderingen in LV functie en aanwezigheid van myocard inflammatie, vastgesteld met CMR, kunnen nuttig zijn om het ziekteproces en het effect van behandeling te monitoren. Daarnaast kan de aanwezigheid van fibrose in het myocard bij sommige patiënten met chronisch vermoeidheidssyndroom, waarbij de gedachte is dat dit wordt uitgelokt door latente virale infecties, suggereren dat toepassing van CMR voor de beoordeling van cardiale betrokkenheid een vereiste is in de wetenschappelijke onderzoekssetting van het chronisch vermoeidheidssyndroom.

Dankwoord
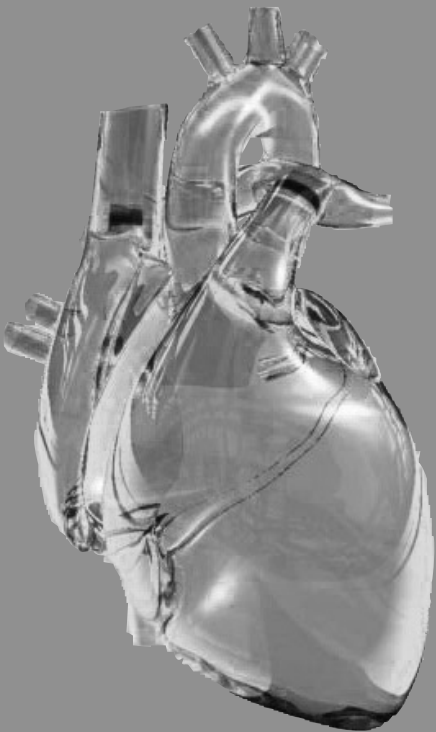
Anno 2007; 'ik ben beland in het grote sprookjesbos!'

Ik werd aan de hand genomen, zoals dat gaat in sprookjes, maar steeds iets meer losgelaten, totdat uiteindelijk de weg was gevonden.

Het was uiteindelijk geen sprookje. Een wetenschapper gelooft ook niet in sprookjes, zij gaat op zoek naar bewijs. En dit werd gevonden. In dit geval bewijs over het nut van de cardiale MRI met behulp van contrast-enhancement. Het werd opgeschreven in een boek. Een boek dat niet thuishoort in het genre fictie maar wetenschap.

Ik ben er blij mee en ik ben er trots op!

Wat overheerst is een gevoel van dankbaarheid aan een ieder die mij in de afgelopen jaren heeft geholpen met de totstandkoming van dit proefschrift. Een aantal personen heeft hieraan een bijzondere bijdrage geleverd.

Allereerst gaat mijn dank uit naar alle patiënten en vrijwilligers die hebben deelgenomen aan dit onderzoek.

Professor von Birgelen, beste Clemens, wat een ongelofelijke inspiratiebron ben je!

Ik bewonder je onuitputtelijke enthousiasme, drijfveer en energie waarmee je me elke keer weer opnieuw wist te stimuleren. Ik heb ontzettend veel van je wetenschappelijke kennis kunnen leren. Daarnaast vind ik het bijzonder waardevol dat je altijd een moment wist in te ruimen als ik je hulp nodig had. Dank voor je vertrouwen, begeleiding en de uiteindelijke totstandkoming van dit proefschrift.

Mijn eerste co-promotor Dr. Galjee, beste Michel. Samen zijn we begonnen aan dit onderzoek! Bedankt voor je inzet om je kennis van de MRI over te brengen op mij. Met je ervaring bewaakte je de klinische relevantie van dit MRI onderzoek en hielp je me om het juiste pad in te slaan. Dank hiervoor.

Mijn tweede co-promoter Dr. Wagenaar, beste Lodewijk, dank voor je waardevolle aanvullingen en opmerkingen tijdens de beoordeling van mijn manuscripten. Daarnaast wist je me altijd weer nieuwe energie te geven met je enthousiasme en humor! Ik hoop ook in de komende jaren nog veel te kunnen leren van jou expertise in de beeldvorming.

De leden van de leescommissie te weten, Prof. dr. M.J. IJzerman, Prof. dr. ir. C.H. Slump, Prof. dr. J.G. Grandjean, Prof dr. A.H.E.M. Maas, Prof. dr. R.J. de Winter en Prof. Dr. med. D. Baumgart wil ik bedanken voor het beoordelen van mijn proefschrift.

Jan van Es, hartelijk dank voor je medebeoordeling van de cardiale MRI beelden.

We zullen het wel nooit eens worden over het klinisch belang van 'de grijzer dan grijs tinten', maar dat geeft ook niet, het heeft af en toe geleid tot interessante en waardevolle discussies tijdens de woensdagmiddag MRI beoordelingen. Ik zal mijn best doen om er binnenkort weer eens aan te schuiven. Wie zet er eigenlijk nu de koffie?

Beste collega's van de research afdeling, dank voor jullie hulp, steun, maar ook gezelligheid op zijn tijd. Harald Verheij wil ik in het bijzonder bedanken voor de ondersteuning en begeleiding van mijn onderzoek.

Professor van der Palen, beste Job, ik wil je ontzettend graag bedanken voor de waardevolle hulp en uitleg betreffende de statistische analyses. De thee stond altijd klaar en dat heeft er mede toe geleid dat ik nu 'iets' meer van de statistiek begrijp.

Mijn opleiders Cardiologie Dr. Verhorst en Dr. Scholten, beste Patrick en Marcoen, dank voor het vertrouwen dat jullie in mij hadden om mij onderzoek te laten verrichten en om dit onderzoek voort te kunnen zetten naast de klinische opleiding.

Daarnaast wil ik alle cardiologen in het MST bedanken voor het feit dat ik mijn opleiding kan genieten in een opleidingskliniek waar onderwijs hoog in het vaandel staat!

De opleiders Interne van het MST Enschede, te weten Dr. Smit en Dr. Wymenga, de Internisten en de collegae assistenten Interne wil ik bedanken voor de tijd die me werd gegeven om dit onderzoek naast de opleiding uit te kunnen voeren. Maar bovenal dank voor de 2 leerzame jaren vooropleiding Interne die ik heb genoten in een warme opleidingssfeer.

Dr. Cramer, beste Maarten Jan, je hebt echt je enthousiasme voor de Cardiologie op mij overgebracht! Na een geweldig inspirerende begeleiding van mijn wetenschappelijke stage gedurende mijn laatste jaar van de opleiding Geneeskunde hielp je me verder; je attendeerde me op een opleidingskliniek in het MST Enschede, daar waar ik vandaan kom. Mede door jou sta ik nu hier, dank voor je inzet.

Mijn collegae onderzoekers wil ik bedanken voor de tijd die ze genomen hebben om mij te helpen en om allerlei vragen te beantwoorden, niet alleen op onderzoeksgebied maar ook op het gebied van allerlei andere relevante levenswijsheden!

Karin Kraaier wil ik in het bijzonder bedanken voor de waardevolle input van kritische opmerkingen en aanvullingen van mijn onderzoeksvragen. Bob, jou wil ik bedanken voor je hulp bij de lay-out van mijn manuscripten, de beoordeling van mijn Nederlandse samenvatting en uiteraard je geduld, steun en gezelligheid tijdens onze gezamenlijke onderzoekstijd.

Ook alle collegae assistenten in het Medisch Spectrum Twente wil ik bedanken voor de interesse in mijn onderzoek, voor de goede samenwerking op de werkvloer, maar ook voor de gezelligheid, niet alleen tijdens maar ook buiten werktijden.

Dr. Vermeulen en Dr. Visser dank ik voor hun inzet en begeleding betreffende het onderzoek naar patiënten met het Chronich Vermoeidheidssyndroom.

Dank ook aan alle MRI laboranten voor de geweldige inzet van het scannen van onze onderzoekspopulatie.
De medewerkers van de hartfunctieafdeling wil ik bedanken voor de tijd die werd ingeruimd voor het verrichten van de fietstesten.

Lieve Lous, vanaf het eerste moment dat we elkaar zagen wisten we allebei, vriendinnen voor het leven. Wat hebben we al ontzettend veel beleefd samen (en herbeleefd onder het genot van heerlijke wijntjes, met onze mannen erbij). Ik vind het fantastisch dat je mijn paranimf wilt zijn, niet alleen omdat je alles altijd zo perfect weet te regelen, maar omdat je ontzettend veel voor me betekent!

Mijn lieve broer Ralph. Dank voor je nooit aflatende steun in goede en slechte tijden! Geweldig om te zien dat het je lukt om probleemloos 2 studies, nl. Rechtsgeleerdheid en Bedrijfskunde te volgen. En daarnaast weet je je studietijd ook nog eens optimaal te benutten om zoveel mogelijk ervaringen op te doen. Het heeft mij o.a. gestimuleerd om dit proefschrift af te ronden. Ik ben er trots op dat je mijn paranimf wilt zijn.

Lieve schoonouders Harry en Suzan. Dank voor jullie waardevolle ondersteuning en voortdurende interesse en belangstelling in mijn werk en onderzoek. Maar vooral dank voor het fantastische tweede 'thuis' voor Eleonora! Het is heel wat waard als je weet dat je dochter op een vertrouwde en warme plek is.
Lieve Matthijs, voorgoed uit ons midden maar altijd in ons hart, zo ben jij er ook bij.

Lieve Papa en Mama, ik heb ontzettend veel bewondering voor jullie als ouders. Alle kansen heb ik gekregen en oneindig hebben jullie me gestimuleerd om 'er uit te halen wat er in zit'. Ik heb altijd kunnen rekenen op jullie onvoorwaardelijke vertrouwen, steun en liefde, en nu nog. Jullie zijn vast trots op mij, maar ik ben trots op jullie! Zonder jullie zou dit proefschrift niet mogelijk zijn.

Ruben, ik mag mezelf niet alleen gelukkig prijzen, maar ik *ben* ook gelukkig met jou aan mijn zijde. Je geeft me alle tijd en ruimte om mijn werk optimaal uit te kunnen voeren. Als het even tegenzit ben jij het die er voor zorgt dat ik het snel weer van de positieve kant bekijk. Maar minstens zo waardevol is onze vrije tijd samen. We hebben het goed met elkaar en ik kijk uit naar de toekomst met je! Binnenkort weer naar onze 'favoriete bestemming'? Ik hou van je.

En ten slotte Eleonora, lieve kleine meid, met jou ben ik opnieuw beland in een prachtig sprookje! Laten we het nog maar even houden zo, afgesproken?

Curriculum Vitae
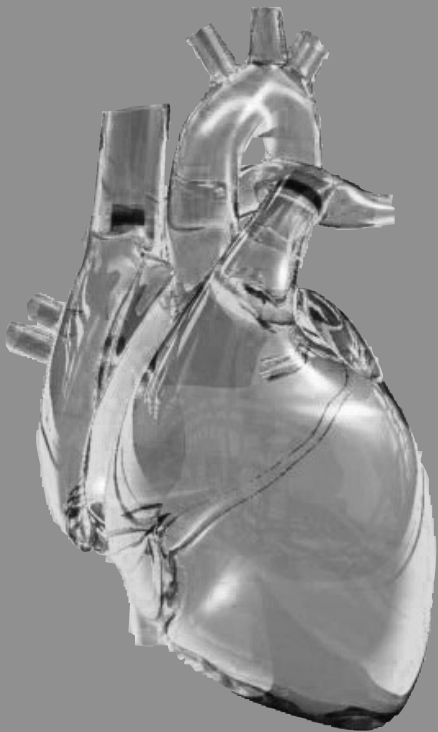
Marlon Anne Gesina Maria Olimulder werd geboren op 28 augustus 1982 te Almelo, Overijssel. In 2000 behaalde zij haar VWO-diploma aan het St.Canisius te Almelo. In september 2000 startte zij met de studie Voeding en Gezondheid te Wageningen en een jaar later, in september 2001 kon ze met de studie Geneeskunde te Utrecht beginnen. Zowel de wetenschappelijke stage als werkzaamheden bij de functie-afdeling binnen de vakgroep Cardiologie van het UMC Utrecht enthousiasmeerde haar voor het specialisme Cardiologie.

Dr. M.J.M. Cramer was degene die haar verwees naar de opleidingskliniek van het thoraxcentrum Twente. In het MST te Enschede volgde zijn haar oudste co-schap Cardiologie en na het voltooien van de opleiding Geneeskunde in augustus 2007 begon zij aansluitend in september van dat jaar met het verrichten van klinisch wetenschappelijk MRI onderzoek. Dit onderzoek werd verricht onder begeleiding van C. von Birgelen, M.A. Galjee en L.J. Wagenaar, die hebben geleid tot de totstandkoming van dit proefschrift.

Zij startte 1 april 2011 met haar opleiding Cardiologie waarbij de eerste twee jaren de vooropleiding Interne Geneeskunde onder leiding van de opleiders Dr. W.M. Smit in het MST te Enschede werd genoten.

Vanaf 1 juli 2013 tot heden is de opleiding tot cardioloog voortgezet in Enschede onder leiding van de opleiders Dr. P.M.J. Verhorst en Dr. M.F. Scholten.

Marlon Olimulder is gehuwd met Ruben Kienhuis en zij hebben samen een dochter, Eleonora.